A NEW ROLE FOR ALDOSTERONE/MINERALOCORTICOID RECEPTOR PATHWAY IN THE DEVELOPMENT OF MITRAL VALVE PROLAPSE

Jaime Francisco Ibarrola Ulzurrun

Diseño de portada: **Unidad de Comunicación y Diseño de Navarrabiomed**

A NEW ROLE FOR ALDOSTERONE/MINERALOCORTICOID RECEPTOR PATHWAY IN THE DEVELOPMENT OF MITRAL VALVE PROLAPSE

Memoria presentada por

D. Jaime Francisco Ibarrola Ulzurrun

para aspirar al grado de Doctor por la Universidad Pública de Navarra

Pamplona-Iruña, 2019

A NEW ROLE FOR ALDOSTERONE/MINERALOCORTICOID RECEPTOR PATHWAY IN THE DEVELOPMENT OF MITRAL VALVE PROLAPSE

La directora e investigadora principal del grupo de investigación de Cardiología Traslacional INFORMA que la presente memoria de tesis doctoral elaborada por Jaime Francisco Ibarrola Ulzurrun ha sido realizado bajo mi dirección y cumple con las condiciones exigidas por la legislación vigente para optar al grado de Doctor.

Y para que así conste, firmo la presente en Pamplona, 20 de Junio del 2019

Natalia López Andrés

Este trabajo ha sido realizado
gracias a las ayudas predoctorales
de la Universidad Pública de Navarra
y los fondos europeos del proyecto
"*European FP7 FIBROTARGETS.*
Targeting cardiac fibrosis
for heart failure treatment".

ACKNOWLEDGEMENTS

El haber completado esta tesis no hubiera sido posible sin la ayuda y el apoyo de muchas personas a las que quiero expresar mi agradecimiento.

En primer lugar, me gustaría agradecer tanto a la Universidad Pública de Navarra como a Navarrabiomed por darme la oportunidad de poder haber realizado esta tesis doctoral y haberme ofrecido sus recursos, medios y financiación necesarios para realizar mi tesis doctoral. También quería agradecer a mi tutor Iñigo Lasa por su disponibilidad y su tiempo dedicado.

Aunque esta tesis doctoral no hubiera sido posible sin la ayuda y apoyo de mi directora Natalia. Hace ya casi 4 años que entré en el laboratorio y siempre te estaré agradecido. Gracias por confiar en mí y apoyarme en todo momento, gracias por enseñarme todo lo que sé de ciencia, por permitirme crecer y dejarme equivocarme (por desgracia demasiadas veces) y siempre acompañado de una sonrisa. Nunca olvidaré nuestro primer congreso (vuelo logroñés incluido), todo ello pasado con escasez de agua, el acopio como si no hubiera mañana de tazas de vino caliente y las numerosas comilonas seguidas de manzanilla que nos hemos pegado. Pero lo que nunca olvidaré será la confianza que tienes en mí, a pesar de mis numerosos fallos, siempre has estado ahí, ayudándome y enseñándome. Y aunque ahora me toca empezar un nuevo camino, sé que siempre estarás ahí y siempre serás un ejemplo a seguir. ¡Mil gracias! (Siempre te quedará ser miembro de la real academia Jaimense (RAJ)).

Aunque tampoco me puedo olvidar de Amaya, le verdadera jefa de poyata. Todo lo que sé de técnicas, la forma de trabajar en el laboratorio y organización de experimentos te lo debo a ti. Durante estos años has sido un pilar y una ayuda incondicional y sin ti esta tesis nunca habría salido. Gracias a ti los días podían ser súper productivos, 10 placas de ELISA, 4 geles de western, poner inmunos, machacar válvulas y recoger un experimento de células, todo ello acompañado de nuestro bocadillo y de placas de PCR cada dos horas. Aunque lo verdaderamente importante es que siempre estuvieras ahí apoyándome, ayudándome en todo momento y respondiendo a mis mismas preguntas una y otra vez siempre con una sonrisa para tu cachorro. Ahora ya no te podré dar sustos por los pasillos o alimentarte con bocadillos, pero sin mí podrás llegar a casa con dinero después de las comidas de empresa.

Gracias también a Alicia, nuestra súper enfermera, y experta en pinchazos, por estar siempre ahí apoyando y respondiendo tan rápido como ella sabe a todas nuestras preguntas de pacientes. Y aunque se unió más tarde, gracias también a Lara, por esas tardes de risa (y bolsas que explotan) y entenderme en mis agobios. Creo que nunca conoceré a nadie que use tanto curry/pesto para todo (eso sí, todo muy rico).

Tampoco me puedo olvidar de nuestra Amaia García de la Peña (comúnmente conocida gracias a mí como nuestra Amaia Mitral). Gracias por tus procrastinaciones, contestar tan rápido como puedes a mis correos

etiológicos y enseñarme toda esa parte clínica que tan desconocida es para mí. Nuestro primer bebé mitral ya está listo, pero necesita un hermanito pronto, así que no procrastines.

Y por supuesto tampoco me puedo olvidar del resto del equipo de Cardiología Traslacional. A Rafa, Virginia, Vanessa y Adela que siempre están allí para ayudarnos con nuestras dudas clínicas y dando esa visión clínica de los proyectos en la que andamos más perdidos.

Je veux remercier tous mes collègues du Centre de Recherche des Cordeliers (Paris) pour l'amitiè et le soutien que j'ai reçu à tout moment. Surtout Benjamin, pour m'avoir appris toute la partie animale et avoir toujours voulu m'aider. Je tiens à remecier tout particulièrement le Proff Frédéric Jaisser pour m'avoir donné l'occasion de travailler avec lui ainsi que son aide et sa contribution à ma dernière annèe de these.

Gracias también a Ernesto, que me ayudó en mi primera estancia en París y que siempre está dispuesto a ayudarte ante cualquier duda.

Esta tesis tampoco hubiera sido posible si no fuera por mis padres. Ellos son los que llevan toda la vida apoyándome y confiando en mí, sacrificándose para que podamos crecer. Mil gracias. Y por supuesto a mi hermana Edurne y nuestro apoyo mutuo con nuestras respectivas tesis, por ayudarme siempre y darme los mejores consejos.

Gracias también a mi Kuadrilla, por estar siempre ahí, apoyarme y dejaros engatusar para acabar de cubateo y txupiteo o simplemente acabar negociando con ladrillo, ovejas, piedras…

Y por último pero no la menos importante, gracias a Nerea. Ya sabes que eres un pilar muy importante en mi vida, con tu apoyo y consejos estos años de tesis han sido un camino muy fácil de seguir. Y aunque estos últimos meses hayamos estado lejos siempre has estado cerca. Ahora nos toca empezar nuestra nueva vida *yankee*, una nueva etapa que seguro que será difícil, pero juntos podemos con todo.

Sin todos vosotros esta tesis no habría sido posible.

MUCHAS GRACIAS

A Natalia

A mis padres

A mi hermana

A Nerea

INDEX

ABBREVIATIONS 29

ABSTRACT 35

RESUMEN 41

INTRODUCTION 47

1. Circulatory system and cardiac valves 49

2. Mitral valve 53

2.1 Structural anatomy 53

2.2 Cellular anatomy 55

2.2.1 Valvular interstitial cells 56

2.2.2 Valvular endothelial cells 58

2.2.3 Interaction between VICs and VECS 60

2.3 Molecular anatomy 61

2.3.1 Extracellular matrix 63

2.3.1.1 Collagen 64

2.3.1.2 Proteoglycans 64

2.3.1.3 Fibronectin 67

2.3.1.4 Elastin 68

2.3.1.5 Matrix metalloproteinases 68

3. Mitral valve disease 69

3.1 Etiology..... 70

3.2 Epidemiology 71

3.3 Natural history, symptoms and diagnosis. 72

3.4 Treatment..... 73

3.5 Mitral valve disease classification 75

3.5.1 Rheumatic mitral valve disease..... 75

3.5.2 Calcific degenerative mitral valve disease..... 76

3.5.3 Functional mitral valve disease 77

3.5.4 Inflammatory mitral valve disease 77

3.5.5 Mitral valve prolapse 78

4. Mitral valve prolapse 78

4.1 Classification..... 79

4.2. Molecular changes..... 80

4.3 Animal models of MVP..... 82

4.3.1 Serotonin (5-HT) pathway as a inductor to develop MVP 84

5. Aldosterone and mineralocorticoid receptor 85

5.1 Aldosterone/MR in cardiovascular disease..... 88

5.2 Aldosterone in mitral valve 90

HYPOTHESIS AND OBJECTIVES..... 95

1. Hypothesis..... 97

2. Objectives 98

MATERIAL AND METHODS 101

I. CLINICAL STUDY 103

1. Patient population 103

2. Mitral valve samples 103

II. CELL CULTURE STUDY 104

3. Cell isolation and culture 104

4. VICs and VECs phenotyping 105

5. Single culture cell assays 106

6. Conditioned media assays 107

7. Cytokine array experiments 108

8. Transfection of cells with siRNA 110

III. ANIMAL STUDIES 111

9. Experimental MVP mice model 111

9.1 Animal groups 112

9.2 Blood pressure 112

9.3 Extraction and sample preparation 113

10. Generation of a MVP mice model in endothelial cell (VE-cadherin)-specific MR knockout mice and in α-SMA cell-specific MR knockout mice 115

10.1 KO induction 115

10.2 Animal groups 115

IV. MOLECULAR BIOLOGY TECHNIQUES 118

11. Real-time reverse transcription PCR 118

12. Western blot analysis 120

13. ELISA 121

14. Histological methods 121

15. Statistical analyses 123

RESULTS 125

1. Expression of MR and Aldo synthesis enzymes in mitral valves 127

***I. IN VITRO* STUDIES** 128

2. Aldosterone induced VICs activation and proteoglycans synthesis in VICs 128

3. Aldo induced EndMT and proteoglycans expression in VECs 131

4. Mitral VECs exacerbated Aldo-induced VICs activation and proteoglycans secretion 135

5. Mitral VICs exacerbated Aldo-induced EndMT and proteoglycans secretion in VECs 137

6. New pathways implicated on Aldo effects in VICs 140

6.1 Cardiotrophin-1 effects in VICs 142

6.2 CT-1 as a mediator of Aldo effects in VICs 145

7. New pathways implicated on Aldo effects in VECs..... 148

7.1 Cardiotrophin-1 effects in VECs 150

7.2 CT-1 is not a mediator of Aldo effects in VECs..... 155

8. New intracellular signaling pathways involved on Aldo effects in VECs..... 160

8.1 CD14 is a mediator of Aldo effects in VECs 161

***II. IN VIVO* STUDIES** 165

9. Effects of Spironolactone in mitral valve morphology and proteoglycans content in a MVP mouse model..... 165

10. Effects on mitral valve morphology and proteoglycans content in conditional SMA-MR-KO mice treated with NDF. 167

11. Effects on mitral valve morphology and proteoglycans content in conditional Vecadh-MR-KO mouse modelmice treated with NDF. 170

III. CLINICAL STUDY..... 174

12. Mitral valve remodeling in MVP patients..... 174

1. Expression of enzymes controlling aldosterone synthesis and MR in the mitral valve...... 188

2. Effects of Aldosterone in mitral valvular interstitial and endothelial cells 190

3. Role of Mineralocorticoid Receptor antagonism in a Mitral Valve Prolapse mouse model. 197

4. Possible beneficial effects of MRA treatment in human MVP patients. 205

CLINICAL RELEVANCE AND PERSPECTIVES OF THE STUDY 209

LIMITATIONS 215

CONCLUSIONS 219

CONCLUSIONES 223

BIBLIOGRAPHY 229

ANNEX 267

ABBREVIATIONS

5-HT: 5-hydroxytryptamine (Serotonin)

5HT2BR: 5-hydroxytryptamine 2B Receptor

ACE: Angiotensin-converting-enzyme

ALCAM: Activated leukocyte cell adhesion molecule

Aldo: Aldosterone

Ang II: Angiotensin II

aVIC: Activated valvular interstitial cell

BMP-5: Bone morphogenetic protein 5

BMP-7: Bone morphogenetic protein 7

CD14: Cluster of differentiation 14

CD31: Cluster of differentiation 31 (PECAM 1)

CD80: Cluster of differentiation 80

Chm-1: Chondromodulin 1

Col: Collagen

CS: Chondroitin sulfate

CT-1: Cardiotrophin 1

CV: Cardiovascular

CXCL16/ DR6: Chemokine (C-X-C motif) ligand 16/DR16

CYP11A1: Cholesterol side-chain cleavage

CYP11B2: Aldosterone synthase

CYP21: 21-hydroxylase

DAB: Diaminobenzidine

DHEA: Dehydroepiandrosterone

DS: Dermatan sulfate

EC: Endothelial cell

ECM: Extracellular matrix

EndMT: Endothelial mesenchymal transition

Erk1/2: extracellular signal–regulated kinases 1/2

GAGs: Glycosaminoglycan

GR: Glucocorticoid receptor

HA: Heparin

HF: Heart failure

HS: Heparan sulfate

HSD3B2: Type 2 3β-hydroxysteroid dehydrogenase

ICAM-2: Intercellular Adhesion Molecule 2

IGF-2: insulin-like growth factor 2

IL: Interleukin

KO: Knock out

KS: Keratan sulfate

LIF: Leukemia inhibitory factor

MATra: Magnet Assisted Transfection

M-CSF R: macrophage colony-stimulating factor receptor

MMP: Matrix metalloproteinase

MPIF-1: Myeloid progenitor inhibitory factor 1

MR: Mineralocorticoid receptor

MRA: Mineralocorticoid receptor antagonist

MVD: Mitral valve disease

MVP: Mitral valve prolapse

NDF: Nordexfenfluramine

NGF R: Nerve growth factor receptor

obVIC: Osteoblastic valvular interstitial cells

PBS: phosphate buffer saline

PDGF : platelet-derived growth factor

PGs: Proteoglycans

pVIC: Progenitor valvular interstitial cells

qVIC: Quiescent valvular interstitial cell

SDF-1 beta: Stromal-derived factor 1 beta

Siglec-5: Sialic acid binding Ig-like lectins 5

SMA: Smooth muscle actin

TGF-β: Transforming growth factor beta

TIMPs: Tissue inhibitors of metalloproteinases

TNFRSF21: Tumor necrosis factor receptor

VCAM-1: Vascular Cell Adhesion Protein 1

VEC: Valvular endothelial cell

VEGFR: Vascular Endothelial Growth Factor Receptor

VIC: Valvular interstitial cell

VSMC: Vascular smooth muscle cell

vWF: Von Willebrand factor

α-SMA: Alpha smooth muscle actin

ABSTRACT

Mitral valve prolapse (MVP) is one of the most common cardiac valvular abnormalities, affecting over 176 million people worldwide. It is defined by typical fibromyxomatous changes in the mitral leaflet tissue. These changes are characterized by an excessive expansion of the spongiosa layer due to the high expression of proteoglycans. However, little is known about the molecular and cellular mechanisms involved in the progression of MVP and surgical intervention is the only available option. Aldosterone/mineralocorticoid receptor (Aldo/MR) has been shown to promote cardiac fibroblast activation as well as fibroblast generation via endothelial mesenchymal transition (EndMT). Moreover, clinical trials showed that MR antagonists (MRAs) improve cardiac function by decreasing cardiac fibrosis.

Our hypothesis is that Aldo/MR could play a role in the development of MVP, modulating valvular interstitial cells (VICs) activation, EndMT and increasing proteoglycans. Furthermore, Aldo/MR pathway could be a new biotarget in MVP and its blockade with a MRA could prevent mitral valve alterations associated with MVP. We tested this hypothesis using human mitral valve samples, human VICs and valvular endothelial cells (VECs), as well as dedicated animal models of MVP.

VICs and VECs were isolated from MVP patients undergoing mitral valve repair. Cells were treated with Aldo +/- MRA. Quiescent VICs markers (Chm-1), VICs activation markers (α-smooth muscle actin (α-SMA),

vimentin, matrix metalloproteinase 2 (MMP-2)), EndMT markers (VE-cadherin, cluster of differentiation 31 (CD31) and von Willebrand factor (vWF)) and proteoglycans (decorin, biglycan, lumican, aggrecan, syndecan-1 and hyaluronan) were measured by RT-PCR, Western Blot and ELISA. Mice were treated with Nordexfenfluramine (NDF) to induce MVP. One group of NDF-treated mice received the MRA Spironolactone. Moreover, two tissue-specific conditional knockout (KO) mice (SMA and VE-cadherin) were treated with NDF. VICs activation markers, EndMT markers and proteoglycans were measured in mitral valves from two subgroups of MVP patients, treated or not with a MRA.

In VICs, Aldo enhanced VICs activation markers and proteoglycans secretion. In VECs, Aldo induced EndMT and increased proteoglycans secretion. The MRA Spironolactone blocked all the above effects. Using a cytokine array, we identified cardiotrophin-1 (CT-1) as a mediator of Aldo-induced VICs activation and proteoglycans secretion, and cluster of differentiation 14 (CD14) as a mediator of Aldo-induced VECs EndMT and proteoglycans secretion. The use of a MRA in an experimental model of MVP reduced mitral valve thickness and proteoglycans content. Furthermore, the specific MR-KO model in endothelial cells (Vecadh-MR-KO) treated with NDF, a drug that induced MVP, revealed that VECs were the primary cell type involved in MVP histological alterations. In human studies, the expression of proteoglycans was partially reduced in mitral valves from MVP patients treated with a MRA.

These findings demonstrate for the first time that Aldo/MR pathway regulates VICs and VECs phenotypic changes associated to MVP. MRA treatment emerges as a promising option to reduce mitral valve remodeling in MVP.

RESUMEN

El prolapso de la válvula mitral (PVM) es una de las enfermedades de las válvulas cardiacas más comunes, afectando a más de 176 millones de personas en el mundo. El PVM se caracteriza principalmente por cambios fibro-mixomatosos que ocurren en el velo de la válvula mitral. Estos cambios consisten en una excesiva expansión de la capa espongiosa debido a una alta expresión de proteoglicanos. Sin embargo, poco se conoce sobre los mecanismos moleculares y celulares involucrados en la progresión del PVM y la única solución disponible es la intervención quirúrgica. La vía de la Aldosterona/Receptor Mineralocorticoide (Aldo/RM) promueve fibrosis cardíaca. Además, Aldo/RM induce la activación de fibroblastos a través de la transición endotelio-mesénquima (TEM). Importantes estudios clínicos muestran que los antagonistas del receptor mineralocorticoide (ARMs) mejoran la función cardiaca mediante la disminución de la fibrosis cardiaca.

Nuestra hipótesis de trabajo es que la vía Aldo/RM podría jugar un papel en el desarrollo del PVM, modulando la activación de las células intersticiales de la válvula (CIVs), la TEM y el incremento de proteoglicanos. Además, la vía de la Aldo/RM podría ser una nueva diana en el PVM y el bloqueo de esta vía con ARMs podría prevenir las alteraciones de la válvula mitral asociadas con el PVM. Hemos testado esta hipótesis usando muestras de válvula mitral humana, CIVs y células endoteliales de válvulas (CEVs) humanas, así como modelos animales de PVM.

CIVs y CEVs fueron obtenidas de pacientes con PVM sometidos a un recambio valvular. Las células fueron tratadas con Aldo +/- ARMs. Se

midieron marcadores de CIVs quiescentes (Chondromodulina-1 (Chm-1)), marcadores de CIVs activadas (α-actina de músculo liso (α-SMA), vimentin, metaloproteinasa 2 (MMP-2)), marcadores del TEM (VE-cadherina, *cluster of differentiation 31* (CD31), factor von Willebrand (vWF)) y proteoglicanos (decorina, biglicano, lumicano, agrecano, sindecano-1 e hialuronano) mediante RT-PCR, Western Blot y ELISA. Se generó un modelo de ratón de PVM mediante la administración de nordexfenfluramina (NDF). A un grupo de ratones tratados con NDF se les administró el ARM Espironolactona. También se administró NDF a dos modelos de ratones transgénicos que no expresan el MR específicamente en células positivas para α-SMA (como las CIVs) o para VE-cadherina (como las CEVs). Por último, se analizaron los marcadores de activación de CIVs, de TEM y la expresión de proteoglicanos en válvulas mitrales de pacientes sometidos a recambio valvular por PVM que habían recibido tratamiento previo con un ARM o no.

En CIVs, la Aldo aumentó los marcadores de CIVs activadas y la secreción de proteoglicanos. En CEVs, la Aldo indujo la TEM y la secreción de proteoglicanos. El ARM Espironolactona bloqueó todos los efectos de la Aldo en CIVs y CEVs. Usando una matriz de citoquinas, se identificó la cardiotrofina 1 como un mediador de la activación de CIVs y de la secreción de proteoglicanos inducida por la Aldo. En CEVs se identificó el CD14 como un mediador de la TEM y de la secreción de proteoglicanos. El uso de ARMs en el modelo experimental de PVM redujo el grosor de la válvula mitral y el contenido total de proteoglicanos. Además, el tratamiento con

NDF en el modelo de ratón condicional que no expresaba el RM específicamente en las células endoteliales demostró que las CEVs son el primer tipo celular involucrado en las alteraciones histológicas del PVM. En los estudios en pacientes, se observó que la expresión de proteoglicanos estaba reducida en las válvulas mitrales de pacientes con PVM tratados con ARM.

Estos hallazgos demuestran por primera vez que la vía de la Aldo/RM regula los cambios fenotípicos de CIVs y CEVs asociados al PVM. El tratamiento con ARMs emerge como una opción prometedora para reducir el remodelado de la válvula mitral en el PVM.

INTRODUCTION

1. Circulatory system and cardiac valves

The circulatory system is a network consisting of blood, blood vessels and the heart. Its main function is to supply the tissues with oxygen, nutrients and other molecules. It can be divided in two different components: the systemic circulation and the pulmonary circulation (Figure 1).

The heart is the principal organ of the circulatory system and it is responsible for pumping oxygenated blood to the body and deoxygenated blood to the lungs. The heart is composed by four chambers; two atria (right and left) and two ventricles (right and left), which in turn are connected to the great vessels (pulmonary artery and aorta). These structures are separated by four valves: aortic, mitral, pulmonary and tricuspid valve. Depending on their anatomical position in the heart, these four heart valves are divided into two types: the semilunar valves (aortic and pulmonary valve), which separate ventricles and great vessels, and the atrio-ventricular valves (mitral and tricuspid valves), between atrium and ventricle (Figure 2).

The right atrium receives deoxygenated blood from the body through the superior and inferior vena cava, and then it flows to the right ventricle through the tricuspid valve. Once the right ventricle is full, it contracts and ejects blood to the pulmonary artery passing through pulmonary valve. After oxygenation in the lungs, blood comes back to the left atrium via the pulmonary veins, then it fills the left ventricle passing through the mitral

valve and finally, when left ventricle contracts, oxygenated blood is ejected to the aorta through the aortic valve [1,2].

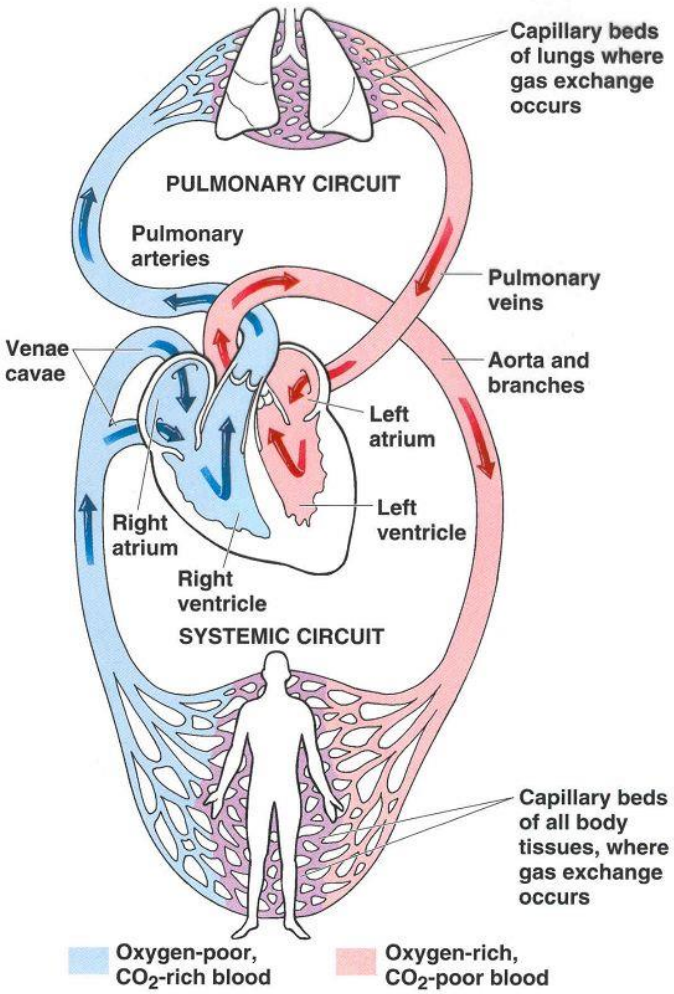

Figure 1. Scheme of the circulatory system. Representation of circulatory system compound by the systemic circulation and pulmonary circulation and the blood journey in the heart (Pearson Education Inc., 2011).

Heart valves are passive cardiac structures, i.e. opening and closure is controlled by the surrounding haemodynamic environment and there are essential to ensure that the blood flows in the appropriate direction, opening or closing depending on the phase of the cardiac cycle.

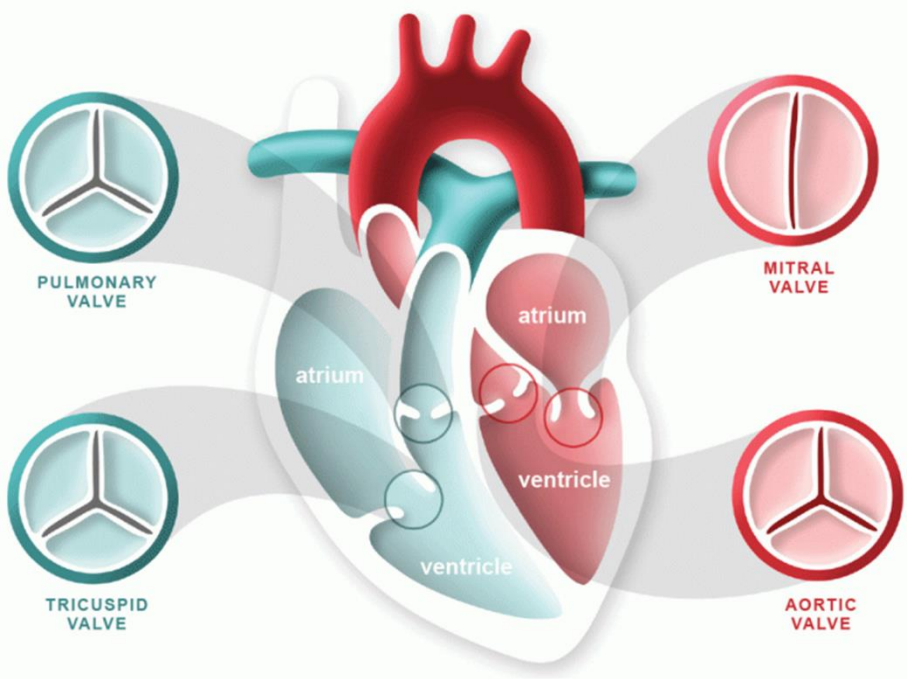

Figure 2. Localization of valves in the heart. Two semilunar valves (aortic and pulmonary valve), which separate ventricles and great vessels, and the atrio-ventricular valves (mitral and tricuspid valves), located between atrium and ventricle (The National Heart Foundation of New Zealand web).

During diastole, when the right and left ventricles are filling, the tricuspid valve and the mitral valve open to allow blood to pass from the atrium into the ventricles. To keep pressure in the ventricles low enough, the pulmonary

valve and aortic valve are closed. Once the ventricles are full, they contract opening the semilunar valves (pulmonary valve and aortic valve), ejecting the blood into the great vessels [2,3]. To prevent retrograde blood flow into the atria, the tricuspid valve and the mitral valve close during systole (Figure 3). This is essential for two reasons: 1) it allows the heart to generate contractile forces sufficient to propel the blood to either the lungs or the systemic circulation; 2) it allows the myocardial muscle tissue of the heart to receive the necessary metabolic nutrients it needs during diastole.

Semilunar valves (i.e. aortic and pulmonary valves) are composed of three leaflets, which are inserted into the root of the corresponding great vessel. Atrio-ventricular valves are more complex anatomical structures that comprise several parts: leaflets (two in mitral valve and three in tricuspid valve), annulus, chordae tendineae and papillary muscles, which are inserted into the ventricular myocardium [4,5].

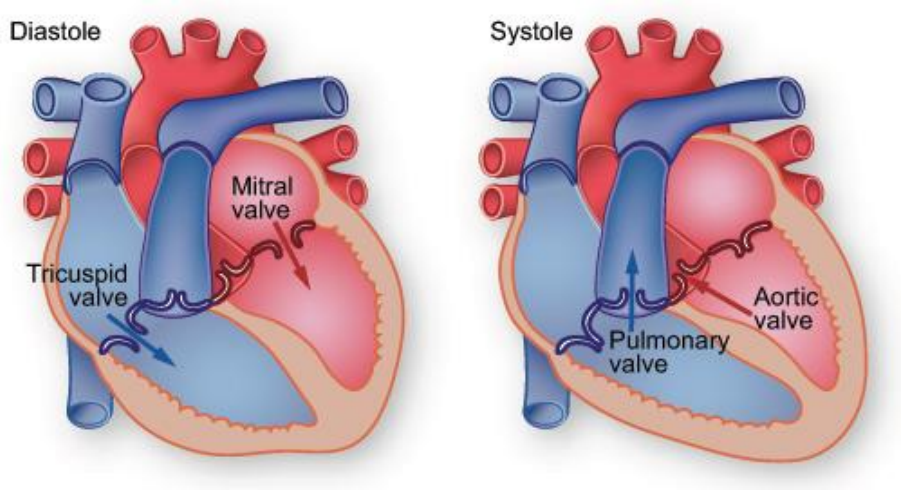

Figure 3. Opening and closing of the heart valves during the cardiac cycle. During diastole the atrio-ventricular valves (mitral and tricuspid valves) are opening and during systole the semilunar valves (aortic and pulmonary valve) are opening.

2. Mitral valve

2.1 Structural anatomy

The mitral valve is a complex and dynamic structure. It is located at the left atrioventricular orifice (Figure 4).

The mitral valve is composed by three parts:

- Leaflets. The leaflet represents a continuous and uninterrupted structure. Mitral valve is formed by two leaflets, the anterior and the posterior leaflet. Each leaflet is separated by the commissural area. The leaflets are attached to the annulus at their bases and multiple tendinous cords (or chordae tendineae) inserted in their ventricular surface. The anterior leaflet is bigger than the posterior leaflet.

Mitral valve leaflets are formed by four distinct histological layers: atrialis, spongiosa, fibrosa and ventricularis. Atrialis layer is composed by aligned collagen and elastin fibers covered with overlying valvular endothelial cells (VECs). Spongiosa layer largely consists of extracellular matrix (ECM) which is rich in proteoglycans and glycosaminglycans. Beneath the spongiosa is the fibrosa layer, composed principally by collagen fibers, and underneath it is the ventricularis layer, a continuous sheet of VECs that overlie the collagen fibers [6]. The most prevalent cell type are valve interstitial cells (VICs), which are found in all layers, and are thought to be responsible for maintaining the structural integrity of the valve [7].

- Annulus. The annulus refers to the circumference of mitral valve orifice located at the left atrioventricular opening. The annulus is a special structure, characterized by a fibrotic structure. The annulus has the shape of a ring or a crown and the function is joining the valve with the heart wall. The annulus is very dynamic throughout the cardiac cycle, and it changes both in shape and dimensions [8–10].
- Subvalvular apparatus. The subvalvular apparatus is composed by two different structures, the tendinous cords and the papillary muscles. The principal function is to join the leaflets with the ventricular wall and to maintain the valvular tension. The tendinous cords have rope-like structures and principally are composed by collagen. They are attached to the ventricular surface of the leaflets

and the papillary muscles or the left ventricular myocardium. The papillary muscles are extensions of the ventricle muscle and contract when the ventricular walls contract (systole). The function is preventing a high retraction of leaflets to the atrium side during systole and maintenance the unidirectional blood flow. The subvalvular apparatus is crucial for the optimum function of the valve [11].

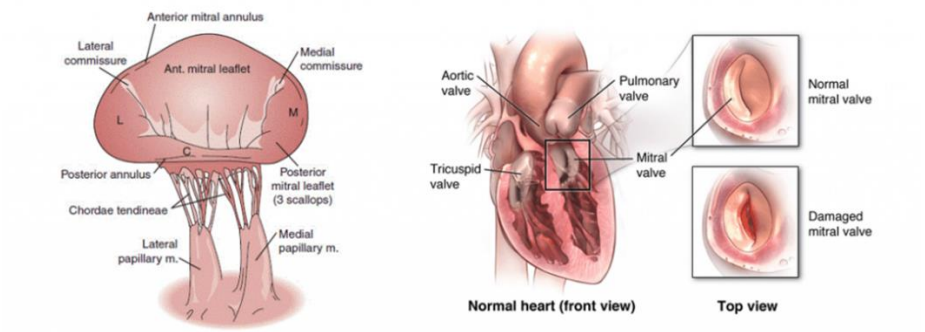

Figure 4. Structural anatomy of mitral valve. Principal parts of mitral valve including the leaflets, annulus, tendinous cords and papillary muscles. (https://mvpresource.com/)

2.2 Cellular anatomy

The mitral valves are composed by two cell populations, VICs and VECs, which play a role in some valvular processes such as proliferation, secretion and contraction. The cell-cell and cell-ECM communications are primordial for the valvular function [11]. Mitral valve leaflets (ventricle and atrial side) are covered from both surfaces by a monolayer of VECs which are

continuous with the endocardium. This monolayer connects with the ECM and the VICs [7,11,12].

2.2.1 Valvular interstitial cells

Cells that reside within the valve are collectively known as VICs. VICs have been ascribed a fibroblastic phenotype due to the absence of specific markers of other cell types and possess a wide range of biological properties that distinguishes them from other fibroblast-like cells and allows them to contribute to maintaining valve function [13]. Their morphology by electron microscopy reveals that they are mostly flattened cells lacking a basement membrane. VICs have the ability to synthesize ECM proteins and matrix-degrading enzymes which include. Based on a review of the literature, five phenotypes represent the VIC family of cells because each of these phenotypes exhibits specific sets of cellular functions essential in normal valve physiology and in pathological processes [7]. The phenotypes are: embryonic progenitor endothelial/mesenchymal cells, quiescent VICs (qVICs), activated VICs (aVICs), progenitor VICs (pVICs), and osteoblastic VICs (obVICs) (Figure 5). The embryonic progenitor endothelial/mesenchymal cells undergo endothelial-to-mesenchymal transformation (EndMT) that initiates the process of valve formation in the embryo. The qVICs are the cells that are at rest in the adult valve and maintain normal valve physiology. The qVICs are noncontractile fibroblast-like cells, which express vimentin and Chm-1 (chondromodulin-1) but do

not express α-SMA (α-smooth muscle actin) (Figura 6). The aVICs are the cells that regulate the pathobiological responses of the valve in disease and injury. aVICs express vimentin and α-SMA but do not express Chm-1 (Figure 6). Furthermore, aVICs expresses MMPs, inflammatory cytokines, proteoglycans, collagens and fibronectin in order to maintain the matrix leaflet homeostasis. The pVICs are the least well defined and consist of a heterogeneous population of progenitor cells that may be important in repair. The obVICs regulate chondrogenesis and osteogenesis. This phenotype principally appears in a few etiologies of mitral valve disease such as degenerative or calcified mitral valve disease and principally occurs as a consequence of the age. Although these phenotypes may exhibit plasticity and convert from one form to another, compartmentalizing VIC function into distinct phenotypes should bring some clarity to our understanding of the complex VIC biology and pathobiology by focusing investigations on the interaction of each specific VIC phenotype with both the tissue and systemic environment in which it resides [7,11,14].

The main function of VICs is to maintain the ECM by a correct control and equilibrium of the different VICs phenotypes, mainly the quiescent and activated phenotype. VICs also synthesize and secrete various mediators, including cytokines, chemokines and growth factors [15]. Although the products released by VICs are well understood, the stimuli that initiate VICs to change their production of various biologically active substances and enzymes is poorly understood. Inflammatory mediators, mechanical loading

and stress, genetic factors, all are potential stimuli that affect the behavior of the VICs [7,11,14,16].

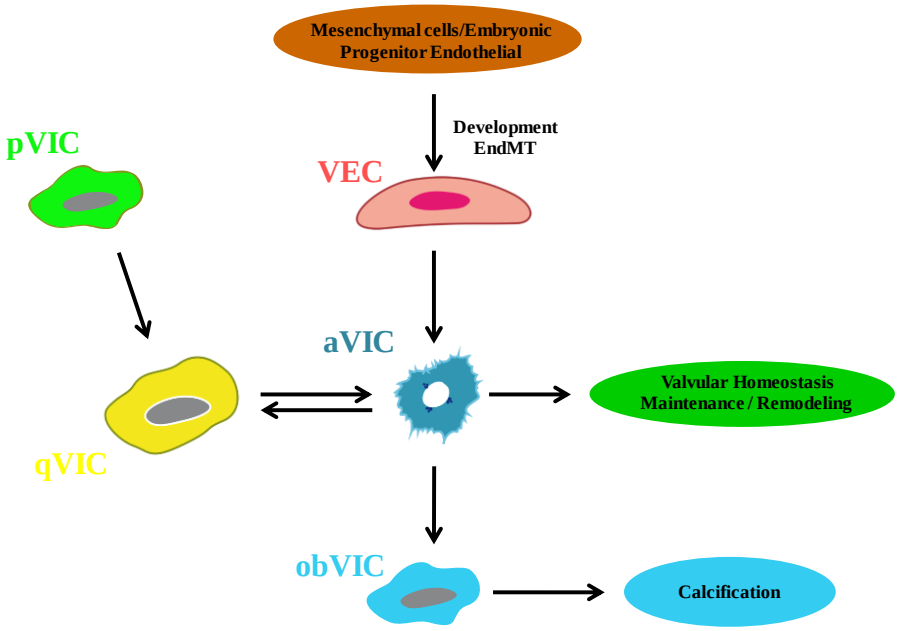

Figure 5. Principal cell types and phenotypes of mitral valve. Five phenotypes of VICs existing; quiescent VICs (qVICs), activated VICs (aVICs), progenitor VICs (pVICs), and osteoblastic VICs (obVICs). The embryonic progenitor endothelial/mesenchymal cells undergo endothelial-to-mesenchymal transformation (EndMT) to VECs.

2.2.2 Valvular endothelial cells

VECs are located as a monolayer around the whole leaflet and provide a barrier between the bloodstream and the tissue. VECs are in constant contact with the atrium and ventricle blood and its function is to regulate the response to their mechanical and humoral environment [17]. VECs are a

special endothelial cell different to other vascular endothelial cells, which maintains the endothelial cell characterization. VECs express CD31, vWF and VE-Cadherin markers. VECs can produce a variety of active molecules and mediators that can be released by diverse vasoactive agents (vasodilators) or by mechanical stimulus (flow of blood), since they are the first barrier in the leaflet [18]. VECs could differentiate to aVIC through the EndMT [7,11,14]. EndMT is an intricate cellular differentiation process whereby endothelial cells detach and migrate away from the endothelium and, to varying extents, decrease endothelial properties and acquire mesenchymal features. This process means the loss of the expression of the VECs markers (CD31, vWF and VE-Cadherin) (Figure 6) and the gain of the expression of the aVICs markers (Vimentin and α-SMA) (Figure 6). EndMT begins in response to an external signal, often transforming growth factor-β (TGF-β). The endothelial cells lose luminal-abluminal polarity, extend filopodia, and migrate into extravascular space where they take up residence, in the case of heart valves, as VICs. Properly controlled EndMT is essential for heart valve development: too little and valves fail to form; too much and the valves thicken and cannot close properly. EndMT seems to persist past embryonic development as endothelial cells expressing EndMT markers can be detected *in vivo* in adult valves. *In vitro*, VECs treated with TGF-β undergo robust EndMT; hence VECs can serve as a prototype for revealing regulators of EndMT [19].

2.2.3 Interaction between VICs and VECS

For the leaflet strength, function, and matrix remodeling, the communication between the cells is primordial. VICs and VECs and its interactions are the principal regulators of the valve homeostasis. VECs are responsible for maintaining levels of VICs, and this event is regulated by multiple cytokines and mediators between both cells types. This robust relation between the two cell types suggests that they are both involved in common pathways to maintain the structure and function of the valve. However, whether VICs and VECs could be similarly affected in various disease processes has not been clarified.

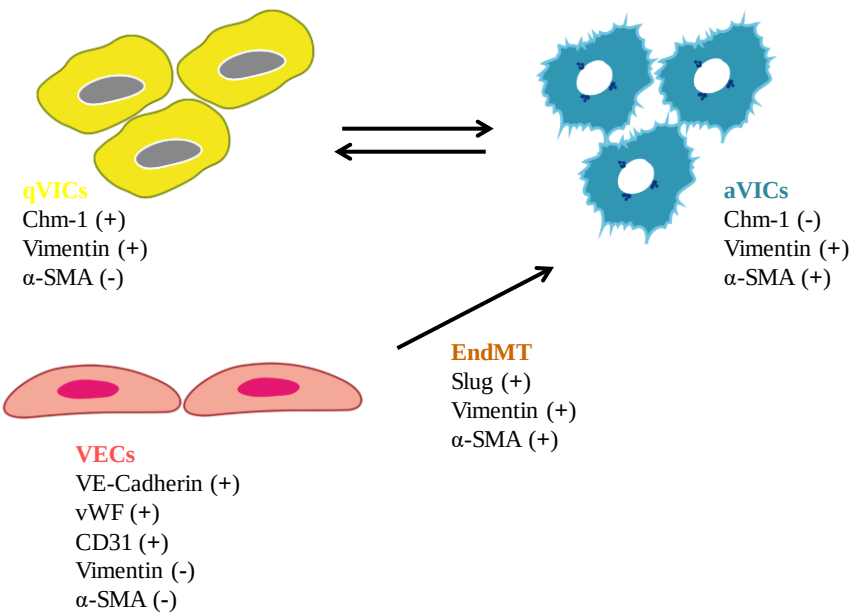

Figure 6. Principal markers of mitral valve cells. qVICs are positive for Chondromodulin 1 (Chm-1) and vimentin. aVICs are positive for vimentin and α-

smooth muscle actin (α-SMA) and VECs are positive for VE-Cadherin, von willebrand factor (vWF) and Cluster of differentiation 31 (CD31).

2.3 Molecular anatomy

Mitral valve leaflets are formed by four distinct histological layers: atrialis, spongiosa, fibrosa and ventricularis. Each layer is composed by different thickness, characteristic cells, ECM composition and biochemical properties [6].

The atrialis layer is composed by aligned collagen and elastin fibers covered with overlying VECs that give elasticity to the leaflet.

The spongiosa layer, located in the middle of the leaflet, is principally composed by free collagen and glycosaminglycans/proteoglycans. The spongiosa layer is the layer most affected under disease conditions. The high amount of glycosaminglycans/proteoglycans produce a high retention of water in the layer and aid to resist the compressive loading imposed by coaptation of the leaflet. Furthermore, spongiosa layer absorbs energy during compression, and facilities the arrangement of collagen fibers in the fibrosa and elastin in the ventricularis during the cardiac cycles.

The fibrosa layer, located under the spongiosa, is composed mainly by collagen fibers, which give the valve its tensile strength.

The ventricularis layer, located in the ventricle side, is constituted by a continuous sheet of endothelial cells. This composition conferred a densely packed and flexibly crimped or wavy [14].

The quantity, quality, and architecture of the ECM, particularly collagen, elastin, and glycosaminglycans/proteoglycans, in addition to the cells in the valve, are the major determinants of the long-term (lifetime) durability of the valve.

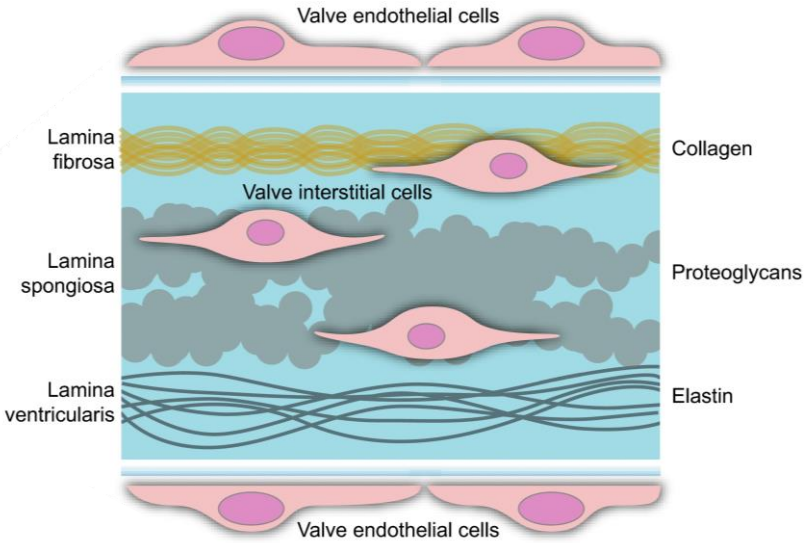

Figure 7. Schematic representation of mitral valve layers [20]. Mitral valve leaflets are formed by four layers: atrialis (not represented in the figure), spongiosa, fibrosa and ventricularis.

2.3.1 Extracellular matrix

The ECM is the fibroskeleton of the valve leaflet. The precise structure of the leaflet ECM, the relative and orientation of fibroskeleton and the contractile capacity contribute to the correct function of the valve.

The ECM presents a special microenvironment with a high regulation between cells and ECM components. VICs are the principal cells that synthetize the ECM components (collagen, elastin, proteoglycans, fibronectin…) and enzymes (MMPs and TIMPs). In healthy mitral valves, there is a low regulation and activity, due to the low activation of qVICs. In disease conditions, the imbalance between VICs phenotypes, due to the proliferation of aVICS, induces a high activity of the ECM through the expression of ECM components and MMPs. These components are divided on the three layers of the mitral valve and are presented in different quantities [21,22]. ECM proteins directly interact with cell surface receptors and start the intracellular signaling contributing to the ECM remodeling [11].

Collagen content in the mitral valve represents 60%, elastin 10% and proteoglycans 30%. This percentage is altered in mitral valve disease. Changes in the ECM composition or distribution are the final common pathway in all mitral valve diseases [11,16,22–26].

2.3.1.1 Collagen

Collagen type I, II and III appear as a crimp interweaving bundles of numerous fibers in the three layers. However, collagen is most common in the atrial and ventricularis layers. In a normal valve, collagen type I represents 74% of the amount of collagen, collagen type III 24% and collagen type II 2%. Collagens are the most abundant ECM component of the mitral valve and confer elasticity, tensile straight and support for the mitral valve cells. Collagen type I fibers have a substantial tensile strength. Collagen type III fibers possess a resilience that is important for maintain an integral structure and distensibility. Synthesis of fibrillar collagen is an essential mechanism for maintaining the valve's mechanical integrity. This complex process originates within VICs and it is completed in the valve ECM. Constant turnover of collagen allows the valve to adapt to regional changes in tensile strength [27–30].

2.3.1.2 Proteoglycans

Proteoglycans are mainly found in the spongiosa layer of the valve where they play a vital role in maintaining normal valve function.

Glycosaminoglycans (GAGs) are composed of long and unbranched chains of repeating disaccharides, which consist of a hexosamine and either, depending on the GAG type, uronic acid or galactose. There exist the following families of GAGs with each group being defined by its

composition: hyaluronan, heparin, heparan sulfate (HS), chondroitin sulfate (CS), dermatan sulfate (DS), and keratan sulfate (KS). Proteoglycans consist of at least one GAG chain attached to a core protein. Proteoglycans provide special properties such as viscoelasticity, hydration, swelling pressure, support compressional forces and resistance to tension. Moreover, proteoglycans also play crucial roles in VICs differentiation [31–34].

Figure 8 summarizes proteoglycans classification proposed by Iozzo and coworkers [34]. This classification attended to three aspects: cellular and subcellular location, overall gene/protein homology and the presence of specific protein nodules within their respective protein cores. Proteoglycans can be divided in five groups, attending to the localization: intracellular, cell surface, pericellular and extracellular [31–34].

Of interest, some of the proteoglycans have been found to be involved in mitral valve pathophysiology:

Syndecan, is included in the transmembrane group, and can interact with a lot of extracellular proteins like MMPs and growth factors, mediating important biological functions. Aggrecan has the property to aggregate with hyaluronan acid. Versican colocalizes with elastic fibers and it is involved in several processes, such as the regulation of cell adhesion, migration and inflammation. Like aggrecan, versican can bind to hyaluronan. Decorin can bind to collagen. In this way, decorin plays an important role in collagen fibrillogenesis and structure. Besides, some studies have demonstrated other

roles of decorin in the modulation of the Wnt (Wingless-type MMTV integration site family member) signaling pathway and in the cellular growth control. Biglycan is very similar to decorin. It is involved in the osteoblast differentiation and presents angiogenic effects. Lumican is involved in inflammation, and could be a target of MMPs [31–34].

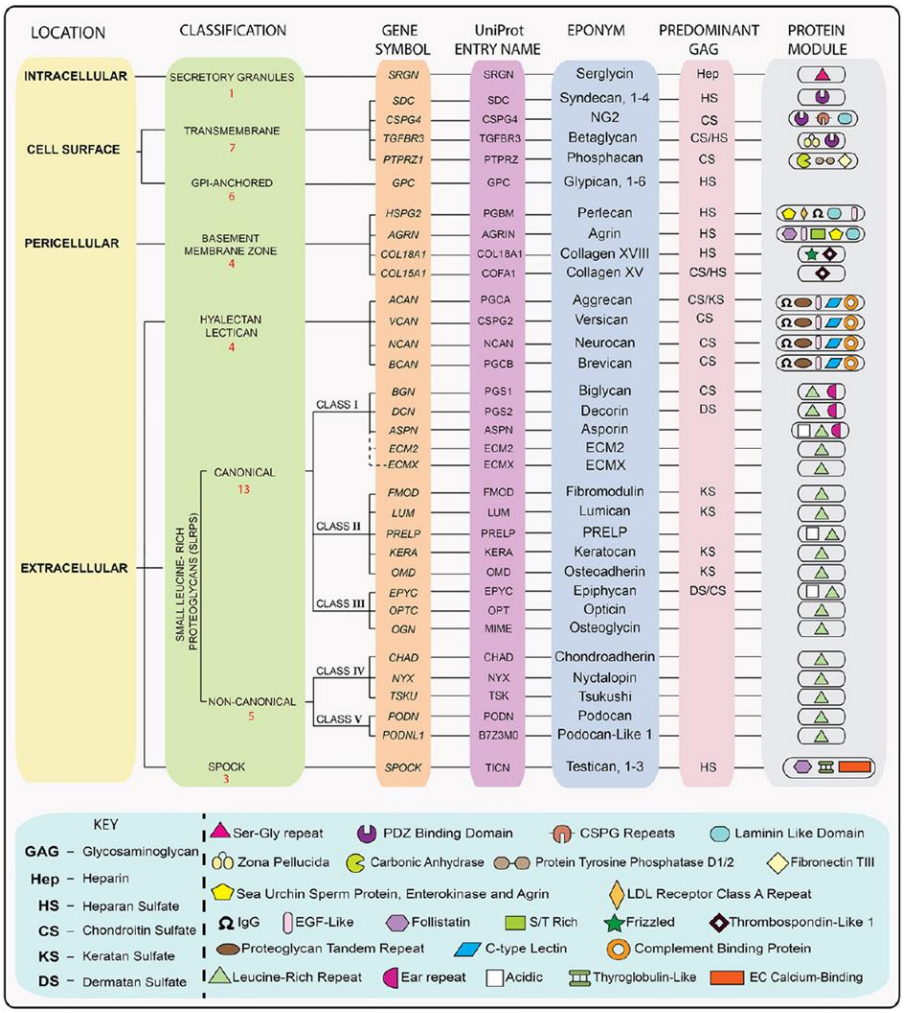

Figure 8. Proteoglycans classification [34]. Classification proposed by Iozzo and coworkers attending to the cellular localization.

2.3.1.3 Fibronectin

Fibronectin is a dimer glycoprotein. Fibronectin in mitral valves principally appears around the endothelial cells. Fibronectin acts binding to integrins, proteoglycans, collagen and other components of the ECM, mediating the

interaction between cells and the ECM proteins. Although fibronectin is not a major ECM component in heart valves, VICs secrete fibronectin in response to valve damage, providing a mean for cell migration [35,36].

2.3.1.4 Elastin

Elastin appears as discrete fibers forming an interlacing structure. The function of elastin is to confer tissue elasticity and it is the principal ECM component to allowing the leaflet opening and closing. It is present in the three layers [14].

2.3.1.5 Matrix metalloproteinases

The ECM turnover or remodeling is a controlled and coordinated process in the mitral valve. This turnover is characterized by a regulation between the synthesis and degradation of the ECM components. The ECM degradation is produced by the extracellular matrix enzymes, where the MMPs are the most common enzymes. MMPs includes the collagenases, gelatinases, stromelysins, metalloelastases and membrane-type MMPs. The majority of pro-MMPs are accumulated in extracellular bound to different ECM components. These pro-MMPs can be rapidly activated and mobilized under any stimulation. The activation of pro-MMPs needs a high regulation to avoid an exacerbated activity of MMPs. The TIMPs bind to activated MMPs

(1:1) and block the MMPs activity rapidly [24,37]. In the mitral valve, MMPs regulation is mediated by VICs.

3. Mitral valve disease

The term heart valve disease refers to an abnormality in the function of the valve. There are two types of valve dysfunction: stenosis, when the opening of the valve is limited and the antegrade flow is hampered, and insufficiency (also termed regurgitation), when there is not a complete coaptation of the leaflets of the valve that causes a backward flow or leak into the preceding chamber. Sometimes both types of valve dysfunction can be present. The physiological consequences and clinical manifestations of the valvulopathy depend on the valve diseased, the type of dysfunction (stenosis or insufficiency) and the degree of the disease. Ultimately, valvular heart disease is one of the main causes of heart failure (HF) and an important cause of cardiovascular mortality. The most prevalent and clinically relevant types of valvular heart disease are those affecting left sided valves, i.e. aortic and mitral valve disease. Among them, the most common in developed countries are aortic stenosis and mitral regurgitation.

Mitral valve has a complex anatomy and the development of mitral valve disease occurs when one of the different parts of the valve is altered: the valve leaflets, the annulus, the tendinous chordae, the papillary muscles or the left ventricle. Mitral valve disease is related with some etiological

factors: myxomatous degeneration, rheumatic disease, calcific degeneration, inflammatory disease or infectious. These etiological factors can affect different structures of the mitral valve, although the different etiologies have common features of changes to the structure, distribution, interaction and function of the ECM components [38]. The changes in the structure including leaflet changes could be prolapse, retraction, calcification, rupture of tendinous chordae, elongation, shortening, annular dilation and papillary muscle dysfunction. The molecular changes affect cell phenotype and function, the extracellular matrix composition and the organization and regional deposition of inflammatory molecules [11].

3.1 Etiology

Mitral valve disease occurs when there is a structural alteration in one of the anatomical parts of the valve, the majority of them affecting the leaflets. Mitral valve disease can be congenital or acquired. Congenital disease is an abnormality that develops before birth, in which valves may be the wrong size, have malformed leaflets or have leaflets that are not attached to the annulus correctly. Acquired disease are the valves disease that develop within the valve over time.

Mitral valve stenosis is predominantly caused by rheumatic fever, although in older patient extensive mitral annular calcification may also cause restricted mitral valve opening.

Mitral regurgitation can be caused by a wide variety of diseases, including mitral valve prolapse, rheumatic heart disease, infective endocarditis, systemic inflammatory disorders, annular calcification, cardiomyopathy and ischemic heart disease [39–42].

3.2 Epidemiology

Heart valve disease, in particular, mitral valve disease is considered a serious global health problem. It has been estimated that around 2,5% of population have some degree of heart valve disease. It is important to acknowledge that one of the principal causes to develop heart valve disease is aging. Currently, there is a high increment of the aging population in the word. For example in Spain, around 26% of the population has more than 65 years. With this progressive aging of the population, the incidence of valve disease is predicted to increase significantly with the increase in the elderly population in the developed world [39–42].

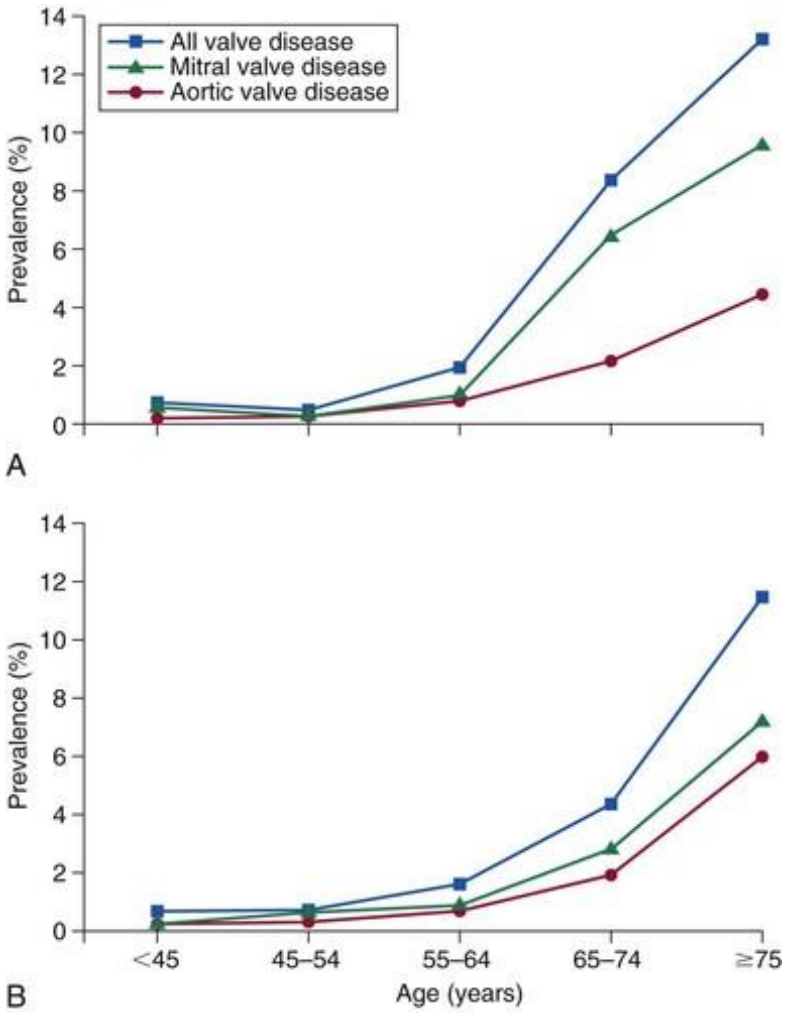

Figure 9. The rising prevalence of valvular heart disease with age [43]. Mitral valve disease is the most prevalent.

3.3 Natural history, symptoms and diagnosis.

In the context of mitral valve disease, the natural history is highly variable, principally due to the different etiologies in the development of mitral valve disease. In chronic primary mitral regurgitation, the asymptomatic period

can last for many years. Among patients with severe mitral regurgitation resulting from flail leaflets, an annual mortality rate of 3% has been reported [44]. Chronic secondary mitral regurgitation is a common consequence of ischemic and nonischemic cardiomyopathy, a condition associated with poor prognosis. In this context, is the cardiomyopathy which determines the clinical course and not the mitral regurgitation *per se*, although is debated whether mitral regurgitation, once established, contributes to progression of left ventricular dysfunction and plays a causative role in the observed worse outcomes in this subgroup of patients.

For the diagnosis of mitral valve diseases, firstly an auscultation is realized to detect any cardiac murmur. If any abnormal murmur is presented, echocardiography should be performed to determine which valve is affected, the mechanism (stenosis or regurgitation), the ventricular function and the etiology. Sometimes, another complementary test is necessary in order to confirm and complete the diagnosis. In these cases, cardiac magnetic resonance, cardiac computed tomography angiography and cardiac catheterization are performed [45].

3.4 Treatment

Currently, no pharmacological treatment has shown to prevent the development or the progression of mitral valve disease. According to current clinical guidelines [45], medical treatment is reserved to palliate the symptoms

caused by the mitral valve disease, such as diuretics for congestion or fluid retention or drugs to slow the heart rate if arrhythmia occurs [45,46].

Medication Category	Goal of Therapy
ACE inhibitors	Reduce blood pressure and slow progression of heart failure
Antiarrhythmics	Restore normal rhythm
Antibiotics	Prevent infections
Anticoagulants	Reduce risk of thromboembolism, which can lead to stroke
Beta-blockers	Reduce cardiac workload via reduction in heart rate; reduce palpitations
Diuretics	Reduce edema and cardiac workload
Vasodilators	Reduce cardiac workload; reduce valvular leakage

Figure 10. Medications for symptoms of valvular heart disease [46]. Principal drugs administrated to mitral valve prolapse patients.

The current management is to follow up the patients until symptoms appears or serial image testing shows an impact on cardiac structure and function; in any of these two situations an mechanical procedure on the valve is indicated. The standard treatment is a surgical intervention, performing replacement of the diseased valve with a prosthetic heart valve or valve repair if anatomically feasible. There are two types of prosthetic valves: mechanical valves or biological valves. Mechanical heart valves are made of synthetic materials (polymers, metals or carbon), whereas bioprosthetic heart valves are made of biologic tissues derived from porcine or calf.

Figure 11. Example of mechanical heart valves and bioprosthetic heart valve. (Myheart.net)

However, nowadays catheter-based interventions are increasingly used in cases with high surgical risk, such as percutaneous mitral valve edge-to-edge repair with Mitraclip® device.

3.5 Mitral valve disease classification

Attending to the European society of cardiology guidelines [45] and American Society of Echocardiography [47], we can divide the mitral valve disease in 5 different etiologies.

3.5.1 Rheumatic mitral valve disease

Rheumatic mitral valve disease is developed as a consequence of late immune reaction to bacterial infection with A, β- hemolytic streptococcus bacteria. It can be associated with stenosis or regurgitation. Structurally, it is characterized by thickened, fibrotic leaflets with partial fusion of the commissures. At molecular level, rheumatic mitral valve disease is

characterized by a high degree of inflammation, and also with a high infiltration of inflammatory cells. Inflammation is a consequence of the humoral and cellular immune response against bacterial infection. Besides, high levels of neovascularization within the leaflets have been described [48].

3.5.2 Calcific degenerative mitral valve disease

The calcific degenerative mitral valve disease principally is associated with age. As a consequence aging, the mitral valve starts some process characterized by accumulation of calcium phosphate complexes in the leaflets. These processes are mediated by several mechanisms. In first place, high differentiation of VEC and therefore high activation of qVICs induce a high ECM remodeling. Secondly, this kind of mitral valvulopathy is characterized by calcium deposition. The expression of calcium is produced by a new subpopulation of VICs. The aVICs, in degenerative mitral valve, can be differentiated to a new phenotype similar to osteoblast, called osteablastic VIC (obVIC). This phenotype is characterized by the high expression of calcification markers. Calcium deposits cause an increment of tightening and thickness. The valve becomes rigid, losses the flexibility and the annular geometry [49].

3.5.3 Functional mitral valve disease

Functional or secondary mitral valve disease is a special kind of mitral valve disease, where the disease occurs in the left ventricle or the annulus but not in the mitral leaflets *per se*. In functional or secondary mitral valve disease the left ventricle is dilated or distorted and in consequence the papillary muscles are displaced. This deviation of papillary muscle that support the mitral valve leaflets induce a stretching of the mitral valve annulus, and as result alter the closing of the valve. The valve leaflets can no longer come together to close the annulus and blood flows back into the atrium [50–52].

3.5.4 Inflammatory mitral valve disease

The inflammatory mitral valve disease occurs as an immune response induced by any bacterial infection (endocarditis) or autoimmune disease. Endocarditis principally is caused by *Staphylococcus aureus* and *Streptococcus viridans*. The principal autoimmune diseases that induce inflammatory mitral valve disease are systemic lupus erythematosous and rheumatoid arthritis. These infections and diseases are characterized by antibody-initiated damaged and activation of the endothelium, followed an increment of inflammatory cells and mediators infiltration. This kind of mitral valve disease presents a similar physiopathology to rheumatic mitral valve disease, but the difference is that rheumatic mitral valve disease

induces mitral valve damage years later to the infection and endocarditis induces destruction and inflammatory reaction directly [53–55].

3.5.5 Mitral valve prolapse

The mitral valve prolapse is the object of this thesis, for this reason, this valvulopathy is explained more in detail.

4. Mitral valve prolapse

MVP is estimated to affect 2-3% of the general population and over 176 million individuals worldwide [56–58] and it is the most common cause for mitral valve surgery.

MVP is a spectrum of disease ranging from a focal abnormality of a mitral leaflet to diffuse involvement of both leaflets. Using echocardiography, MVP is defined as systolic displacement of the mitral leaflet into the left atrium of at least 2 millimeters from the mitral annular plane, measured in the parasternal long-axis window. MVP is defined by a leaflet protrusion to left atrium in each beat. As a consequence, there is not a perfect closing and a retrograde blood flow occurs. This happens because the leaflets are elongated, thickened, there are a partial or total interchordal ballooning and the annulus is enlarged, as a result of the molecular changes in the leaflet [59]. This causes mitral regurgitation, which may progress and cause HF [47,60,61].

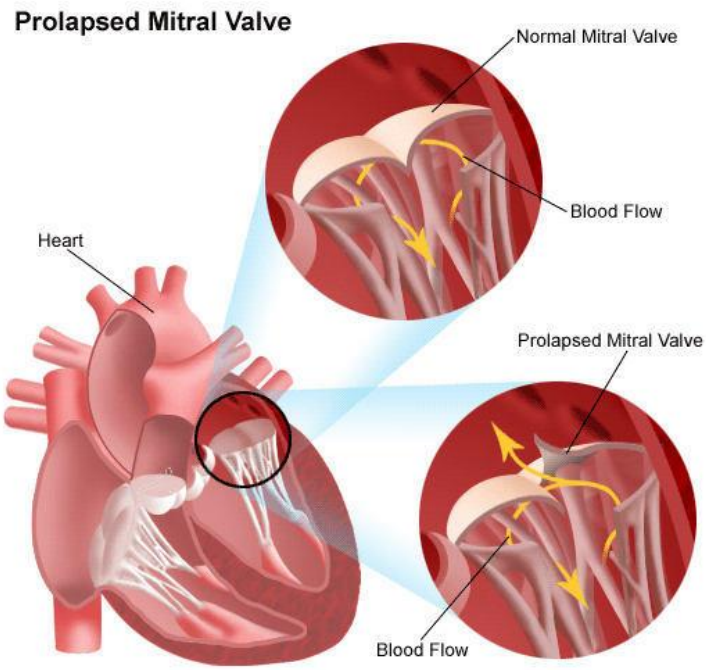

Figure 12. Schematic representation of mitral valve prolapse disease. (Heart valve surgery web).

4.1 Classification

The classification of MVP is very diffuse and few characterized. The literature classifies the MVP in three groups: myxomatous or Barlow's disease, fibroelastic deficiency and genetic syndromes. Fibroelastic deficiency refers to focal segmental pathology with thin leaflets, while Barlow's disease refers to diffuse thickening and redundancy, typically affecting multiple segments of both leaflets and chordae. Traditionally, fibroelastic deficiency was defined as an early stage of Barlow disease.

Fibroelastic deficiency is characterized by a high presence of elastin in the leaflet and a high expression of collagen and elastin in the tendinous cords. In these conditions, there is a high prevalence to tendinous cords rupture. However, in Barlow disease, collagen and proteoglycans increment and elastin fragmentation is characteristic. In Barlow disease it is not common to observe changes in tendinous cords [62]. The genetic syndromes include the Marfan syndrome and Loeys-Dietz syndrome. Marfan syndrome is characterized by a specific mutation in the Fibrilin 1 gene. The Loeys-Dietz syndrome is characterized by a mutation in the TGF-β receptor gene. In both cases, as a result of a mutation there is an up-regulation and a high activation of the TGF-β signaling, that induces VECs differentiation and VICs activation [60].

4.2. Molecular changes

At cellular level, MVP is characterized by two up-regulated phenomenons; VECs monolayer presents an aberrant activation, and differentiation to activated VIC phenotype through the EndMT. The pattern of gene expression changes; there is a down-regulation in the expression of endothelial genes markers and an up-regulation of the aVIC makers. The endothelial cells swollen, loss the cell contact and start to migrate inside the other leaflet layer. This mechanism is highly regulated, by the control of expression of genes involved in the activation of EndMT. The majority of studies focus on TGF-β like the principal inductor of VICs activation. As a

consequence of the high VECs differentiation, the mitral valve presents a high number of activated VICs [63–67].

Otherwise, in MVP there is a high activation of quiescent VICs due to the high mobilization of qVIC niche. As a consequence, there is a high proliferation and activation of qVICs to aVICs. This high proliferation of aVICs through the three layers of the mitral valve implicate a loss of the valvular homeostasis [7,64,65,68].

Shifting to the aVIC phenotype is a key component in mediating the synthesis of proteoglycans, MMPs, inflammatory cytokines, and other extracellular components in the leaflet [14,64,65], which reduce the structural integrity [6,14,16,69].

The most characteristic of MVP is the increment of the spongiosa layer due to the high increment of proteoglycans synthesis by aVICs. Hyaluronan, biglycan, decorin and versican are the principal and most abundant proteoglycans synthesized. The high accumulation of proteoglycans is diffuse and poorly organized [14,16,70].

Apart from proteoglycans, aVIC in MVP induce an anomalous expression of MMPs. Therefore, there is a high leaflet remodeling through the ECM components degradation. In this way, in MVP there is an extensive disorganization of the collagen fibers in the leaflet, thus compromising the structural integrity of the valve. It is important to consider that the aVICs are dispersed in the three layers; for this reason, the alteration of the ECM

components and the ECM remodeling induce disorganization in all the layers resulting in the loss of the layer pattern [14]. Some studies have revealed the high expression of versican, decorin or biglycan in MVP, where co-localized with elastic and collagen fibers. This contributes to the collagen fibrillogenesis and elastic fiber genesis. Collagen fragmentation has been shown during myxomatous remodeling and the link between proteoglycans and the ECM fibrous proteins may explain the compensatory mechanism during myxomatous valve remodeling and it is responsible for the floppy valves [14,47,60,61]. These numerous matrix changes suggest that there may not be a single primary cause of myxomatous degeneration, although more studies are needed to clarify this issue [31,33,71].

4.3 Animal models of MVP

Mouse, rat, sheep, pig and dog are the principal animal models used to study MVP, as summarized in table 1.

In all animals models, MVP and left ventricle dilatation were confirmed by echocardiography or by histological analyses.

To perform our studies, we have selected the Serotonin dependent model. For this reason, this model is expanded with more detail in the next section.

Mitral valve disease	Model	Procedure/Method	Molecular/structural alterations	Reference
Marfan syndrome	Transgenic Mouse	Knock Out (KO) for Fibrilin 1	Connective tissue disease	Ng *et al.* (2004) Judge *et al.* (2004)
Mitral regurgitation	Surgery: Sprague-Dawley Rats	Hole on the mitral leaflet	Left ventricle remodeling	Kim *et al.* (2012)
MVP	Transgenic Mouse	Constitutively cardiac-specific expression of MMP-2	Mitral valves and chordae tendinous exhibit severe myxomatous changes	Mahimkar *et al.* (2009)
MVP	Yorkshire Pigs	Cardiopulmonary bypass and cutting chordae supporting the P2 segment of the posterior leaflet	Median Mitral Regurgitation grade increased from trivial to moderate-severe	Feins *et al.* (2014)
MVP-*Pseudoxanthoma elasticum*	Transgenic Mouse	Abcc6-Deficient:	Mineralization and fragmentation of elastic fibers in connective tissue	Prunier *et al.* (2013)
MVP	Sheep	Cardiopulmonary bypass and papillary muscle retraction with apical myocardial infarction created by coronary ligation	Increment of total diastolic leaflet area	Dal-Bianco *et al.* (2009)
MVP	Beagle Dogs	Spontaneously	Echocardiography mitral valve disease parameters	Suzuki *et al.* (2013) Häggström *et al.* (2013)
MVP	Pharmacologically treated Mouse	Activation Serotonin pathway by Nordexfenfluramine treatment (28 days)	aVICs proliferation and PGs expression	Ayme-Dietrich *et al.* (2017)

Table 1. Principal mitral valve disease models used on other studies.

4.3.1 Serotonin (5-HT) pathway as a inductor to develop MVP

Serotonin or 5-hydroxytryptamine (5-HT) is a monoamine neurotransmitter. It has a popular image as a contributor to feelings of well-being and happiness, though its actual biological function is complex and multifaceted, modulating cognition, reward, learning, memory, and numerous physiological processes [72]. Serotonin pathway has been also demonstrated to be involved in the development of MVP. Serotonin signaling is characterized by the activation of 5-HT receptors (2a/2b). The receptors transmit the intracellular signal and activate the Erk1/2 (Extracellular signal-regulated kinase 1/2) signaling. Classically, Erk1/2 signaling is involved in cellular proliferation, phenotype transformation and ECM remodeling. Currently some commercial drugs are prescribe in cases of depression; Ergot derivatives (ergotamine (Gynergene®), methysergide and dihydroergotamine), dopamine agonists (pergolide (Celance®)) and cabergoline (Dostinex®), amphetamine derivatives (fenfluramine (Ponderal®), dexfenfluramine and MDMA (Ecstasy®)) and Obesity drugs (anorexigens). All these drugs have been shown to strongly stimulate 5HT2BR in valvular cells [73]. 5-HT2R could increase VICs proliferation through activation protein C Kinase, Scr-protein, p-Erk 1/2, TGF-β R activation. For this reason, some MVP animal models are based in the up-regulation of 5-HT receptors, by the administration of the drugs. However, the precise mechanism is not well known [73–79].

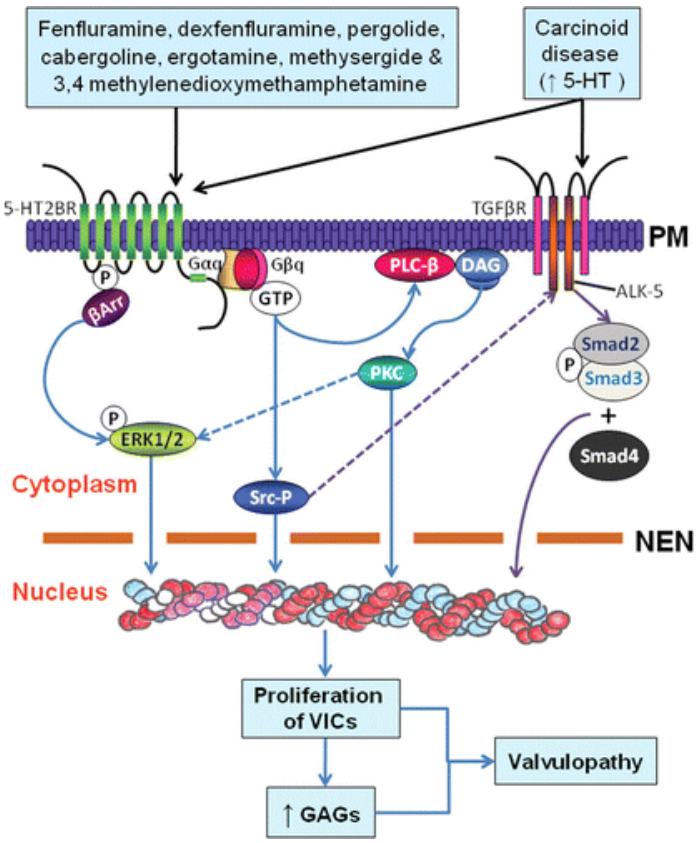

Figure 13. Intracellular mechanism of MVP development through the serotonin pathway [80]. Several drugs induce the 5HT2BR activation. VICs (Valvular interstitial cells); GAGs: Glycosaminoglycans; 5-HT: 5-hidroxitriptamina.

5. Aldosterone and mineralocorticoid receptor

The adrenal gland cortex synthetizes three different groups of corticoids hormones:

- Glucocorticoids (Cortisol and corticosterone). These hormones are involved in the regulation of carbohydrate metabolism, acting via glucocorticoid receptor.
- Adrenal androgens: sex hormones mainly dehydroepiandrosterone (DHEA) and testosterone. They play a role in the early development of the male sex organs in childhood, and female body hair during puberty.
- Mineralocorticoid (Aldosterone (Aldo)). Aldo is a steroid hormone implicated in the regulation of sodium homeostasis, volume regulation, and thus, systemic blood pressure [81–83].

In mammals, Aldo biosynthesis occurs almost solely in the adrenal zona glomerulosa. Aldo is synthetized through a series of enzymatic steps that involve three cytochrome P450 enzymes and one hydroxysteroid dehydrogenase (Figure 14). The enzymes cholesterol side-chain cleavage (CYP11A1), 21-hydroxylase (CYP21) and aldosterone synthase (CYP11B2) belong to the cytochrome P450 family of enzymes. CYP11A1 and CYP11B2 are localized to the inner mitochondrial membrane, while CYP21 is found in the endoplasmic reticulum. Cytochrome P450 enzymes are heme-containing proteins that accept electrons from NADPH via accessory proteins and utilize molecular oxygen to perform hydroxylations (CYP21 and CYP11B2) or other oxidative conversions (CYP11A1). The fourth enzyme, type 2 3β-hydroxysteroid dehydrogenase (HSD3B2), is a member of the short-chain dehydrogenase family and is localized in the endoplasmic reticulum. Aldo

and cortisol share the first few enzymatic reactions in their biosynthetic pathways (cholesterol to progesterone); however, adrenal zone-specific expression of CYP11B2 (aldosterone synthase) in the glomerulosa and that of CYP11B1 (11β-hydroxylase) in the fasciculata leads to the functional zonation observed in the adrenal cortex [81–84].

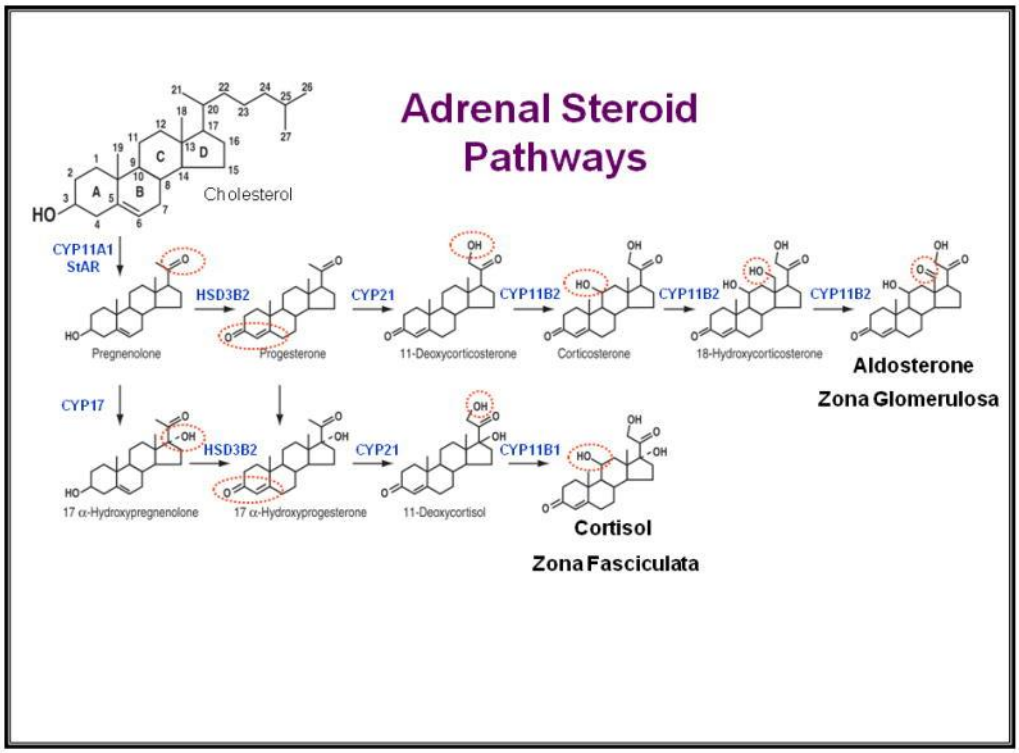

Figure 14. Principal enzymes implicated in the synthesis of mineralocorticoids and glucocorticoids [84].

Aldo is an essential hormone implicated in the regulation of electrolyte and fluid balance and subsequent blood-pressure homoeostasis. Aldo synthesis is

regulated by the renin-angiotensin system and potassium ions and it exert the effects by the union with mineralocorticoid receptor (MR), that it is the principal agonist [84–86].

Corticosteroid hormones such as Aldo and corticosterone are synthesized by specific enzymes in the adrenal cortex but now there is strong evidence that these enzymes are also present in other tissues [87]. Although these extra-adrenal sites are not capable of corticosteroid production on the same scale as the adrenal cortex, due to a much lower level of relevant gene expression, their proximity to glucocorticoid receptors (GR) and MR is consistent with a paracrine/autocrine mode of steroid hormone action.

MR is a cytosolic steroid receptor, member of the nuclear receptor family and acts as a ligand-dependent transcription factor [88]. The MR is not a specific receptor of Aldo, because Aldo and cortisol bind to human MR with equal affinity. However, Aldo-responsive tissues also express the cortisol-inactivating enzyme 11β-HSD2, which confers Aldo specificity to MR [89–91].

5.1 Aldosterone/MR in cardiovascular disease

Aldo binds to the MR which works as a transcription factor of the nuclear receptor family present in the kidney and also in various other non-epithelial cells including the heart and the vasculature [92]. Indeed, new extra-renal pathophysiological effects of this hormone have been characterized, extending its actions to the cardiovascular system [93]. Consequently, MR

hyperactivation can be either responsible or a factor in the onset and progression of several cardiovascular diseases, including metabolic syndrome, hypertension, coronary artery disease, and congestive HF [94]. During the development of HF, changes in cardiac geometry and gene expression/regulation do occur. A growing body of clinical and pre-clinical evidence suggests that Aldo and MR play an important pathophysiological role in cardiovascular remodeling by promoting changes involving cardiac hypertrophy, fibrosis, arterial stiffness, as well as in inflammation and oxidative stress [95–98]. Some studies have demonstrated that Aldo could be an inductor of cardiac fibrosis. Thus, in animal models, Aldo treatment increase cardiac hypertrophy and fibrosis [88,98–100]. Moreover, Aldo induces inflammation in heart; in mice treated with Aldo and salt, there is a mobilization of macrophages, lymphocytes and an increase in proliferation of endothelial, vascular smooth muscle cells and fibroblasts. As a consequence, there is a high expression of several inflammatory factors and adhesion molecules. One of the principal causes of the infiltration of inflammatory cells is the endothelial dysfunction induced by Aldo [88,99].

Evidence from the RALES and the EPHESUS studies in patients with HF (with or without previous myocardial infarction) showed that chronic MR blockade reduces blood collagen peptides, suggesting the contribution of anti-fibrotic effects to the clinical benefits associated with the use of MR antagonists (MRAs). Moreover, results of the recently completed REMINDER (Impact Of Eplerenone On cardiovascular Outcomes In

Patients Post Myocardial Infarction); (clinical trial number NCT01176968) trial and TOPCAT (NCT00094302) trial suggest that MR blockade might be clinically beneficial respectively for acute myocardial infarction healing and progression of HF with preserved ejection fraction. The ongoing ALCHEMIST (NCT01848639) trials are currently exploring the benefit of Spironolactone in acute myocardial infarction and in cardiovascular prevention in end stage renal disease [101–107]. Taken together published data indicate the potential contribution of Aldo and MR to cardiovascular remodeling. These findings reinforce the importance of MRA prescription by providing strong evidence of survival extension that can be used to explain patients why they should be on MRA treatment [103]. However, the precise mechanisms responsible for Aldo/MR-induced cardiac remodeling, fibrosis and dysfunction remain to be determined.

5.2 Aldosterone in mitral valve

The information regarding the role of Aldo in mitral valve physiology or pathology is scarce. Moreover, there is no studies that analyze Aldo effects in valvular cells. However, some indirect evidences suggest that Aldo could play a role in valvular remodeling.

Focusing on cellular experiments, some studies have shown the effects of Aldo and MRAs in cardiac fibroblasts and vascular smooth muscle cells (VSMCs) (phenotype similar to VICs) as well as in endothelial cells (ECs)

(phenotype similar to VECs). Studies in VSMCs and ECs from pulmonary artery show that Aldo, via MR hyperactivation, could potentiate the hypertrophic effects of Angiotensin II (Ang II) [108]. VSMCs from rats treated with MRAs showed a reduction of vascular remodeling associated with the abnormal VSMCs migration [109,110]. In human cardiac fibroblasts, it has been demonstrated that Aldo induces fibroblast activation and collagen production promoting cardiac fibrosis [96–98,111,112]. Interestingly, in HUVECs treated with TGF-β, Chen et al observed that Spironolactone blocks EndMT induced by TGF-β [113]. Moreover, *in vivo*, in Aldo/salt-treated rats, ECs present a proinflammatory and fibrogenic phenotype and Spironolactone attenuates this response [114]. Gravez et al observed that Aldo induces cardiac ECs proliferation *in vivo* [115]. Furthermore, some studies observed that the use of MRAs in models of ischemic HF and chronic Ang II infusion improve endothelial dysfunction and vascular remodeling [116–120].

Focusing on mitral valve disease animal models, most of the studies showed the implication of the renin-angiotensin-Aldo system in the context of HF associated with mitral valve disease. In dog models of mitral valve disease, circulating Aldo levels have been found to be increased as compared to controls [121–124]. It has been demonstrated that treatment with Spironolactone reduced cardiac remodeling in a dog model with myxomatous mitral valve disease [125]. Moreover, the safety of the Spironolactone treatment has been also analyzed in dogs presenting chronic HF because of degenerative valvular disease [126]. In a myocardial infarction sheep model, where the mitral

valve was fibrotic, treatment with Losartan (antagonist of the type I angiotensin II receptor) decreased TGF-β expression [127].

In humans, Aldo circulating levels have been found to be increased in early phases of mitral valve regurgitation as compared with healthy patients [128,129]. Moreover, Yongjun et al demonstrated that local and circulating renin-angiotensin-Aldo system activation exist simultaneously in atrial fibrillation associated with mitral valvular disease. Besides, the levels of local and circulating Ang II and Aldo are different depending to the etiology of the mitral valve disease. The authors explain that the pathophysiological changes in different types of mitral valve disease causes different changes on the left atrial pressure and volume load, which release different pathophysiological substrates potentially causing different expression of local and circulating renin-angiotensin-aldosterone system [130].

Nevertheless, there are no studies aiming at analyzing the possible role of Aldo in the development of mitral valve disease. Importantly, there are no studies demonstrating that MR is expressed in mitral valve cells.

Model system used	Summary of the study	Reference
Human mitral regurgitation patients	Aldo levels were elevated in mitral regurgitation patients as compared with healthy subjects	Leszek *et al.* (2010)
Human mitral valve disease patients	Aldo levels were increased in mitral stenosis patients as compared with mitral regurgitation patients	Hayashi *et al.* (2004)
Dog with myxomatous mitral valve disease	Aldo concentrations were not associated to histological changes in the myocardium	Falk *et al.* (2013)
Dog with Mitral valve insufficiency	Aldo concentration was significantly higher in MVD as compared to controls	Pedersen *et al.* (1995)
Dog with Mitral valve regurgitation	Aldo concentration was similat in MR as compared to controls	Kanno *et al.* (2006)
Dog with Myxomatous mitral valve disease	Dogs with cardiac disease treated with spironolactone, in addition to conventional therapy, are not at higher risk for adverse events than those receiving solely conventional therapy.	Lefebvre et al (2013)
Dog with Mitral valve regurgitation	Aldo was not elevated after the administration of carperitide (human recombinant natriuretic peptide) but it was elevated after furosemide (diuretic) treatment	Suzuki *et al.* (2013)
Dog Myxomatous mitral valve disease	Spironolactone had significant beneficial effect on fibrosis. Eplerenone treatment decrease significantly the volume fraction of reactive interstitial fibrosis	Bernay *et al.* (2010)

Table 2. Aldosterone in mitral valve diseases. A systematic review of the literature

HYPOTHESIS AND OBJECTIVES

1. Hypothesis

Our primary working hypothesis is that Aldo/MR pathway plays a role in the development of MVP by modulating VICs activation and VECs differentiation through the EndMT, leading to an increase in proteoglycans production.

Furthermore, Aldo/MR pathway could be a new biotarget in MVP and its blockade with a MRA could prevent mitral valve alterations associated with this pathophysiological condition. To test this hypothesis, human mitral valve samples, human VICs and VECs, and dedicated animal models of MVP in which MR expression has been specifically inactivated were used.

2. Objectives

1. Demonstrate the expression of MR and Aldo synthesis in the mitral valve.
2. Study the effects of Aldo in VICs isolated from human MVP patients:
    a. On VICs activation markers
    b. On proteoglycans expression and secretion
3. Study the effects of Aldo in VECs isolated from human MVP patients:
    a. On VECs differentiation markers to aVICs
    b. On proteoglycans expression and secretion
4. Analyze the effects of MRA treatment in a mice model of MVP:
    a. On mitral valve size
    b. On mitral valve composition
5. Study the consequences of specific deletion of MR in α-SMA cells in a MVP mice model:
    a. On mitral valve size
    b. On mitral valve composition
6. Study the consequences of specific deletion of MR in VE-Cadherin cells in a MVP mice model:
    a. On mitral valve size

b. On mitral valve composition

7. Examine the differences in human MVP patients treated with MRA versus human MVP patients without MRA treatment:

   a. On the expression of VECs differentiation markers to aVICs
   b. On proteoglycans expression
   c. On mitral valve composition

MATERIAL AND METHODS

I. CLINICAL STUDY

1. Patient population

This prospective, observational study included a total of 105 patients with severe mitral regurgitation due to MVP, referred to our center for mitral valve replacement from June 2015 to November 2018. MVP was defined by transthoracic echocardiography if there was systolic displacement of the mitral leaflet into the left atrium at least 2 mm from the mitral annular plane in the parasternal long axis window, following current guidelines [59]. Exclusion criteria were other etiologies of mitral valve disease other than myxomatous degeneration, such as rheumatic, senile degenerative, infectious, ischemic. All patients were evaluated by transthoracic echocardiography and in 63% transesophageal echocardiography was performed, based on clinician's criterion. Informed consent was obtained from each patient and control and the study protocol conforms to the ethical guidelines of the 1975 Declaration of Helsinki as reflected in a priori approval by the institution's human research committee (*Comité Ético de Investigaciones Clínica del Complejo Hospitalario de Navarra 2015/26*).

2. Mitral valve samples

Human mitral valves were obtained from mitral valve replacement surgery. The selected controls were similar to the cases with respect to age and sex. The valve samples were quickly sectioned in three pieces. One part was used

for VICs and VECs isolation; other part was fixed in formaldehyde and embedded in paraffin for histological analysis; and the third part was frozen in liquid nitrogen to perform molecular biology techniques (RT-PCR, Western Blot and ELISA). Cell isolation, histological and molecular biology techniques are detailed below.

II. CELL CULTURE STUDY

3. Cell isolation and culture

Human VICs and VECs were isolated from 7-9 human mitral valves obtained from mitral valve replacement surgery. Mitral valves were incubated with Collagenase type 2 (240 U/mg) (Worthington Biochemical Product) for 10 minutes four times for VECs isolation and for 1 hour for VICs isolation. For VECs isolation, supernatants were re-collected and centrifuge 5 minutes at 1100 rpm. VECs were grown on 2% gelatin-coated dishes in EBM-2 medium supplemented with GA1000, Hydrocortisone solution, Fetal Bovine Serum, Human Fibroblast Growth Factor basic (hFGFb), Human Vascular Endothelial Growth Factor (hVEGF), Analog of Human Insulin-Like Growth Factor-1, Long R3-IGF-1, Ascorbic Acid Solution and Human Epidermal (Lonza). For VICs, after 1 hour in Collagenase type 2 (240 U/mg), supernatant was centrifuged 5 minutes at 1100 rpm. VICs were cultured on DMEM F-12 (Gibco) medium supplemented with 10% FBS. All assays were performed at 37°C, 95%

sterile air and 5% CO_2 in a saturation humidified incubator. VECs were used between passages 3-4 and VICs between passages 3-6.

4. VICs and VECs phenotyping

VICs and VECs phenotype was routinely checked by immunocytochemistry and immunofluorescence as shown in the representative pictures below (Figure 15). Cells were cultured in Nunc™ Lab-Tek™ II Chamber Slide™ (Thermo Fisher) at 37°C, 95% sterile air, and 5% CO_2 in a saturation humidified incubator. After reached 50-60% of confluence, cells were washed three times for 5 minutes with Phosphate-buffered saline (PBS). Then, cells were fixed with formaline (Sigma Aldrich) for 20 minutes and washed three times for 5 minutes with PBS. After fixation, immunochemistry or immunofluorescence was performed. VICs were positive for alpha-smooth muscle actin (α-SMA) and vimentin and negative for CD31; VECs were positive for CD31 and VE-cadherin and negative for vimentin and α-SMA**.**

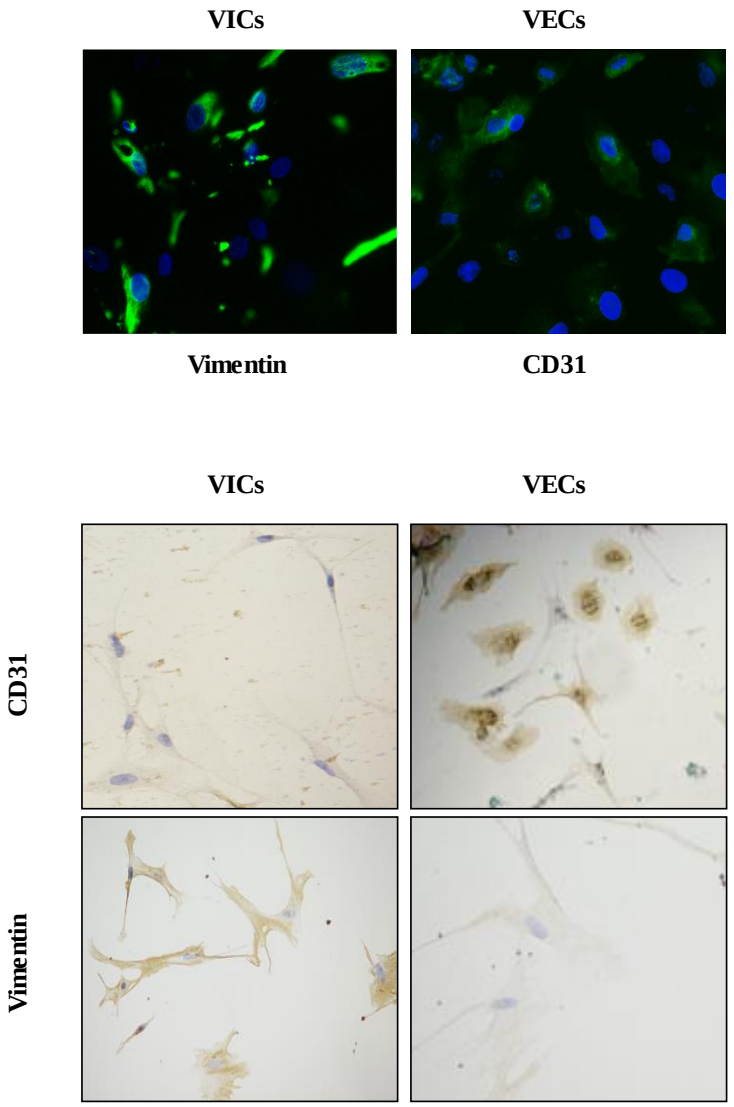

Figure 15. Representative images of immunofluorescence and immunocytochemistry in VICs and VECs for the selected markers. VICs are positive for vimentin and negatives for CD31 and VECs are positive for CD31 and negative for vimentin. Magnification 40x

5. Single culture cell assays

VICs were treated with Aldo (10^{-8}, Sigma Aldrich) for 6 hours for mRNA studies and for 24 hours for protein studies. VECs were treated with Aldo (10^{-8}, Sigma Aldrich) for 24 hours for mRNA studies and for 96 hours for protein studies. In VECs cultures, the duration of the treatment was chosen based on previous studies that analyze EndMT [131]. Cells were treated with Spironolactone (10^{-6}, Sigma Aldrich) for MR blockade 30 minutes before Aldo stimulation.

6. Conditioned media assays

Cells were treated with conditioned media that had been produced by the specified cell type for 24 hours (in VICs) or 96 hours (in VECs), at which point it was sterile filtered and added to target cells. Media was replaced with fresh conditioned media obtained in VICs every 2 days for VECs treatment.

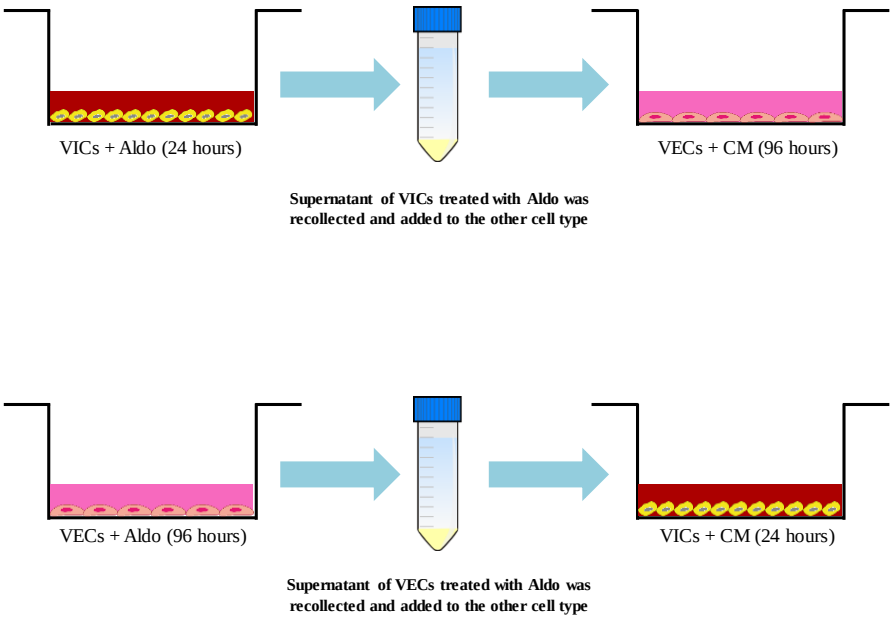

Figure 16. Outline of the conditioned media assays. CM: Conditioned media

7. Cytokine array experiments

VICs and VECs were treated with Aldo (10^{-8}, Sigma Aldrich) for 24 hours. Cell supernatants were collected and analyzed using a human cytokine array kit following manufacturer's instructions (ab169816) (Abcam) (Figure 17), which detects 54 human soluble cytokines (*Activin A, ALCAM, CD80, BMP-5, BMP-7, Cardiotrophin-1, CD14, CXCL16/ DR6 , TNFRSF21, Endoglin, ErbB3, E-Selectin, Fas Ligand, ICAM-2, IGF-2, IL-1 RII, IL-10 R beta, IL-13 R alpha 2, IL-18 BP alpha, IL-18 R beta, MMP-3, IL-2 R beta, IL-2 R gamma, IL-21R, IL-5 R alpha, IL-9, IP-10, TGF beta 1, Leptin R, LIF, L-Selectin, M-CSF R, MMP-1, MMP-13, MMP-9, MPIF-1, NGF R, PDGF-AA, PDGF-AB, PDGF R alpha, PDGF R beta, PECAM-1, Prolactin, SCF R, SDF-1 beta, Siglec-5, TGF alpha, TGF beta 2, Tie-1, Tie-2, TIMP-4, VE-*

Cadherin, VEGFR2, VEGFR3). Among the 54 cytokines we can find cytokines involved in the endothelial function (adhesion, migration…), VICs activators, cardiovascular mediators, inflammatory molecules and MMPs family. Array membranes were blocked 30 minutes with specific blocking buffer and following incubated 2 hours with supernatants. Subsequent incubation with a detection antibody cocktail, antibody conjugation, and recommended washes, the immunoblots on the membrane were developed with Chemiluminescent Substrate Reagent. The results were normalized to the control condition in each cell type. Data was expressed as a fold change relative to controls.

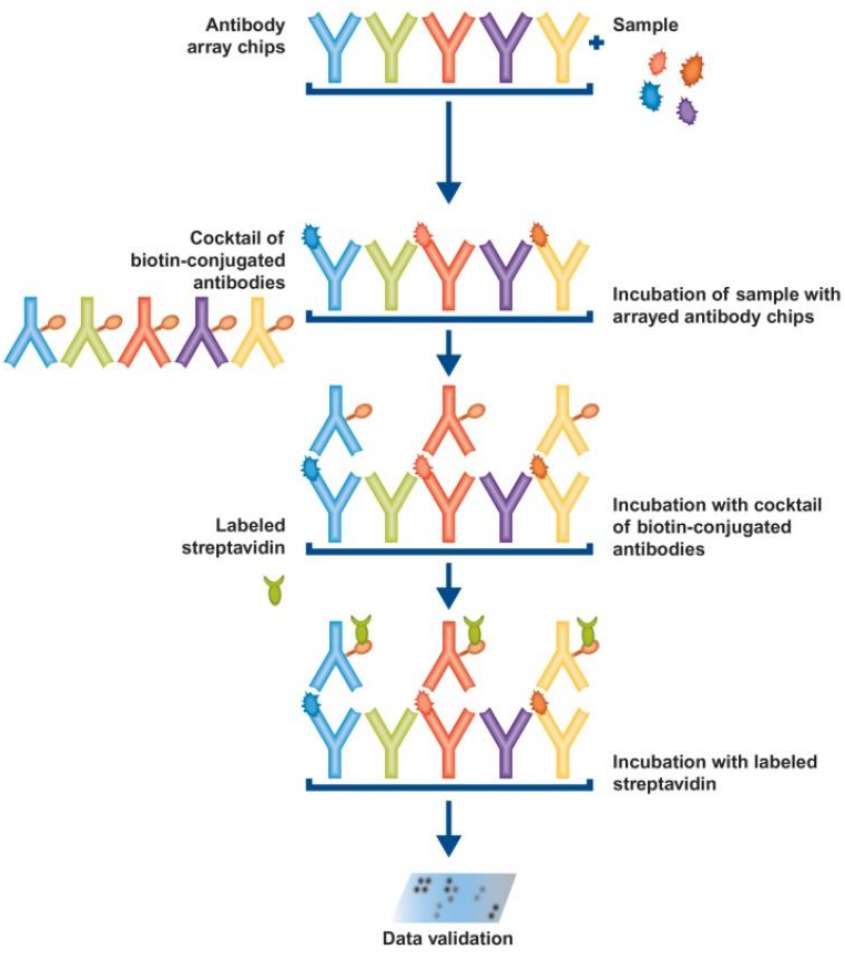

Figure 17. Schematic representation of cytokine array technique (Abcam)

8. Transfection of cells with siRNA

Cells were seeded into twelve-well plates at 100% confluence and transfected with a pool of five siRNAs (GeneCust) for CT-1 and for CD14 target-specific using Magnet Assisted Transfection siRNA (MATra-si, Promokine-Promocell) (Figure 18). MATra solution was incubated with the pool of siRNAs during 20 minutes at room temperature. The MATra-sirNA

mix was added with medium to cells and it was incubated during 15 minutes at 37°C, 95% sterile air, and 5% CO_2 in a saturation humidified incubator with the magnetic plate under the cell plate. After 3 hours, the medium was changed with fresh medium. Cells were allowed to recover for 24 h before stimulation. Scramble siRNAs were used as controls.

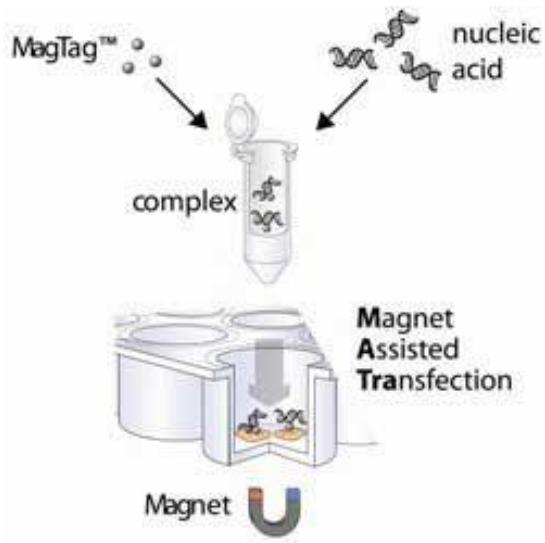

Figure 18. Schematic representation of MATra technology.

III. ANIMAL STUDIES

9. Experimental MVP mice model

Three-month old male Wild Type 129S2/Sv mice were obtained from Charles River Laboratories (France). Mice were maintained in specific pathogen free condition and with *ad libitum* access to food and water. Animals were housed in a climate-controlled facility with a 12- hours/12-

hours light/dark cycle. Experiments were approved by the Darwin ethics committee of Pierre et Marie Curie University, and conducted according to the INSERM animal care and use committee guidelines.

Osmotic minipumps (Alzet) delivering Nordexfenfluramine (NDF) (1 mg/kg/day; Sigma Aldrich) were implanted subcutaneously under general anaesthesia (Imalgene 500, Ketamine mixed with Rompun 2% Bayer). The MRA Spironolactone (1 mg/kg/day) was administered as a food additive for 28 days.

9.1 Animal groups

Mice were divided in three groups; Control group (n=6) (minipumps with saline serum), NDF group (n=7) (minipumps with NDF, 1 mg/kg/day) and NDF + Spironolactone group (n=7) (minipumps with NDF (1 mg/kg/day) and Spironolactone (1 mg/kg/day) as a food additive) (Figure 20).

9.2 Blood pressure

Systolic blood pressure and heart rate were measured at the beginning and at the end of the treatment after 2 days of training using Visitech BP-2000 Series II Blood Pressure Analysis SystemTM (Figure 19). Mice were placed inside a black box over the platform at 37ºC. The tail of mouse was passed through an inflatable sleeve and fixed with an adhesive tape. The system realized 15 cycles (5 cycles of training and 10 cycles of measurements) of inflated. In each cycle, this device performs a photoplethysmographic

measurement by illuminating the tail of the animal with a light emitting diode (red) emitting radiation whose variations through the tail reflect the pulsations of blood flow at the level of the caudal artery (heart rate).

Figure 19. System for measuring blood pressure and heart rate. (BP-2000 SERIES II Blood Pressure Analysis System ™, VISITECH, USA).

9.3 Extraction and sample preparation

Heart samples were obtained after euthanasia and cut in two parts between the atrium and the ventricle. Then, hearts were fixed in formaldehyde and embedded in paraffin for histological analysis.

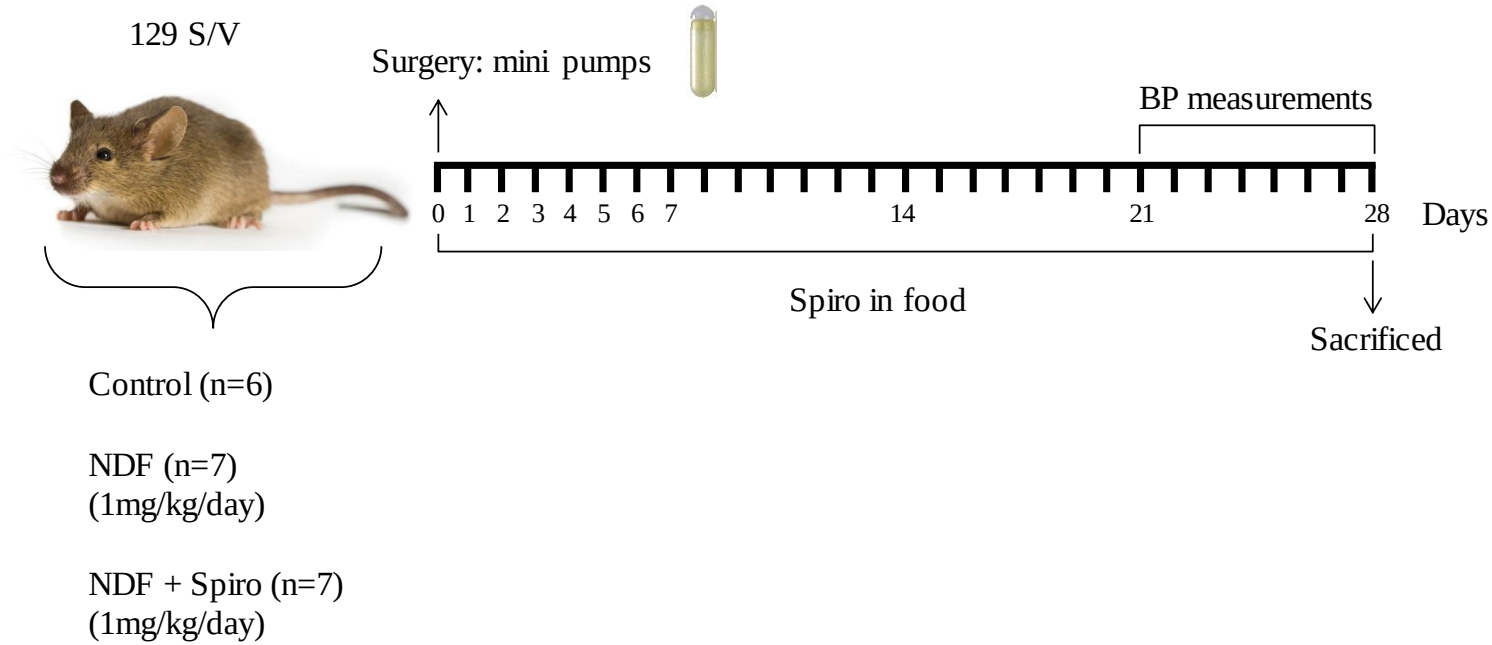

Figure 20. Experimental design of 129SV mouse model

10. Generation of a MVP mice model in endothelial cell (VE-cadherin)-specific MR knockout mice and in α-SMA cell-specific MR knockout mice

Three-month old male mice with cell-type-specific MR deletion in endothelial and smooth muscle (Vecadh-MR-KO and SMA-MR-KO mouse models, respectively), were generated in the C57BL/6 genetic background as previously described [132–134]. Floxed MR ($MR^{f/f}$) mice [135] (kindly provided by Dr. Berger, Heidelberg, Germany) were crossed with mice expressing an inducible Cre-ERT2 recombinase driven by the VE-Cadherin promoter (Cdh5(PAC)-Cre-ERT2 line, kindly provided by Prof. Adams, London, UK [136]; to generate Vecadh-MR-KO mice) or by the α-SMA promoter [137] (kindly provided by Dr. Metzger, Strasbourg, France; to generating SMA-MR-KO mice). $MR^{f/f}$ littermates lacking the Cre transgene were used as controls.

10.1 KO induction

Cell-specific MR inactivation was induced by tamoxifen injection (10 mg/ml in corn oil for 4 consecutive days) 14 days before MVP induction. Both KO and control mice received same tamoxifen regimen.

10.2 Animal groups

Mice were divided in four groups; Control group (n=5) (minipumps with saline serum), Control + NDF group (n=12) (minipumps with NDF),

Vecadh-MR-KO + NDF group (n=8) and SMA-MR-KO + NDF group (n=8) (Figure 21).

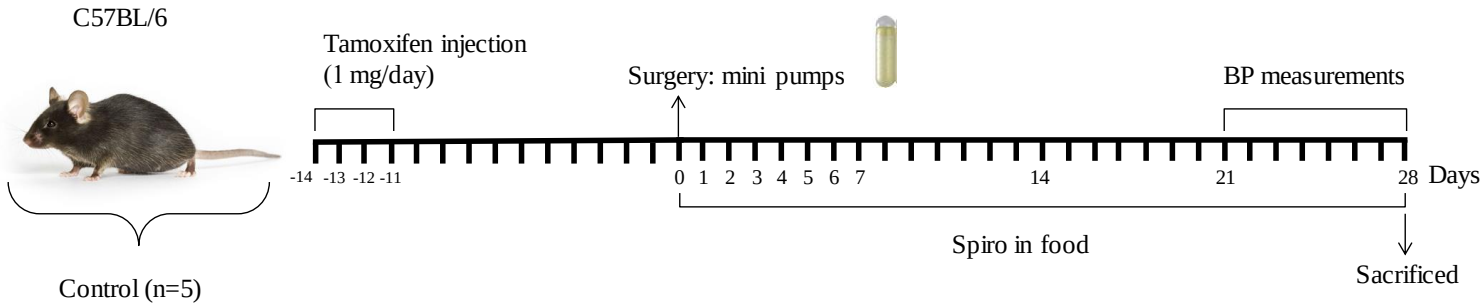

Control (n=5)

Control + NDF (n=12)
(1mg/kg/day)

Vecadh-MR-KO + NDF
(n=8) (1mg/kg/day)

SMA-MR-KO + NDF
(n=8) (1mg/kg/day)

Figure 21. Experimental design of mineralocorticoid receptor-knock out mouse model

IV. MOLECULAR BIOLOGY TECHNIQUES

11. Real-time reverse transcription PCR

Total RNA from cells and mitral valves was extracted with Trizol Reagent (Qiagen), according to the manufacturer's instructions, using chloroform and isopropanol for purification. Purified total RNA was quantified using a Nanodrop 1000 (Thermo Fisher). Equal amounts of total RNA were processed with iScript™ Advanced cDNA Synthesis Kit for RT-qPCR (Bio-Rad) using oligo (dT) as primer according to the manufacturer's instructions. Quantitative PCR analysis was performed using cDNA as template and the oligonucleiotide pairs specific in table 3. Each qPCR reaction was performed in triplicate using the iQ SYBR Green Supermix (Bio-Rad) in a CFX Connect Real-Time System (Bio-Rad). Threshold cycle (Ct) analysis was performed with the manufacter's software. All primers had efficiencies between 90-110%. Melting curves analysis was to ensure specific amplification. Data were normalized by HPRT, GADPH and β-actin levels and expressed as percentage relative to controls. Relative quantification of mRNA abundance was used the ΔΔCt method [138].

The names and sequences of all the primers used during this thesis are shown in Table 3.

Gene	Primer	Sequence (5´to 3´)
VE-Cadherin	Forward	CAG CCC AAA GTG TGT GAG AA
	Reverse	CGG TCA AAC TGC CCA TAC TT
α-SMA	Forward	ACT GCC TTG GTG TGT GAC AAT GG
	Reverse	TGG TGC CAG ATC TTT TCC ATG
MMP-2	Forward	CGA CCA CAG CCA ACT ACG AT
	Reverse	GTC AGG AGA GGC CCC ATA GA
Decorin	Forward	CCT GAT GAC CGC GAC TTC GAG
	Reverse	TTT GGC ACT TTG TCC AGA CCC
Versican	Forward	ACG GGA TTG AAG ACA CAC AAG
	Reverse	AGC CTC AAA ATT CAG TGT GTA
Biglycan	Forward	TCT GTC ACA CCC ACC TAC AGC
	Reverse	AGG GGA GAT CTC TTT GGG CAC
Lumican	Forward	TGA GCT GGA TCT GTC CTA TAA
	Reverse	ATC TTG CAG AAG CTC TTT ATG
Chm-1	Forward	CAT CGG CCT TCT ACT TCT
	Reverse	GGC ATG ATC TTG CCT TCC AG
Vimentin	Forward	GTT TCC CCT AAA CCG CTA GG
	Reverse	AGC GAG AGT GGC AGA GGA
CD31	Forward	TTC CCA CGC CAA AAT GTT A
	Reverse	CAC AGC ACA TTG CAG CAC A
Slug	Forward	GGA CGC ACA CCT TAC CTT GT
	Reverse	CGA GAA GGT TTT GGA GCA AC
VWF	Forward	TAA GTC TGA AGT AGA GGT GG
	Reverse	AGA GCA GCA GGA GCA CTG GT
Syndecan-1	Forward	CCC CTG AAG ATC AAG ATG GC
	Reverse	GGT TCT GGA GAC GTG GGA AT
Hyaluronan	Forward	TGT TGT GGT AGC ACT GGA CT
	Reverse	TCT GGG CTT TGT GAT GGG AT
CT-1	Forward	CTG GAC CCC CAG ACT GAT TC
	Reverse	CCT GGA GCT GCA CAT ATT CCT
CD14	Forward	CTG CAA CTT CTC CGA ACC TC
	Reverse	CCA GTA GCT GAG CAG GAA CC
HPRT	Forward	TTG CTT TCC TTG GTC AGG CA
	Reverse	ATC CAA CAC TTC GTG GGG TC
β-actin	Forward	GCC GCC AGC TCA CCA T
	Reverse	TCG ATG GGG TAC TTC AGG GT
GADPH	Forward	ACC AGC CCC AGC AAG AGC ACA AG
	Reverse	TTC AAG GGG TCT ACA TGG CAA CTG F

Table 3. Description of the primers used for this work: name and sequence of each primer are shown.

12. Western blot analysis

Aliquots of 20 µg of total proteins were prepared from cells and mitral valves, electrophoresed on SDS polyacrylamide gels and transferred to Hybond-c Extra nitrocellulose membranes (Bio-Rad). Membranes were incubated with primary antibodies. Stain free detection was used as loading control. After washing, detection was made through incubation with peroxidase-conjugated secondary antibody, and developed using an ECL chemiluminescence kit (Amersham biosciences biosciences). After densitometric analyses, optical density values were expressed as arbitrary units. All Western Blots were performed at least in triplicate for each experimental condition.

All the antibodies and the working concentrations are listed in Table 4.

Target	Oringin	Type	Method	Supplier	Cat#	Dilution
α-SMA	Mouse	Monoclonal	WB	Sigma	A7607	1:50
Biglycan	Mouse	Monoclonal	WB	Santa Cruz	sc-100857	1:100
CD14	Rabbit	Polyclonal	WB	Abcam	ab203294	1:100
CD31	Mouse	Monoclonal	WB	Santa Cruz	sc-376764	1:100
CT-1	Mouse	Monoclonal	WB	Abcam	ab13975	1:100
Decorin	Rabbit	Polyclonal	WB	Santa Cruz	sc-22753	1:100
MMP-2	Rabbit	Polyclonal	WB	Santa Cruz	ab37150	1:50
Slug	Mouse	Monoclonal	WB	Santa Cruz	sc-166476	1:100
VE-Cadherin	Mouse	Monoclonal	WB	Abcam	sc-9989	1:50
Vimentin	Mouse	Monoclonal	WB	Santa Cruz	sc-373717	1:100
vWF	Mouse	Monoclonal	WB	Santa Cruz	sc-365712	1:100

Table 4. Description of the antibodies used for Western Blot.

13. ELISA

Decorin, Lumican, Aggrecan, Syndecan-1, Hyaluronan, Fibronectin, and CD14 were measured in valve extracts, serum and cells supernatants by ELISA according to the manufacturer's instructions (R&D Systems). CT-1 was measured in valve extracts, serum and cells supernatants by ELISA according to the manufacturer's instructions (Abcam).

14. Histological methods

a) Histological processing

Heart samples kept in formaldehyde at the time of sacrifice were dehydrated in increasing solutions of ethyl alcohol (70%, 96% and absolute ethyl alcohol), embedded in paraffin and cut with a microtome (HM 340 E Microm) in 5 µ-thick sections.

b) Immunohistochemistry

Immunohistochemistry was performed in 5 µm-thick sections. Slides were incubated at 60ºC for 1 hour and hydrated in decreasing solutions of ethyl alcohol (absolute ethyl alcohol, 96% and 70%) and finally in water. Slides were treated with H_2O_2 for 10 min to block peroxidase activity. All samples were blocked with 5% normal goat serum in PBS for 1 h and incubated for 1h with primary antibodies. After incubation, tissues were washed three times, and then incubated for 30 min with the horseradish peroxidase-labeled polymer conjugated to secondary antibodies (Dako Cytomation). The signal

was revealed by using Diaminobenzidine (DAB) Substrate Kit (BD Pharmingen). As negative controls, samples followed the same procedure described above but in the absence of primary antibodies were used.

c) Stainings

For Alcian blue-Sirius red staining, slides were hydrated and first incubated with Alcian-blue (1% in 3% acetic acid, pH 2.5) (Sigma Aldrich) for 20 minutes. After washing, slides were incubated with 1% Sirius red diluted in picric acid for and 30 minutes.

d) Image analysis

The average of each area leaflet was done from the Alcian blue-Sirius red staining. For thickness, the average of three measurements of thickness along the leaflet were done from the Alcian blue-Sirius red staining. The quantification of immunochemistry was done in each leaflet using a manual threshold of the more staining slide per antibody. All measurements and quantifications were performed blind in an automated image analysis system (Nikon).

All the antibodies and the working concentrations are listed in Table 5.

Target	Oringin	Type	Method	Supplier	Cat#	Dilution
Aggrecan	Rabbit	Polyclonal	IHC	Abcam	ab140707	1:50
Biglycan	Mouse	Monoclonal	IHC	Santa Cruz	sc-100857	1:2000
CD31	Mouse	Monoclonal	IHC	Santa Cruz	sc-376764	1:10000
Decorin	Rabbit	Polyclonal	IHC	Santa Cruz	sc-22753	1:100
Lumican	Rabbit	Polyclonal	IHC	Abcam	ab108286	1:50
VCAM-1	Mouse	Monoclonal	IHC	BD pharmingen	559165	1:100
Versican	Rabbit	Polyclonal	IHC	Santa Cruz	ab19345	1:50
Vimentina	Mouse	Monoclonal	IHC	Santa Cruz	sc-373717	1:1000

Table 5. Description of the antibodies used for IHC.

15. Statistical analyses

For *in vitro* studies, data were expressed as mean ± SEM. Normality of distributions was verified by means of the Kolmogorov–Smirnov test. Data were analyzed using a one-way analysis of variance, followed by a Newman-Keuls to assess specific differences among groups or conditions using GraphPad Software Inc. For animal studies, data were expressed as mean ± SEM. The normality of distributions was verified by means of the Kolmogorov–Smirnov test. Data were analyzed using a one-way ANOVA, followed by a Newman–Keuls test to assess specific differences among groups or conditions, using GraphPad Software Inc. For human studies, data were expressed as mean ± SEM. Spearman's correlation coefficients were calculated to determine correlations. Categorical variables were expressed as percentages and compared using χ2-test, or Fisher exact test when the expected value in any cell of the contingency table was below 5. Quantitative variables were analyzed by T student test or Mann-Whitney U test if the normality was not met. Clinical data of the patients enrolled were analyzed with IBM SPSS statistics 25 software.

RESULTS

1. Expression of MR and Aldo synthesis enzymes in mitral valves

Our first goal was to analyze the expression of MR and Aldo synthesis enzymes in the mitral valve. Adrenal cortex was used as a control tissue in which these enzymes are expressed [139,140].

We examined the expression of MR and the principal enzymes involved in Aldo synthesis (11β-hydroxysteroid dehydrogenase type 2 (11β-HSD2), 11β-Hydroxylase and Aldosterone synthase). Results showed that MR and 11β-HSD2 were expressed in mitral valves. (Figure 22).

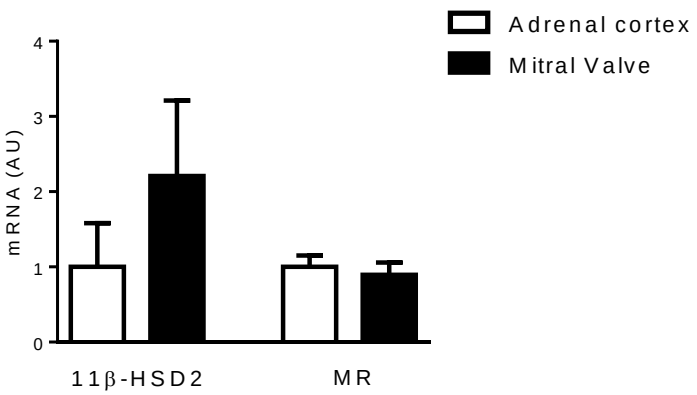

Figure 22. Expression of MR and Aldo synthesis enzymes in mitral valves. Quantification of 11β-HSD2 and MR expression at mRNA levels in adrenal cortex and human mitral valves. Histograms with bars represents the mean ± SEM of each group in arbitrary units (AU) normalized to HPRT, GADPH and β-actin for cDNA.

***I. IN VITRO* STUDIES**

2. Aldosterone induced VICs activation and proteoglycans synthesis in VICs

At the mRNA levels, Aldo decreased the qVICs marker Chm-1 ($p<0.05$) and induced the expression of the VICs activation markers α-SMA, vimentin and MMP-2 ($p<0.05$) as compared to control conditions (Figure 23A). At the protein levels, Aldo significantly induced the expression of the VICs activation markers α-SMA, vimentin and MMP-2 ($p<0.05$) (Figure 23B). All the above effects were blocked by Spironolactone treatment.

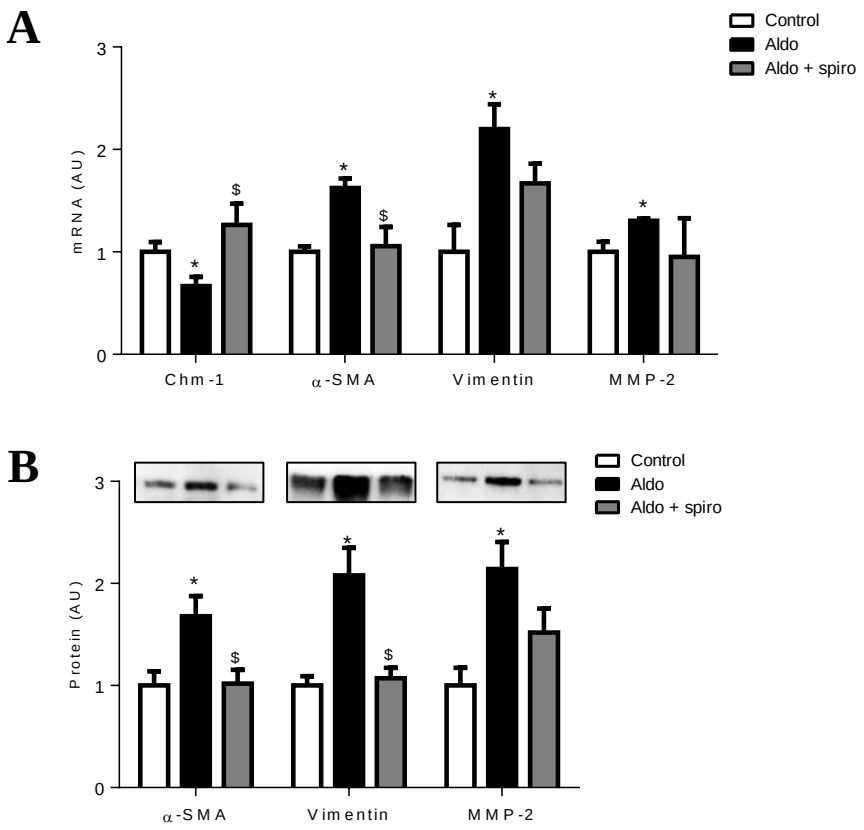

Figure 23. Effect of Aldo on quiescent VICs markers VICs activation markers in VICs. Quantification of the qVICs marker Chm-1 and the VICs activation markers α-SMA, vimentin and MMP-2 at mRNA **(A)** and protein levels **(B)**. All conditions were performed at least in triplicate. Histograms with bars represents the mean ± SEM of each group in arbitrary units (AU) normalized to HPRT, GADPH and β-actin or stain free gel for cDNA and protein respectively. * $p<0.05$ vs. control. $ $p<0.05$ vs. Aldo.

In VICs, Aldo treatment increased significantly ($p<0.05$) the expression and secretion of the proteoglycans decorin, biglycan, lumican, aggrecan,

syndecan-1, hyaluronan and versican at the mRNA (Figure 24A) and the protein levels (Figure 24B). All the above effects were blocked by Spironolactone treatment.

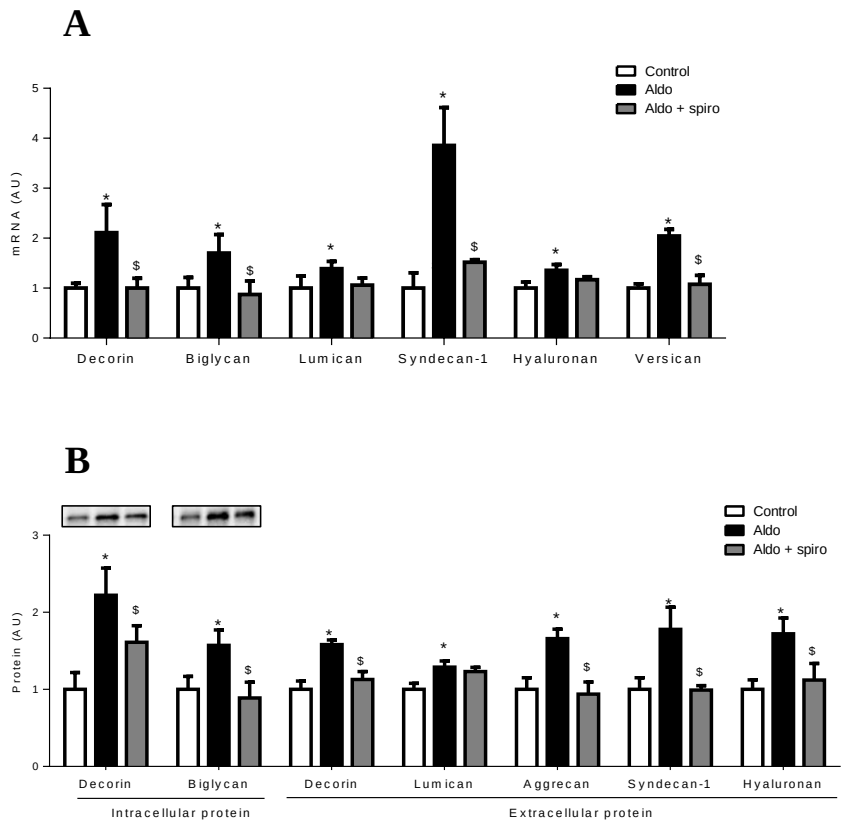

Figure 24. Effects of Aldo on proteoglycans expression in VICs. mRNA expression of decorin, biglycan, lumican, syndecan-1, hyaluronan and versican **(A)**. Quantification of intracellular proteoglycans (decorin and biglycan) and extracellular proteoglycans (decorin, lumican, aggrecan, syndecan-1 and hyaluronan) at protein levels **(B)**. All conditions were performed at least in triplicate. Histograms with bars represents the mean ± SEM of each group in arbitrary units

(AU) normalized to HPRT, GADPH and β-actin or stain free gel for cDNA and protein respectively. * $p<0.05$ vs. control. $ $p<0.05$ vs. Aldo.

3. Aldo induced EndMT and proteoglycans expression in VECs

VECs markers VE-cadherin and vWF decreased significantly ($p<0.05$) in Aldo-treated VECs as compared to controls. However, stimulation with the mineralocorticoid did not modify the expression of CD31 (Figure 25A). At the protein levels, Aldo diminished ($p<0.05$) the expression of the VECs markers CD31, VE-cadherin and vWF (Figure 25B). All these effects were blocked by Spironolactone treatment.

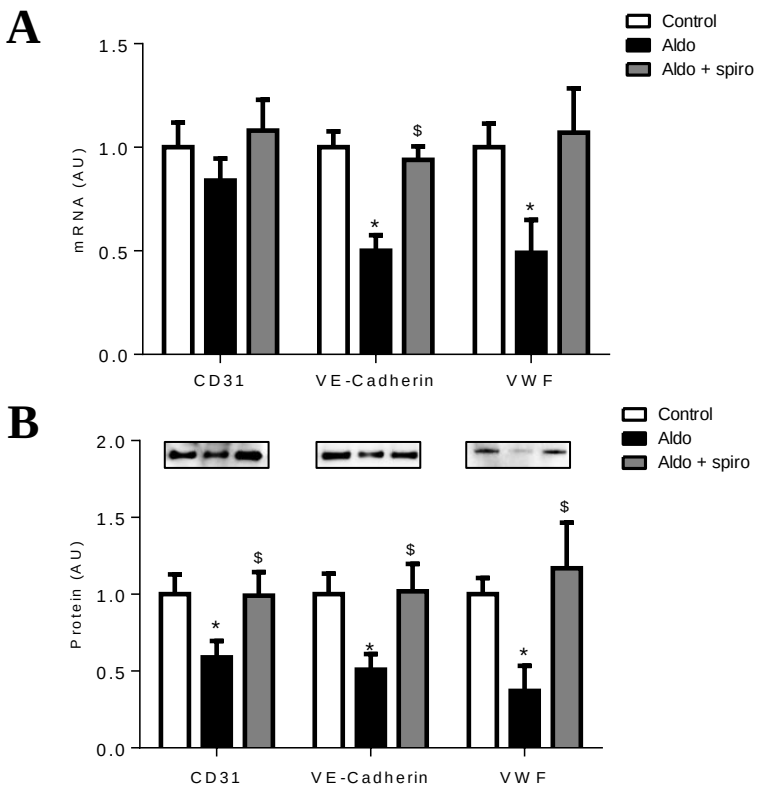

Figure 25. Effects of Aldo on VECs markers in VECs. Quantification of VECs markers (CD31, VE-Cadherin and vWF) at mRNA **(A)** and protein levels **(B)**. All conditions were performed at least in triplicate. Histograms with bars represents the mean ± SEM of each group in arbitrary units (AU) normalized to HPRT, GADPH and β-actin or stain free gel for cDNA and protein respectively. * $p<0.05$ vs. control. $ $p<0.05$ vs. Aldo.

Aldo treatment enhanced ($p<0.05$) the expression of the VICs activation markers α-SMA, vimentin, MMP-2 and slug at the mRNA levels (Figure 26A). At the protein levels, Aldo increased ($p<0.05$) the expression of α-SMA and vimentin as compared to controls, while stimulation with the

mineralocorticoid did not modify the expression of MMP-2 (Figure 26B). All this effects were blocked by Spironolactone treatment.

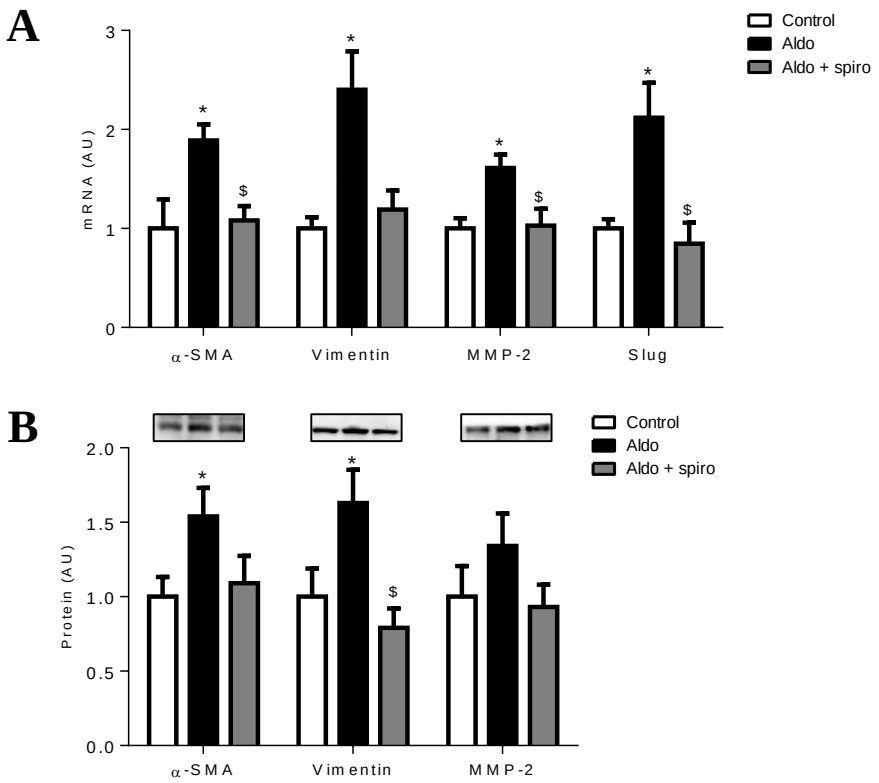

Figure 26. Effects of Aldo on VICs activation markers in VECs. Quantification of qVICs marker (Chm-1) and VICs activation markers (α-SMA, vimentin, MMP-2 and slug) at mRNA **(A)** and protein levels **(B)**. All conditions were performed at least in triplicate. Histograms with bars represents the mean ± SEM of each group in arbitrary units (AU) normalized to HPRT, GADPH and β-actin or stain free gel for cDNA and protein respectively. * $p<0.05$ vs. control. $ $p<0.05$ vs. Aldo.

The expression of the proteoglycans biglycan, lumican, syndecan-1, hyaluronan and versican was significantly increased ($p<0.05$) by Aldo treatment at the mRNA levels. However, decorin mRNA expression remained unchanged (Figure 27A). At the protein levels, decorin, biglycan and syndecan-1 were significantly increased ($p<0.05$) by Aldo treatment, whereas stimulation with the mineralocorticoid did not significantly change lumican, aggrecan or hyaluronan levels (Figure 27B). All these effects were blocked by Spironolactone treatment.

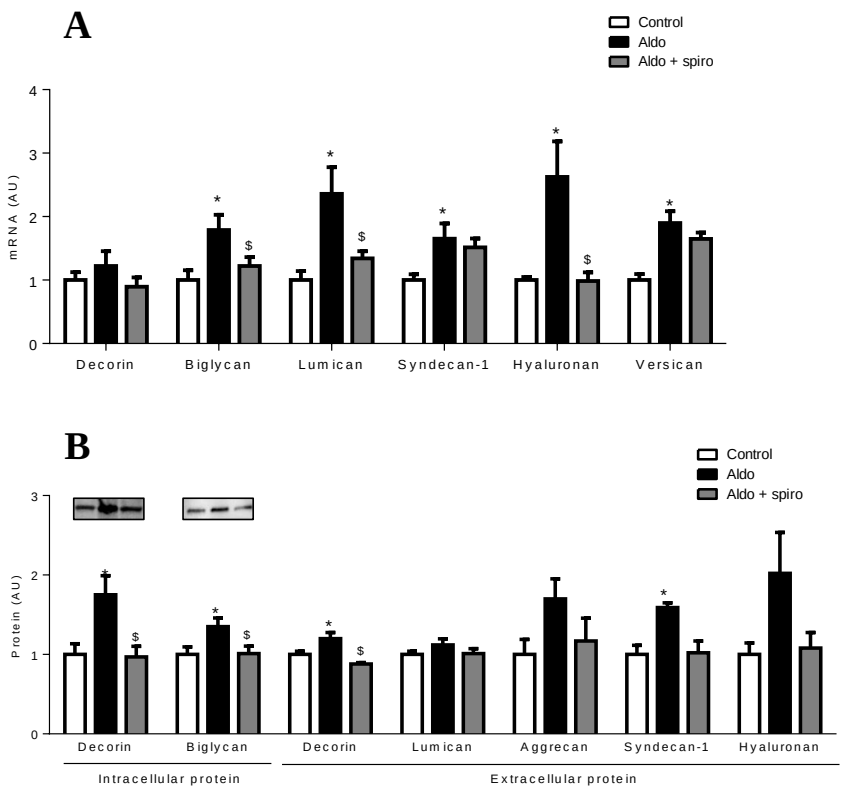

Figure 27. Effects of Aldo on proteoglycans expression in VECs. mRNA expression of decorin, biglycan, lumican, syndecan-1, hyaluronan and versican **(A)**. Expression of intracellular proteoglycans (Decorin and biglycan) and extracellular proteoglycans (Decorin, lumican, aggrecan, syndecan-1 and hyaluronan) at protein levels **(B)** in VECs. All conditions were performed at least in triplicate. Histograms with bars represents the mean ± SEM of each group in arbitrary units (AU) normalized to HPRT, GADPH and β-actin or stain free gel for cDNA and protein respectively. * $p<0.05$ vs. control. $ $p<0.05$ vs. Aldo.

4. Mitral VECs exacerbated Aldo-induced VICs activation and proteoglycans secretion

We next investigated whether mitral VECs could produce factors or signals that induce VICs activation and proteoglycans secretion. For this purpose, mitral VICs were incubated with conditioned media from the culture of mitral VECs treated with Aldo (Figure 16).

The expression of the VICs activation markers α-SMA, vimentin and MMP-2 increased 2-fold ($p<0.05$) in cells incubated with conditioned medium from VECs treated with Aldo as compared to VICs treated with conditioned medium from control VECs, being these effects blocked by Spironolactone (Figure 28).

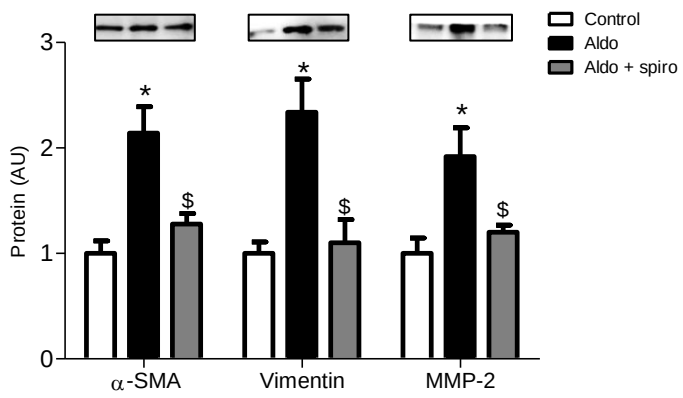

Figure 28. Effects on VICs activation markers in VICs treated with conditioned media from the culture of mitral VECs treated with Aldo. Quantification of VICs activation markers (α-SMA, vimentin and MMP-2) at protein levels. All conditions were performed at least in triplicate. Histograms with bars represents the mean ± SEM of each group in arbitrary units (AU) normalized to stain free gel for protein. * $p<0.05$ vs. control. $ $p<0.05$ vs. Aldo.

Conditioned medium from VECs treated with Aldo enhanced significantly ($p<0.05$) the expression of decorin, biglycan, aggrecan and the secretion of aggrecan, syndecan-1 and hyaluronan in VICs, whereas the secretion of decorin and lumican was not modified. Spironolactone blocked all the above effects (Figure 29).

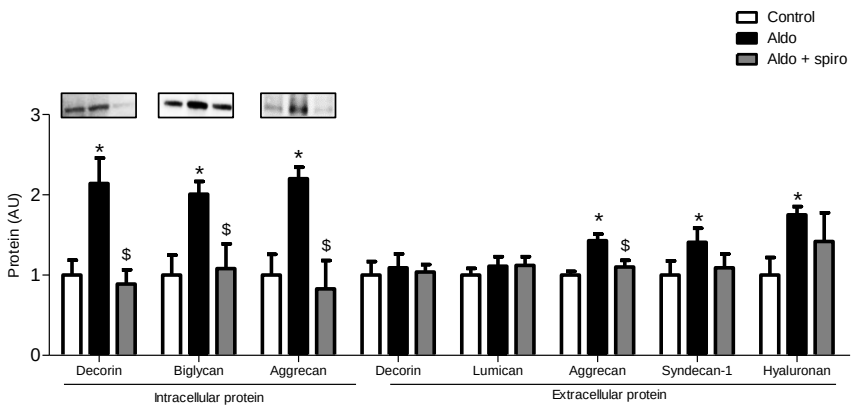

Figure 29. Effects on proteoglycans expression in VICs treated with conditioned media from the culture of mitral VECs treated with Aldo. Quantification of intracellular proteoglycans (decorin, biglycan and aggrecan) and extracellular proteoglycans (decorin, lumican, aggrecan, syndecan-1 and hyaluronan) at protein levels. All conditions were performed at least in triplicate. Histograms with bars represents the mean ± SEM of each group in arbitrary units (AU) normalized to stain free gel for protein. * $p<0.05$ vs. control. $ $p<0.05$ vs. Aldo.

5. Mitral VICs exacerbated Aldo-induced EndMT and proteoglycans secretion in VECs

Primary mitral VECs were incubated with conditioned media from mitral VICs treated with Aldo in order to determine if mitral VICs produce factors or signals that can induce EndMT and proteoglycans secretion.

VECs incubated with VICs supernatant previously treated with Aldo exhibited a decrease in the expression of the VECs markers CD31, VE-

cadherin and vWF ($p<0.05$) being all these effects blocked by Spironolactone (Figure 30).

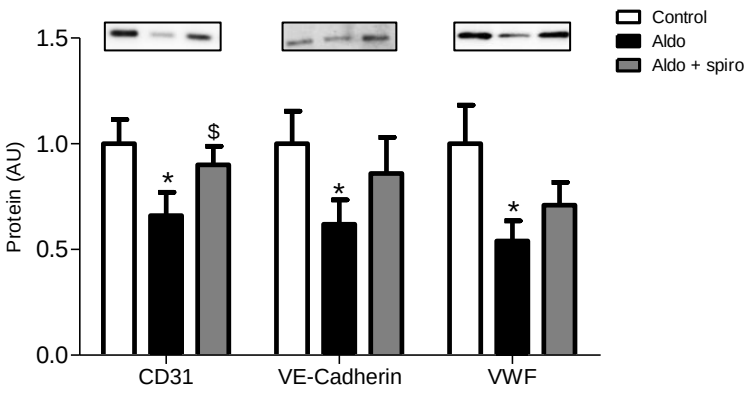

Figure 30. Effects on VECs markers in VECs treated with conditioned media from mitral VICs treated with Aldo. Quantification of VECs markers (CD31, VE-Cadherin and vWF) at protein levels. All conditions were performed at least in triplicate. Histograms with bars represents the mean ± SEM of each group in arbitrary units (AU) normalized to stain free gel for protein. * $p<0.05$ vs. control. $ $p<0.05$ vs. Aldo.

Complementary, the expression of the VICs differentiation markers α-SMA, vimentin and MMP-2 were significantly increased ($p<0.05$) in VECs treated with conditioned medium from VICs stimulated with Aldo, whereas the expression of slug was not changed. Spironolactone blocked the above effects (Figure 31).

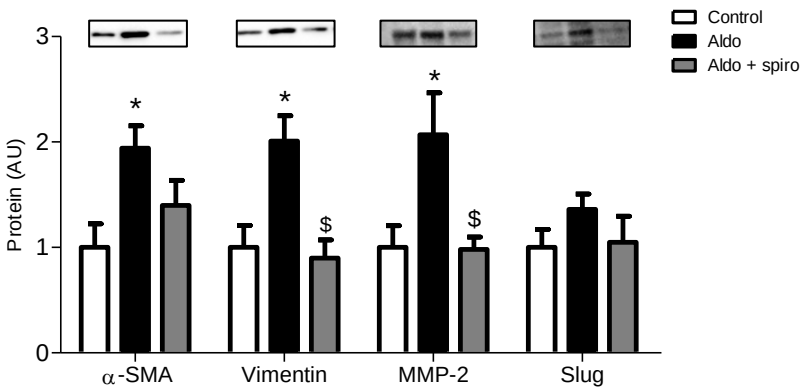

Figure 31. Effects on VICs markers in VECs treated with conditioned media from mitral VICs treated with Aldo. Quantification of VICs activation markers (α-SMA, vimentin, MMP-2 and slug) at protein levels. All conditions were performed at least in triplicate. Histograms with bars represents the mean ± SEM of each group in arbitrary units (AU) normalized to stain free gel for protein. * $p<0.05$ vs. control. $ $p<0.05$ vs. Aldo.

The expression of decorin and lumican and the secretion of decorin, lumican, aggrecan and syndecan-1 was also augmented significantly ($p<0.05$) in VECs treated with conditioned medium from Aldo-stimulated VICs. However, the expression of biglycan and the secretion of hyaluronan remained unchanged. All the above effects were blocked by Spironolactone (Figure 32).

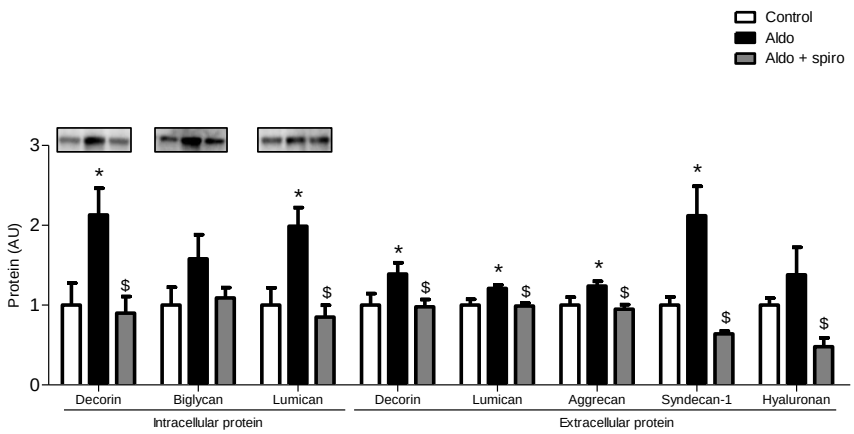

Figure 32. Effects on proteoglycans expression in VECs treated with conditioned media from mitral VICs treated with Aldo. Quantification of intracellular proteoglycans (decorin, biglycan and lumican) and extracellular proteoglycans (decorin, lumican, aggrecan, syndecan-1 and hyaluronan) at protein levels. All conditions were performed at least in triplicate. Histograms with bars represents the mean ± SEM of each group in arbitrary units (AU) normalized to stain free gel for protein. * $p<0.05$ vs. control. $ $p<0.05$ vs. Aldo

6. New pathways implicated on Aldo effects in VICs

To analyze in depth Aldo effects in VICs, a cytokine array was performed in Aldo-treated VICs supernatants.

Aldo up-regulated 53 cytokines in VICs supernatant (ANNEX). Cardiotrophin-1 (CT-1), a cytokine previously shown to be up-regulated by Aldo in other cell types [141,142] was one of the principal up-regulated molecules, presenting a 32% increment in its expression in Aldo-treated

VICs as compared to controls (Figure 33). This result was validated by western blot and ELISA showing a significant increment ($p<0.05$) in CT-1 expression and secretion in VICs treated with Aldo (Figure 34). Of note, Spironolactone prevented CT-1 up-regulation induced by Aldo.

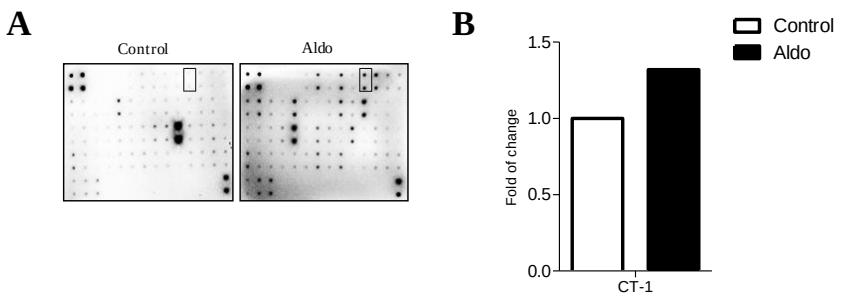

Figure 33. Identification of cytokines from VICs supernatant treated with Aldo in a cytokine array. Representative images of human cytokine array blots probed with the cell supernatant samples **(A)**. Each blot represents the immunoreactive staining with each cytokine. The lack of dots represented the negative and blank control. The blots marked inside the box are the CT-1 expression. The fold of change of CT-1 was determined by comparing the pixel intensity of the respective blots to that of the positive control on the same array **(B)**.

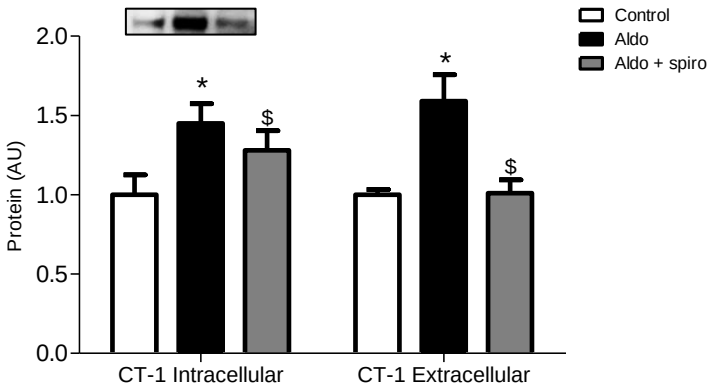

Figure 34. Cytokine array validation in VICs treated with Aldo. Quantification of extracellular and intracellular CT-1. All conditions were performed at least in triplicate. Histograms with bars represents the mean ± SEM of each group in arbitrary units (AU) normalized to stain free gel for protein. * $p<0.05$ vs. control. $ $p<0.05$ vs. Aldo

6.1 Cardiotrophin-1 effects in VICs

We next analyzed CT-1 effects in VICs. CT-1 treatment decreased significantly the qVIC marker Chm-1 ($p<0.05$) and increased significantly ($p<0.05$) the VICs activation markers α-SMA, vimentin, MMP-2 and slug both at the mRNA (Figure 35A) and the protein levels (Figure 35B) as compared with control cells.

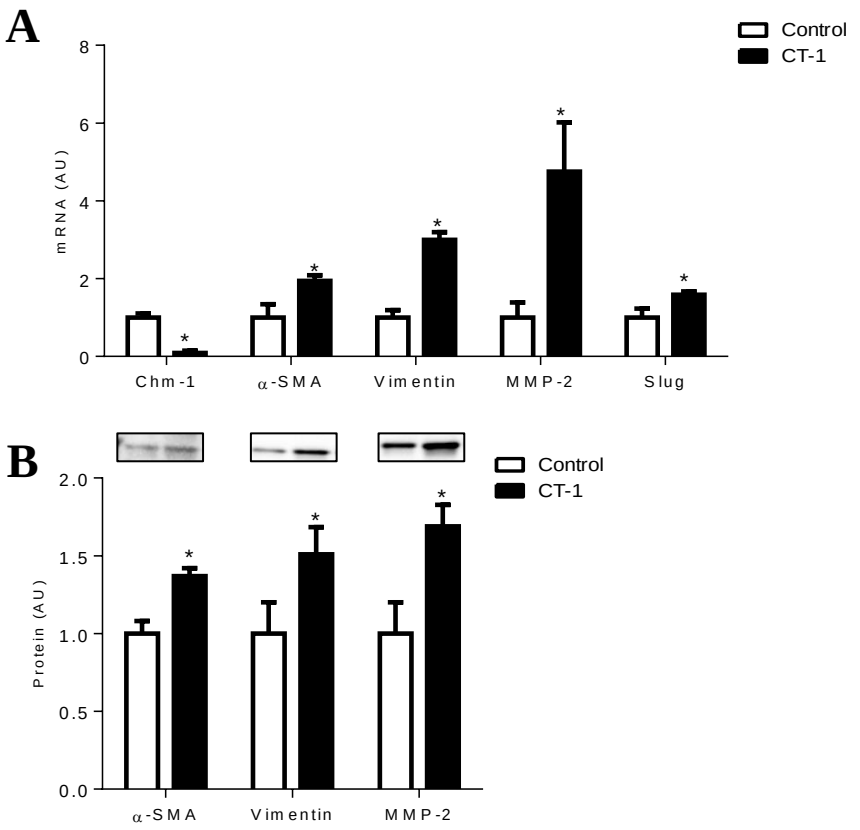

Figure 35. Effects on quiescent VICs markers and VICs activation markers in VICs treated with CT-1. Quantification of the qVICs marker Chm-1 and the VICs activation markers α-SMA, vimentin, MMP-2 and slug at mRNA **(A)** and protein levels **(B)**. All conditions were performed at least in triplicate. Histograms with bars represents the mean ± SEM of each group in arbitrary units (AU) normalized to HPRT, GADPH and β-actin or stain free gel for cDNA and protein respectively. * $p<0.05$ vs. control.

The expression of the proteoglycans decorin, biglycan, lumican and versican was significantly increased ($p<0.05$) by CT-1 treatment at the mRNA levels

(Figure 36A). At the protein levels, the expression of decorin and biglycan and the secretion of decorin and lumican was significantly increased ($p<0.05$) by CT-1 treatment, whereas the secretion of syndecan-1 and hyaluronan remained unchanged (Figure 36B).

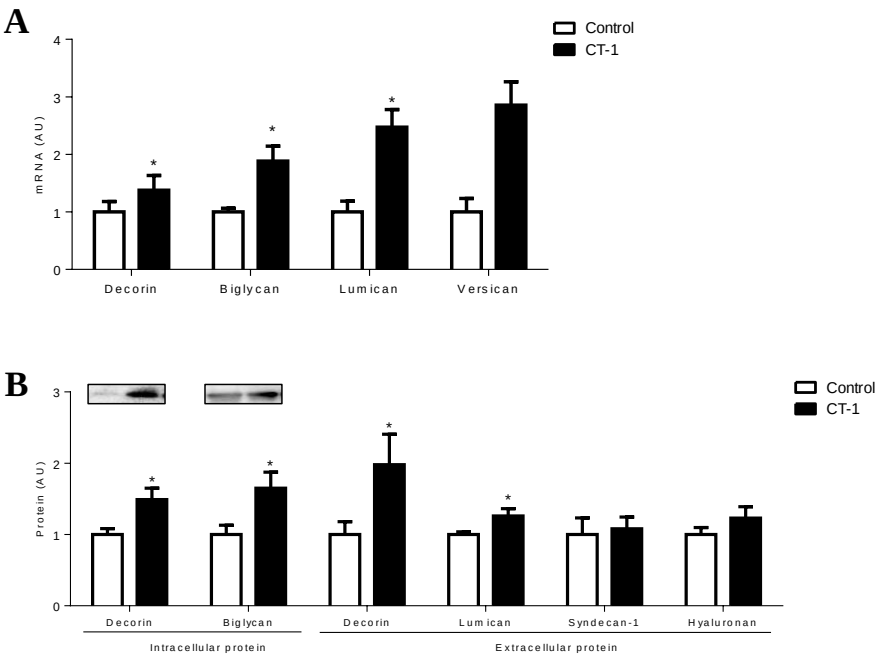

Figure 36. Effects on proteoglycans expression in VICs treated with CT-1. Quantification of proteoglycans (decorin, biglycan, lumican and versican) at mRNA levels **(A)**. Quantification of intracellular proteoglycans (decorin and biglycan) and extracellular proteoglycans (decorin, lumican, syndecan-1 and hyaluronan) at protein levels **(B)**. All conditions were performed at least in triplicate. Histograms with bars represents the mean ± SEM of each group in arbitrary units (AU)

normalized to HPRT, GADPH and β-actin or stain free gel for cDNA and protein respectively. * $p<0.05$ vs. control.

6.2 CT-1 as a mediator of Aldo effects in VICs

Our next step was to study whether CT-1 could mediate Aldo effects in VICs. To validate this objective, CT-1 expression was knocked-down using a specific siRNA in VICs. Then, CT-1 silenced VICs were treated with Aldo. As a control, a scramble siRNA was used.

In CT-1 silenced cells, Aldo did not decrease Chm-1 nor induce the VICs activation markers α-SMA, vimentin and MMP-2 at the mRNA (Figure 37A) and the protein levels (Figure 37B). However, the mRNA expression of vimentin and MMP-2 was unchanged in CT-1 knock-down cells treated with Aldo.

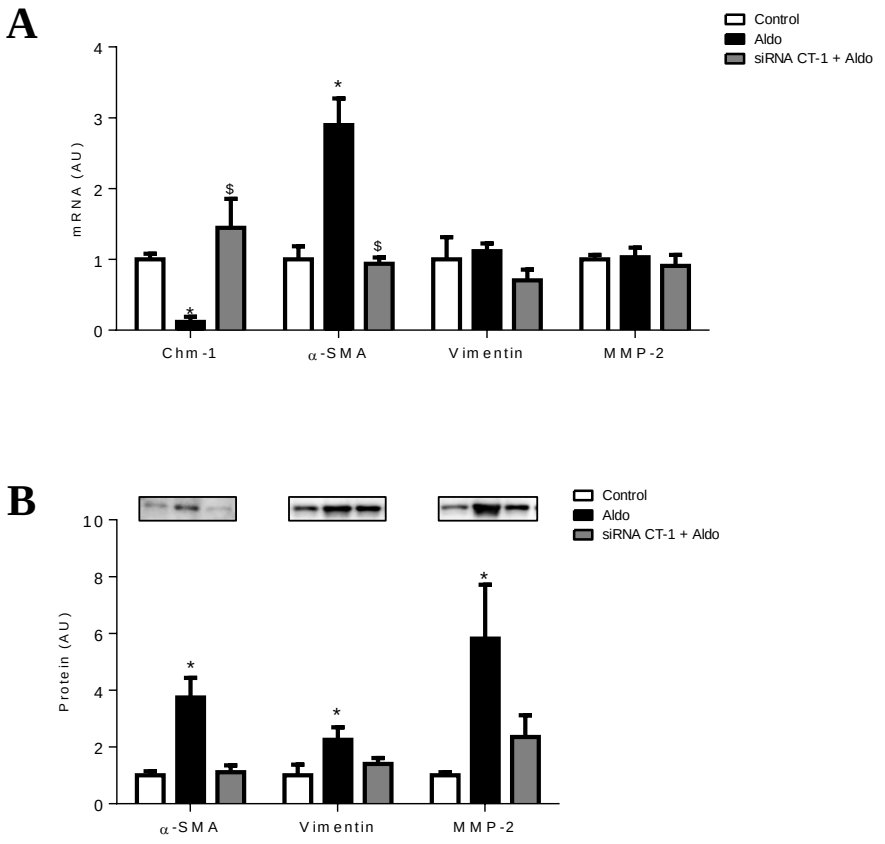

Figure 37. Effects on quiescent VICs markers and VICs activation markers in CT-1-knock down VICs treated with Aldo. Quantification of the qVICs marker Chm-1 and the VICs activation markers α-SMA, vimentin, MMP-2 and slug at mRNA **(A)** and protein levels **(B)**. All conditions were performed at least in triplicate. Histograms with bars represents the mean ± SEM of each group in arbitrary units (AU) normalized to HPRT, GADPH and β-actin or stain free gel for cDNA and protein respectively. * $p<0.05$ vs. control. $ $p<0.05$ vs. Aldo.

Moreover, in CT-1 silenced cells, Aldo was unable to increase the expression of decorin and biglycan both at the mRNA (Figure 38A) and the

protein levels as well as the secretion of decorin, lumican and syndecan-1 (Figure 38B). However, the mRNA expression of lumican and versican and the protein expression of hyaluronan were unchanged in CT-1 knock-down cells treated with Aldo.

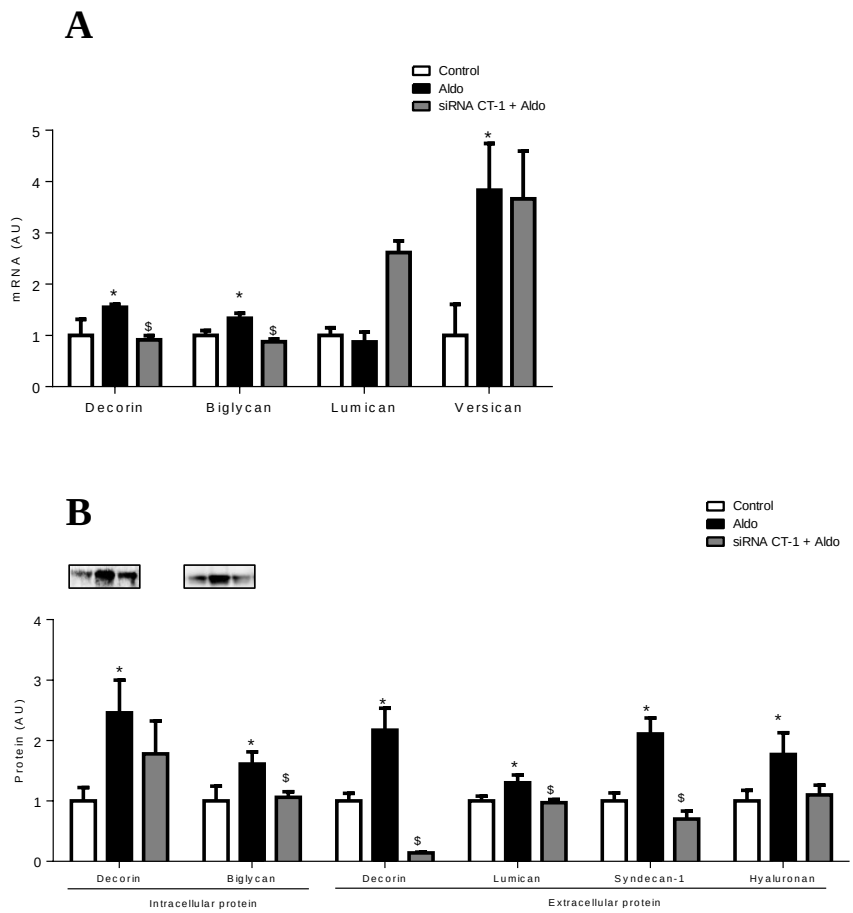

Figure 38. Effects on proteoglycans expression in CT-1-knock down VICs treated with Aldo. Quantification of proteoglycans (decorin, biglycan, lumican and

versican) at mRNA levels **(A)**. Quantification of intracellular proteoglycans (decorin and biglycan) and extracellular proteoglycans (decorin, lumican, syndecan-1 and hyaluronan) at protein levels **(B)**. All conditions were performed at least in triplicate. Histograms with bars represents the mean ± SEM of each group in arbitrary units (AU) normalized to HPRT, GADPH and β-actin or stain free gel for cDNA and protein respectively. * $p<0.05$ vs. control. $ $p<0.05$ vs. Aldo.

7. New pathways implicated on Aldo effects in VECs

To analyze more in depth Aldo mediators in VECs, a cytokine array of 54 targets was performed in Aldo-treated VECs supernatant at 24 hours.

Aldo up-regulated 44 cytokines in VECs supernatant (ANNEX). As it was described in VICs, CT-1 was one of the most up-regulated cytokine, presenting a 92% increment in its expression in Aldo-treated VECs as compared to controls (Figure 39). This result was validated by western blot and ELISA showing a significant increment ($p<0.05$) in CT-1 expression in VECs treated with Aldo (Figure 40). Of note, Spironolactone prevented CT-1 up-regulation induced by Aldo.

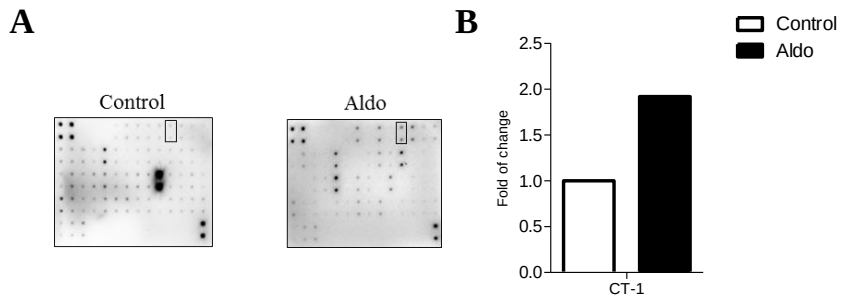

Figure 39. Identification of cytokines from VECs supernatant treated with Aldo in a cytokine array. Representative images of human cytokine array blots probed with the cell supernatant samples **(A)**. Each blot represents the immunoreactive staining with each cytokine. The lack of dots represented the negative and blank control. The blots marked inside the box are the CT-1 expression. The fold of change of CT-1 was determined by comparing the pixel intensity of the respective blots to that of the positive control on the same array **(B)**.

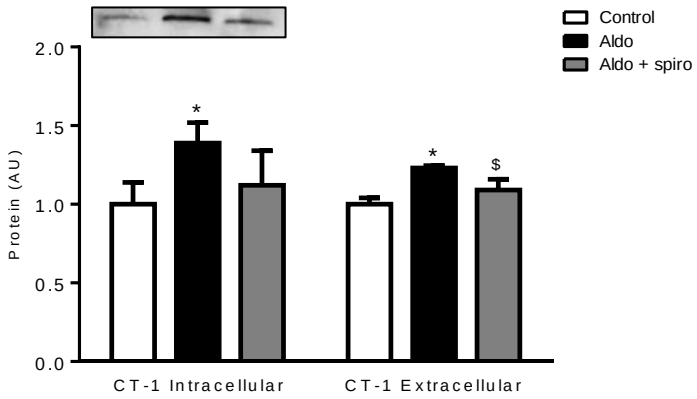

Figure 40. Cytokine array validation in VECs treated with Aldo. Quantification of intracellular and extracellular CT-1. All conditions were performed at least in

triplicate. Histograms with bars represents the mean ± SEM of each group in arbitrary units (AU) normalized to stain free gel for protein. * $p<0.05$ vs. control.

7.1 Cardiotrophin-1 effects in VECs

Our next step was to study CT-1 effects in VECs. CT-1 treatment decreased significantly ($p<0.05$) the expression of VE-Cadherin at the mRNA (Figure 41A) and the protein levels (Figure 41B) and the expression of vWF at the mRNA levels. However, the mRNA and protein expression of CD31 remained unchanged as compared to controls.

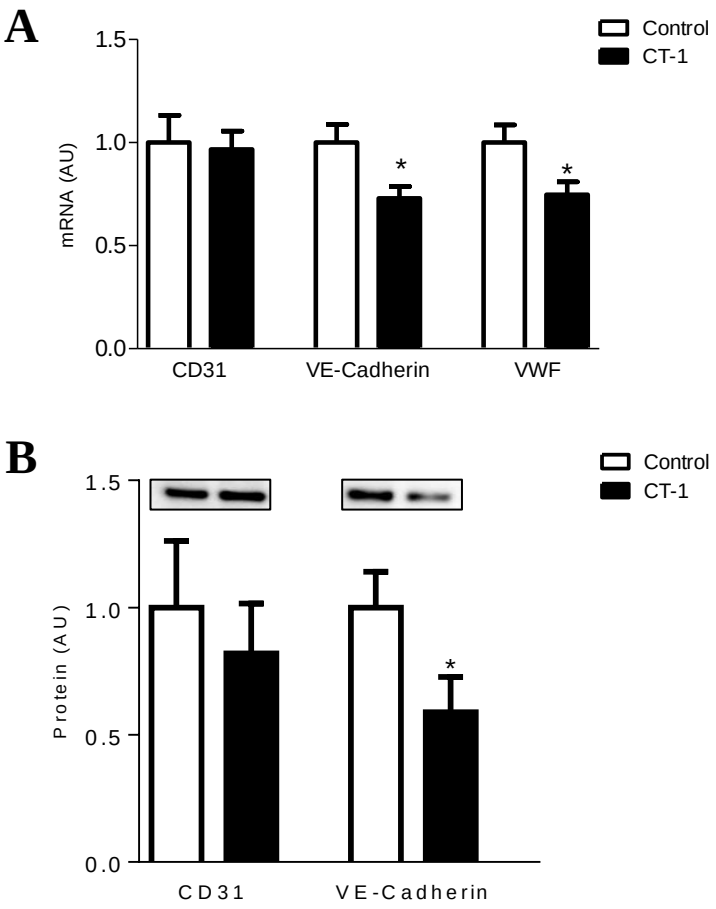

Figure 41. Effects on VECs markers in VECs treated with CT-1. Quantification of VECs markers (CD31, VE-Cadherin and vWF) at mRNA levels **(A)** and protein levels **(B)**. All conditions were performed at least in triplicate. Histograms with bars represents the mean ± SEM of each group in arbitrary units (AU) normalized to HPRT, GADPH and β-actin or stain free gel for cDNA and protein respectively. * $p<0.05$ vs. control.

CT-1 treatment significantly increased ($p<0.05$) the VICs activation markers α-SMA and vimentin both at the mRNA (Figure 42A) and the protein levels

(Figure 42b) as compared to control cells. The mRNA expression of slug and the protein expression of MMP-2 did not change.

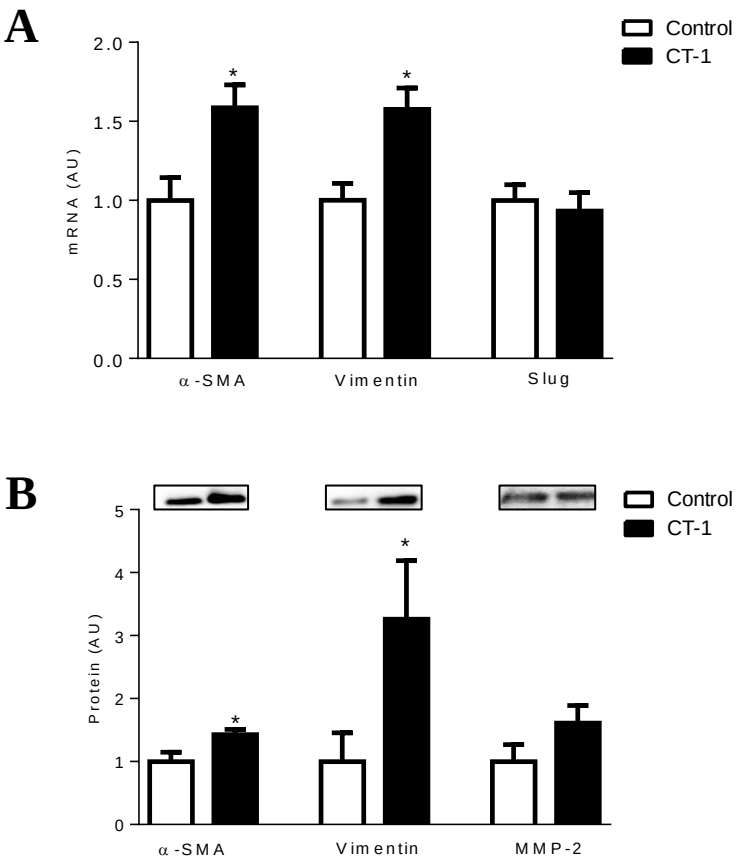

Figure 42. Effects on VICs activation markers in VECs treated with CT-1. Quantification of VICs activation markers (α-SMA, vimentin, MMP-2 and slug) at mRNA **(A)** and protein levels **(B)**. All conditions were performed at least in triplicate. Histograms with bars represents the mean ± SEM of each group in

arbitrary units (AU) normalized to HPRT, GADPH and β-actin or stain free gel for cDNA and protein respectively. * $p<0.05$ vs. control.

Concerning proteoglycans, the mRNA expression of decorin and lumican was significantly increased ($p<0.05$) in CT-1-treated VECs as compared to controls. However, stimulation with CT-1 did not significantly modify the mRNA expression of biglycan and versican (Figure 43A). At the protein levels, CT-1 significantly increased ($p<0.05$) the intracellular expression of biglycan and the secretion of decorin and lumican as compared to controls. However, stimulation with CT-1 did not significantly modify the expression of decorin and the secretion of hyaluronan (Figure 43B).

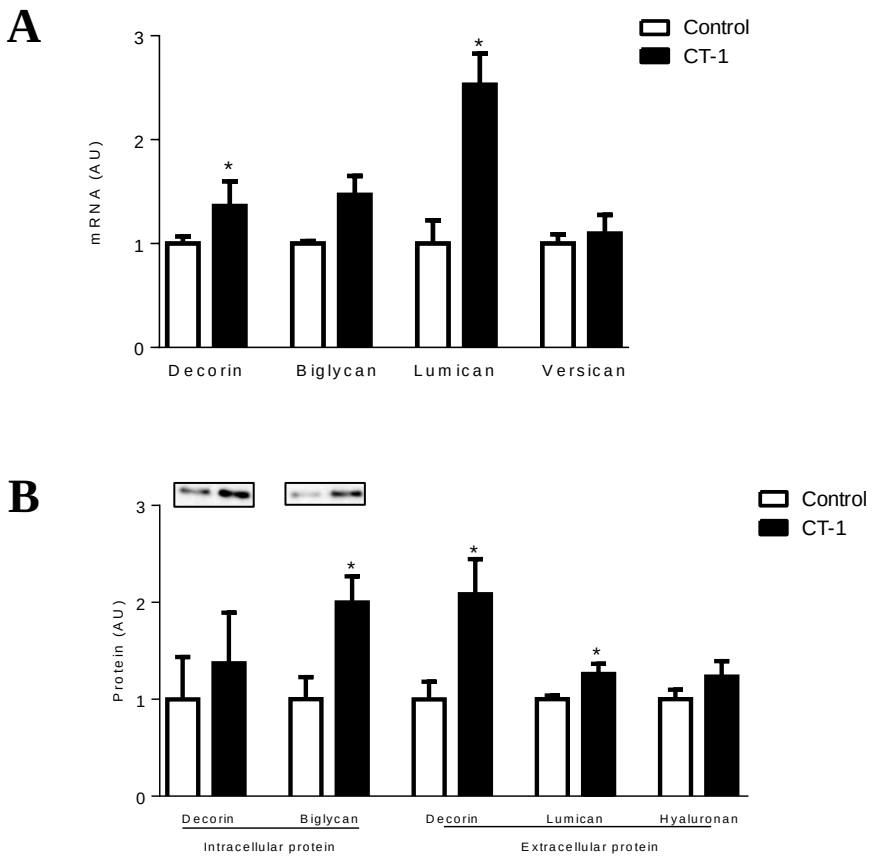

Figure 43. CT-1 effects on proteoglycans expression in VECs. Quantification of proteoglycans (decorin, biglycan, lumican and versican) at mRNA levels **(A)**. Quantification of intracellular proteoglycans (decorin and biglycan) and extracellular proteoglycans (decorin, lumican and hyaluronan) at protein levels **(B)**. All conditions were performed at least in triplicate. Histograms with bars represents the mean ± SEM of each group in arbitrary units (AU) normalized to HPRT, GADPH and β-actin or stain free gel for cDNA and protein respectively. * $p<0.05$ vs. control.

7.2 CT-1 is not a mediator of Aldo effects in VECs

Likewise to what was previously shown in VICs, we next hypothesized that CT-1 could mediate Aldo effects in VECs.

In CT-1 knock-down cells, Aldo diminished the expression of CD31, VE-cadherin and vWF at mRNA (Figure 44A) and protein levels (Figure 44B) in the same way than Aldo incubated in control cells.

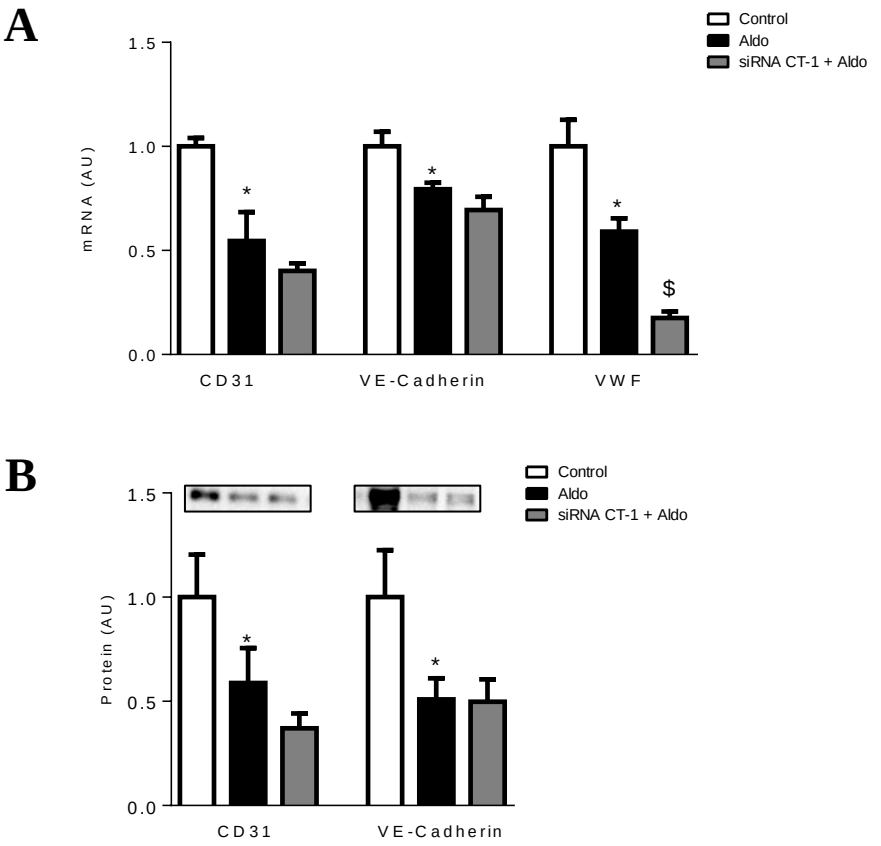

Figure 44. Effects of CT-1-knock down on VECs markers. Quantification of VECs markers (CD31, VE-Cadherin and vWF) at mRNA **(A)** and protein levels **(B)**. All conditions were performed at least in triplicate. Histograms with bars represents the mean ± SEM of each group in arbitrary units (AU) normalized to HPRT, GADPH and β-actin or stain free gel for cDNA and protein respectively. * $p<0.05$ vs. control. $ $p<0.05$ vs. Aldo.

In CT-1 silenced cells, Aldo induced the expression of the VICs activation markers α-SMA, vimentin, MMP-2 and slug at the mRNA in the same way than Aldo incubated in control cells (Figure 45A). Nevertheless, in CT-1-

silenced cells, Aldo did not induce the expression of the VICs activation markers α-SMA, vimentin and MMP-2 at the protein levels (Figure 45B).

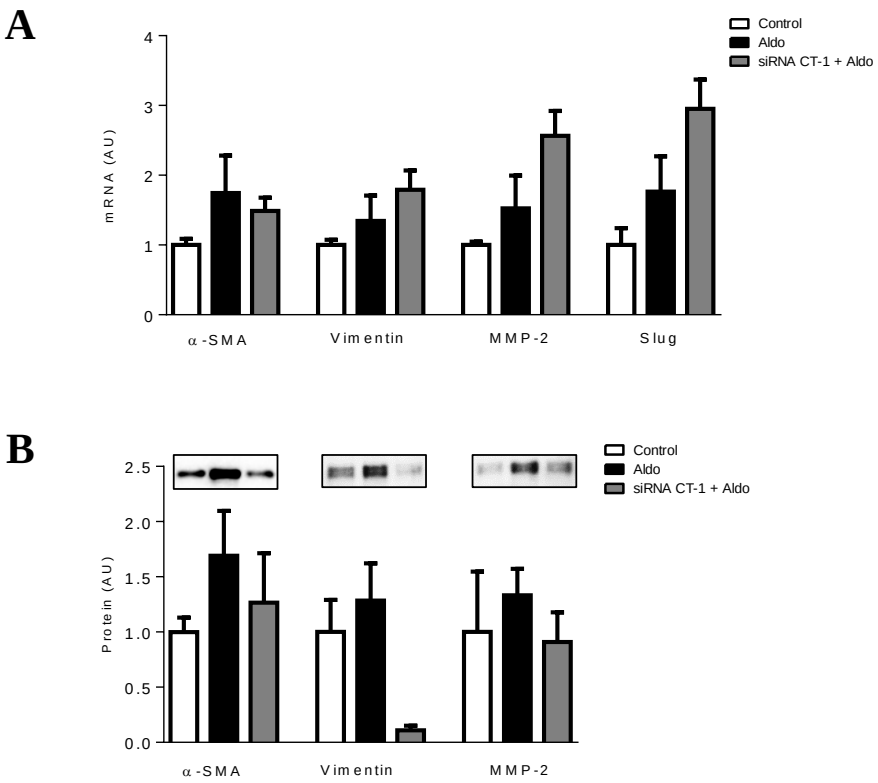

Figure 45. Effects of CT-1-knock down on VICs activation markers in VECs. Quantification of VICs activation markers (α-SMA, vimentin, MMP-2 and slug) at mRNA **(A)** and protein levels **(B)**. All conditions were performed at least in triplicate. Histograms with bars represents the mean ± SEM of each group in arbitrary units (AU) normalized to HPRT, GADPH and β-actin or stain free gel for cDNA and protein respectively. * $p<0.05$ vs. control.

Interestingly, Aldo increased the mRNA expression of decorin, biglycan, versican and lumican in CT-1 knock-down cells. These increases were similar than those found in Aldo-treated control VECs (Figure 46A). At the protein levels, the expression and secretion of proteoglycans in CT-1 knock-down cells were similar as those found in Aldo–treated control cells (Figure 46B).

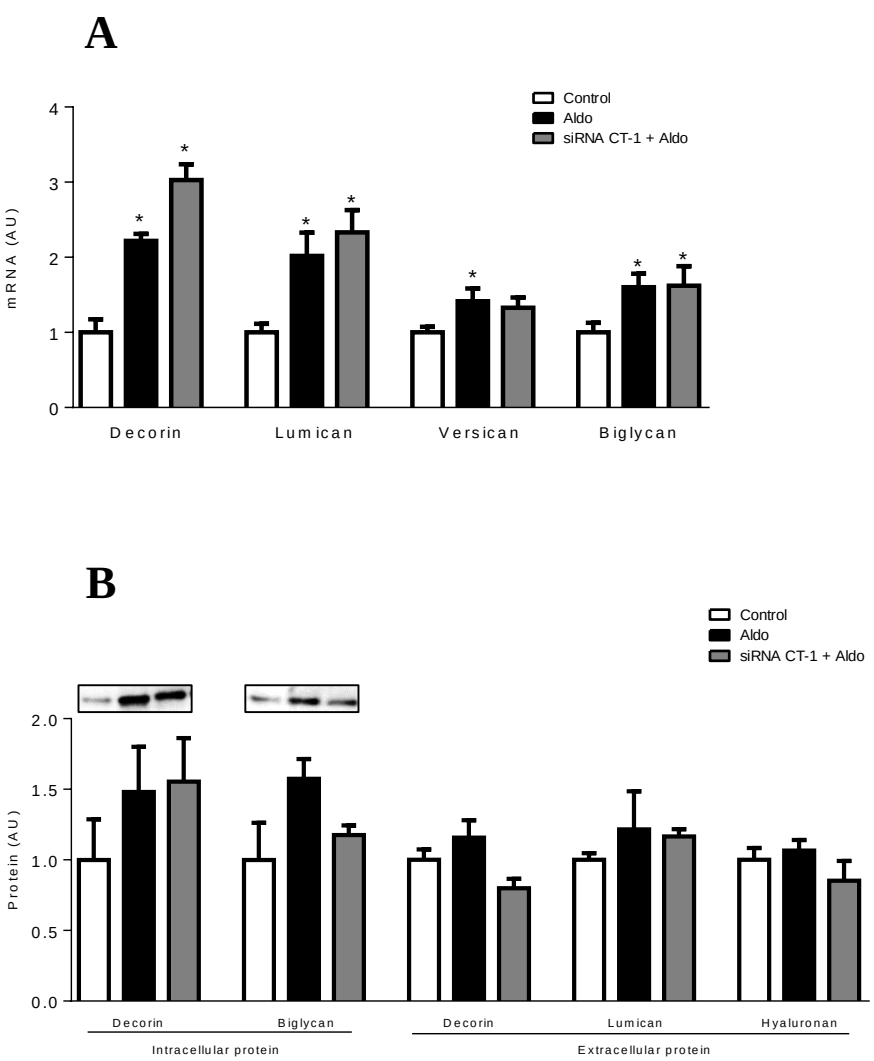

Figure 46. Effects of CT-1-knock down on proteoglycans expression in VECs. Quantification of proteoglycans (decorin, biglycan, lumican and versican) at mRNA levels **(A)**. Quantification of intracellular proteoglycans (decorin and biglycan) and extracellular proteoglycans (decorin, lumican and hyaluronan) at protein levels **(B)**. All conditions were performed at least in triplicate. Histograms with bars represents the mean ± SEM of each group in arbitrary units (AU) normalized to HPRT, GADPH and β-actin or stain free gel for cDNA and protein respectively. * $p<0.05$ vs. control.

8. New intracellular signaling pathways involved on Aldo effects in VECs

The cytokine array revealed that Aldo up-regulated CD14 (129%), a ligand of Toll Like Receptor-4 (TLR4) signaling that has been shown to mediate mineralocorticoid effects in cardiomyocytes [143] (Figure 47). In VECs treated with Aldo, CD14 increased at 24 hours (Figure 48).

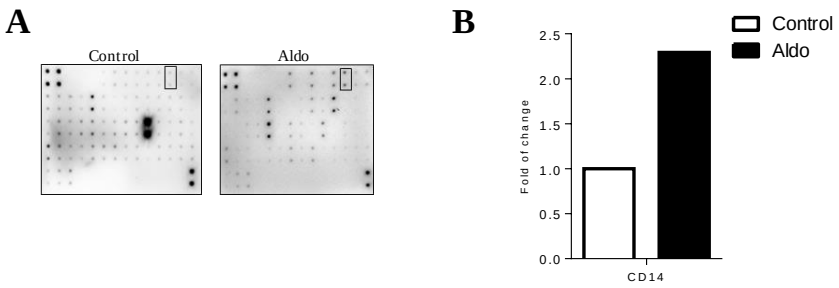

Figure 47. Identification of cytokines from VECs supernatant treated with Aldo in a cytokine array. Representative images of human cytokine array blots probed with the cell supernatant samples **(A)**. Each blot represents the immunoreactive staining with each cytokine. The lack of dots represented the negative and blank control. The blots marked inside the box are the CD14 expression. The fold of change of CD14 was determined by comparing the pixel intensity of the respective blots to that of the positive control on the same array **(B)**.

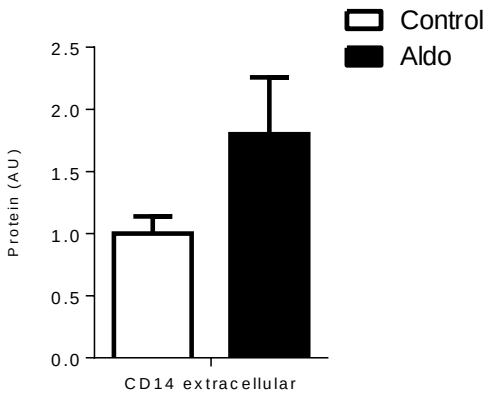

Figure 48. Cytokine array validation in VECs treated with Aldo. Quantification of extracellular CD14. All conditions were performed at least in triplicate. Histograms with bars represents the mean ± SEM of each group in arbitrary units (AU) normalized to stain free gel for protein. * $p<0.05$ vs. control

8.1 CD14 is a mediator of Aldo effects in VECs

We next studied the involvement of CD14 in Aldo effects in VECs, using a siRNA against CD14 to knock-down its expression.

In CD14 knock-down cells, Aldo did not decrease VE-cadherin at mRNA (Figure 49A) and protein levels (Figure 49B). However, in CD14-silenced cells, Aldo diminished the expression of CD31.

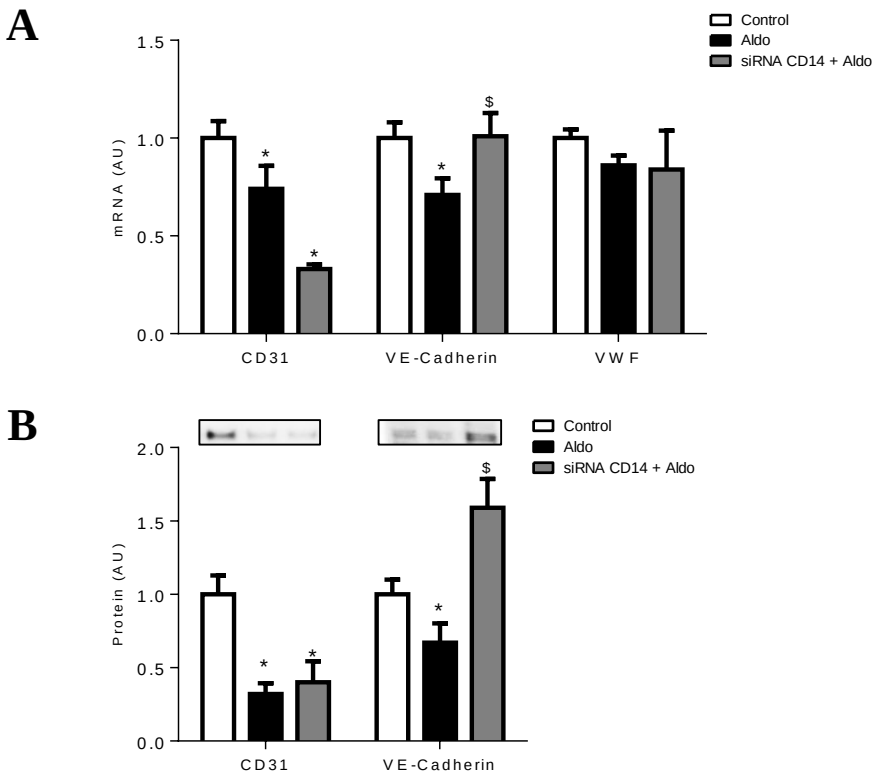

Figure 49. Effects of CD14-knock down on VECs markers. Quantification of VECs markers (CD31, VE-Cadherin and vWF) at mRNA **(A)** and protein levels **(B)**. All conditions were performed at least in triplicate. Histograms with bars represents the mean ± SEM of each group in arbitrary units (AU) normalized to HPRT, GADPH and β-actin or stain free gel for cDNA and protein respectively. * $p<0.05$ vs. control. $ $p<0.05$ vs. Aldo.

Interestingly, Aldo treatment did not increase the VICs activation markers α-SMA, vimentin, MMP-2 and slug in CD14 knock-down cells both at the mRNA (Figure 50A) and the protein levels (Figure 50B).

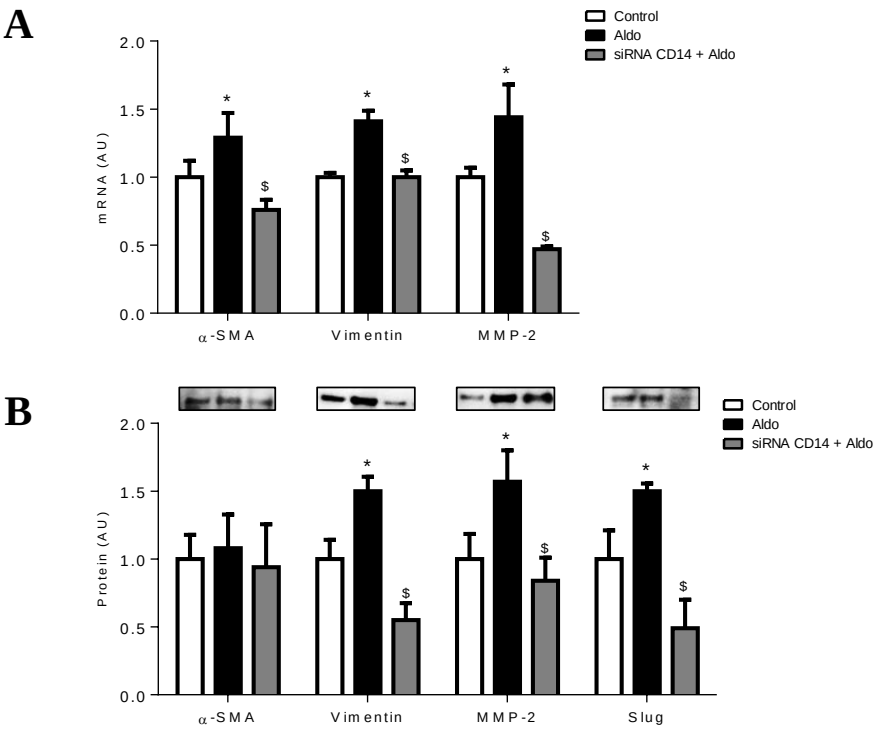

Figure 50. Effects of CD14-knock down on VICs markers in VECs. Quantification of VICs activation markers (α-SMA, vimentin, MMP-2 and slug) at mRNA **(A)** and protein levels **(B)**. All conditions were performed at least in triplicate. Histograms with bars represents the mean ± SEM of each group in arbitrary units (AU) normalized to HPRT, GADPH and β-actin or stain free gel for cDNA and protein respectively. * $p<0.05$ vs. control. $ $p<0.05$ vs. Aldo.

Cells silenced for CD14 treated with Aldo presented a reduction in the expression of most of the proteoglycans analyzed, being significant ($p<0.05$) for decorin, lumican and syndecan-1 at the mRNA levels (Figure 51A) and for decorin and aggrecan at the protein levels (Figure 51B).

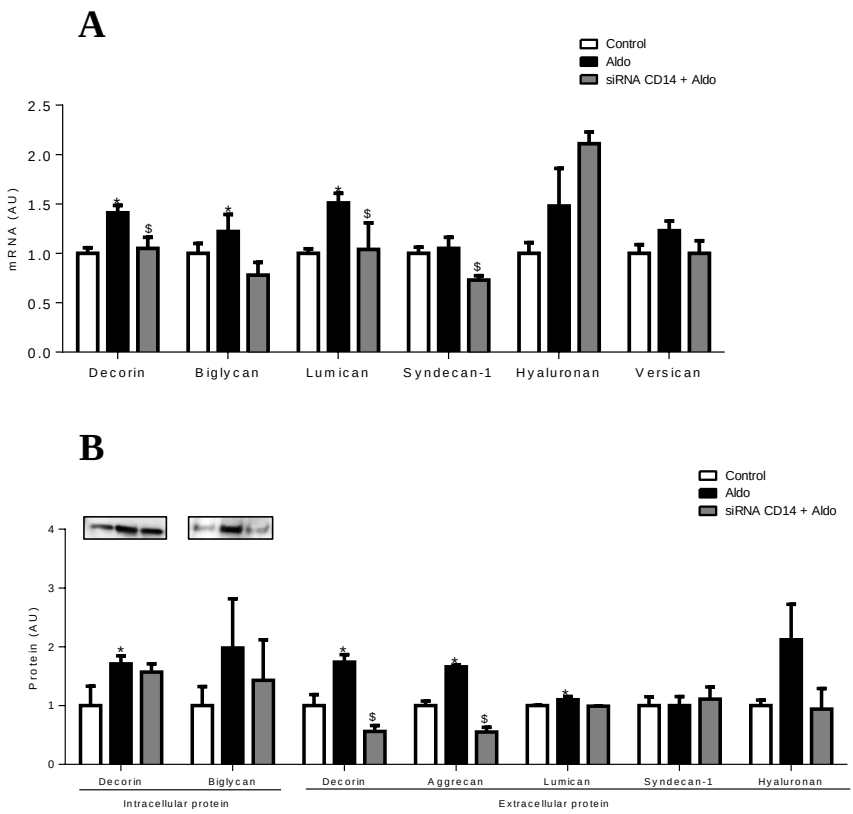

Figure 51. **Effects on proteoglycans expression in CD14-knock down VECs.** Quantification of proteoglycans (decorin, biglycan, lumican, syndecan-1, hyaluronan and versican) at mRNA levels **(A)**. Quantification of intracellular proteoglycans (decorin and biglycan) and extracellular proteoglycans (decorin, lumican, aggrecan, syndecan-1 and hyaluronan) at protein levels **(B)**. All conditions were performed at least in triplicate. Histograms with bars represents the mean ± SEM of each group in arbitrary units (AU) normalized to HPRT, GADPH and β-actin or stain free gel for cDNA and protein respectively. * $p<0.05$ vs. control. $ $p<0.05$ vs. Aldo.

II. IN VIVO STUDIES

9. Effects of Spironolactone in mitral valve morphology and proteoglycans content in a MVP mouse model

We generated a MVP mouse model according to the literature [144]. 129/sv mice were treated with nordexfenfluramine (NDF), in the presence of the MRA Spironolactone as an additive in the food. Mice treated with NDF or with NDF+Spironolactone presented similar body weight, heart weight, systolic blood pressure and heart rate as compared to control mice. These data are summarized in table 6.

Parameters	Control	NDF	NDF + Spiro
Body weight (g)	26.54 ± 0.6	28.33 ± 0.71	27.45 ± 0.71
HW/TL (g/cm)	0.07 ± 0.002	0.08 ± 0.001	0.08 ± 0.002
SBP (mm Hg)	128.56 ± 5.08	120.10 ± 4.36	119.19 ± 2.54
HR (bpm)	674.33 ± 15.61	694.05 ± 16.28	668.19 ± 20.08

Table 6. Effect of the administration of NDF on body weight, heart weight, systolic blood pressure and heart rate. Summary data of blood pressure and weights. Data values represent mean ± SEM. HW: Heart weight; TL: tibia length; SBP: systolic blood pressure; HR: heart rate; bpm: beats per minute.

The analysis of mitral valve morphology revealed that both mitral valve area and thickness were significantly increased ($p<0.05$) in NDF mice as compared to controls (Figure 52). This effect was fully prevented by Spironolactone treatment.

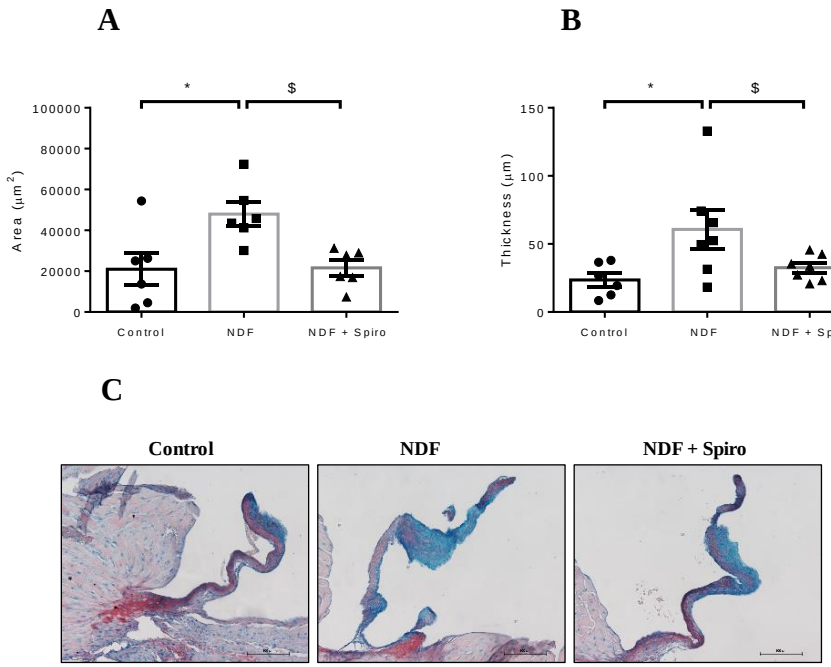

Figure 52. Effects of NDF administration on mitral valve area and thickness. Quantification of mitral valve area **(A)** and thickness **(B)**. Representative microphotographs of murine mitral valve sections stained for Sirius red and Alcian blue **(C)**. Histogram bars represent the mean ± SEM in arbitrary units versus control group. Magnification 20x *p<0.05 vs. control. $p<0.05 vs. NDF.

Moreover, NDF-treated mice presented greater staining (p<0.05) for total proteoglycans content and particularly for decorin, biglycan, lumican and aggrecan immunostainings as compared to controls. Spironolactone treatment reversed NDF effects on mitral valve proteoglycans expression (Figure 53).

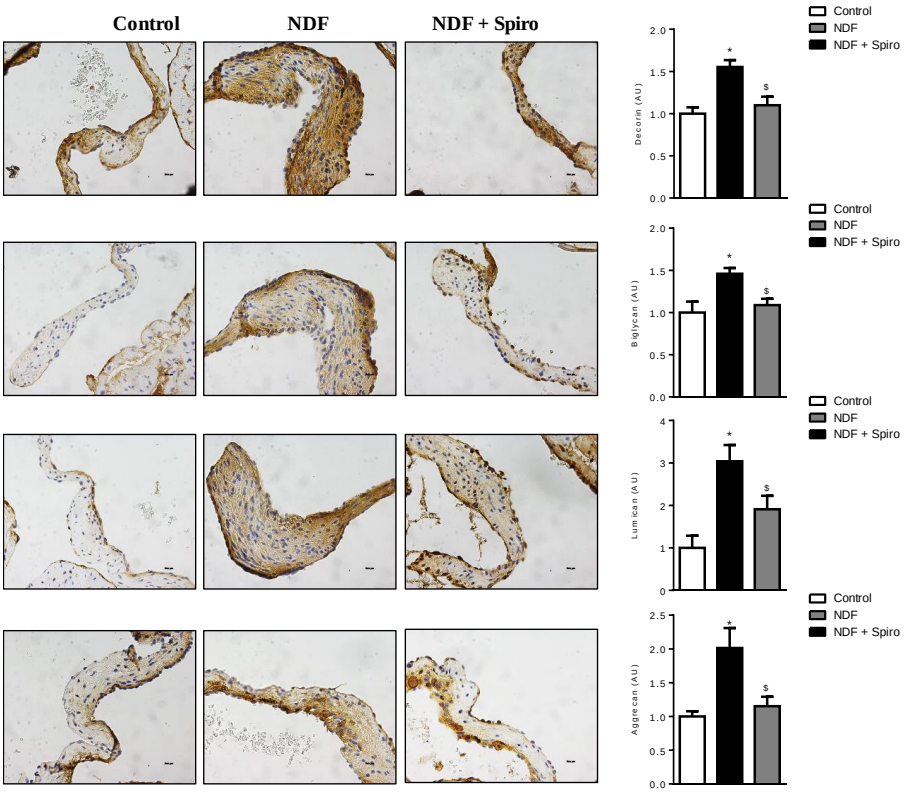

Figure 53. Effects of NDF administration on proteoglycans content in mitral valves. Representative microphotographs of murine mitral valve sections stained for decorin, biglycan, lumican, aggrecan, and quantification of immunochemistry staining. Histogram bars represent the mean ± SEM in arbitrary units versus control group. Magnification 40x. *p<0.05 vs. control. $p<0.05 vs. NDF.

10. Effects on mitral valve morphology and proteoglycans content in conditional SMA-MR-KO mice treated with NDF.

In collaboration with Dr. Frédéric Jaisser laboratory (*Centre de Recherche des Cordeliers*, Paris, France) we had access to the SMA-MR-KO mice, which lack MR specifically in α-SMA positive cells (VICs). These mice

were treated with NDF to explore if VICs were the principal cell type involved in the development of MVP. Littermates C57BL6 mice were used as controls. All groups presented similar body weight, heart weight, systolic blood pressure and heart rate. These data are summarized in table 7.

Parameters	Control	Control + NDF	SMA-MR-KO + NDF
Body weight (g)	30.24 ± 0.84	31.43 ± 0.43	30.46 ± 0.57
HW/TL (g/cm)	0.08 ± 0.003	0.08 ± 0.004	0.08 ± 0.001
SBP (mm Hg)	97.17 ± 2.32	95.22 ± 1.99	97.65 ± 1.48
HR (bpm)	548.83 ± 15.13	549.5 ± 11.77	592.75 ± 14.62

Table 7. Effect of the administration of NDF on body weight, heart weight, systolic blood pressure and heart rate. Data values represent mean ± SEM. HW: Heart weight; TL: tibia length; SBP: systolic blood pressure; HR: heart rate; bpm: beats per minute.

The analysis of the mitral valve morphology revealed that both mitral valve area and thickness were significantly increased ($p<0.05$) in NDF-treated control mice as compared to controls. There were no differences between controls and SMA-MR-KO treated with NDF and between NDF-treated control mice and SMA-MR-KO mice (Figure 54).

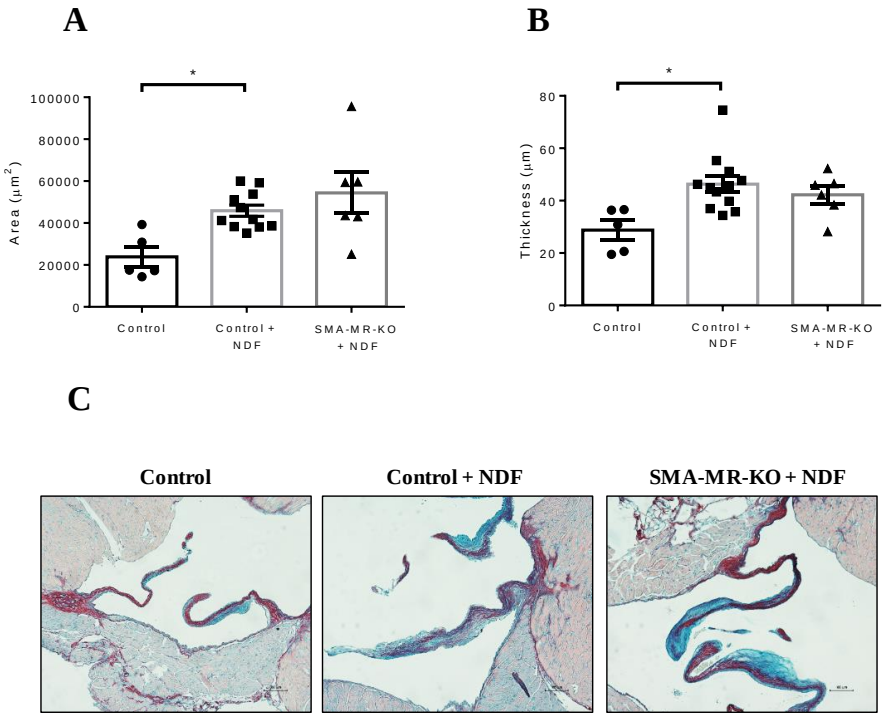

Figure 54. Effects of NDF administration on mitral valve area and thickness in SMA-MR-KO mice. Quantification of mitral valve area **(A)** and thickness **(B)**. Representative microphotographs of murine mitral valve sections stained for Sirius red and Alcian blue **(C)**. Histogram bars represent the mean ± SEM in arbitrary units versus control group. Magnification 20x . *p<0.05 vs. control.

Control mice treated with NDF presented greater staining for total proteoglycans content and particularly greater (p<0.05) immunostaining for biglycan, lumican and aggrecan as compared to controls. SMA-MR-KO treated with NDF presented similar staining for total proteoglycans content as compared to controls treated with NDF (Figure 55).

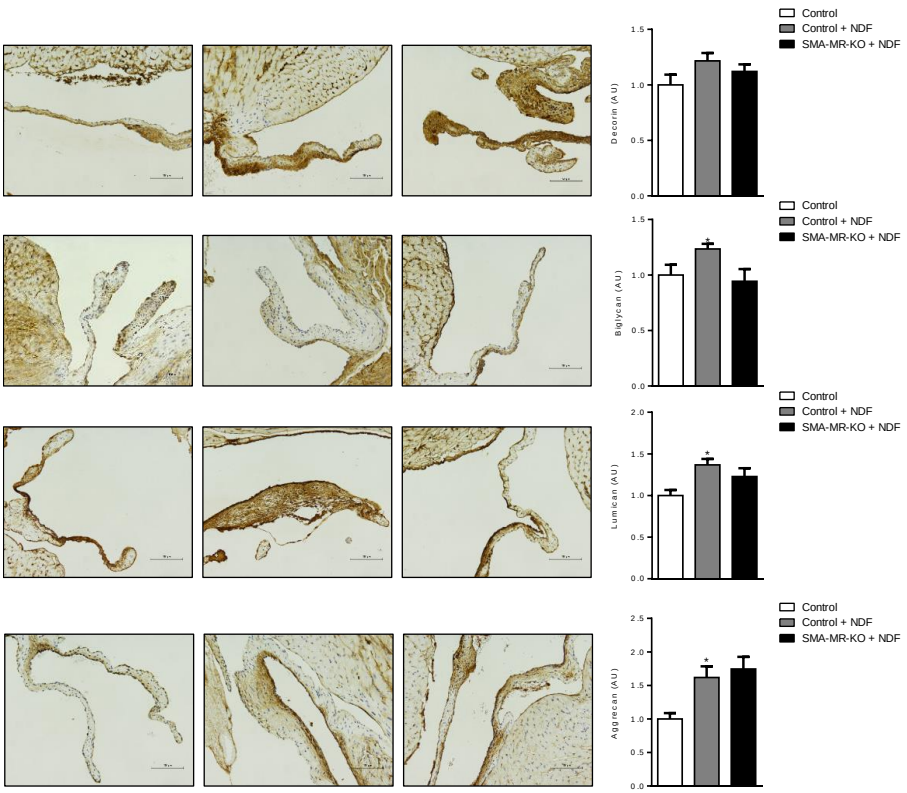

Figure 55. Effects of NDF administration on proteoglycans content in mitral valve from SMA-MR-KO mice. Representative microphotographs of murine mitral valves sections stained for decorin, biglycan, lumican and aggrecan and quantification of immunochemistry staining. Histogram bars represent the mean ± SEM in arbitrary units versus control group. Magnification 20x and 40x. *p<0.05 vs. control.

11. Effects on mitral valve morphology and proteoglycans content in conditional Vecadh-MR-KO mice treated with NDF.

In collaboration with Dr. Frédéric Jaisser laboratory we next used the Vecadh-MR-KO mouse model, which lack specifically MR in endothelial

cells (VECs). Littermates C57Bl6 mice were used as controls. All groups presented similar body weight, heart weight, systolic blood pressure and heart rate. These data are summarized in table 8.

Parameters	Control	Control + NDF	Vecadh-MR-KO + NDF
Body weight (g)	**28.75 ± 0.09**	**29.15 ± 0.71**	**30.63 ± 0.54**
HW/TL (g/cm)	**0.08 ± 0.003**	**0.08 ± 0.004**	**0.09 ± 0.004**
SBP (mm Hg)	**93 ± 1.44**	**98.39 ± 1.42**	**97.38 ± 2.26**
HR (bpm)	**550.33 ± 22.69**	**586.89 ± 18.04**	**575.29 ± 9.39**

Table 8. Effect of the administration of NDF on body weight, heart weight, systolic blood pressure and heart rate in Vecadh-MR-KO mice. Data values represent mean ± SEM. HW: Heart weight; TL: tibia length; SBP: systolic blood pressure; HR: heart rate; bpm: beat per minute.

The analysis of mitral valve morphology revealed that both mitral valve area and thickness were significantly increased ($p<0.05$) in control mice treated with NDF. Interestingly, the Vecadh-MR-KO mice treated with NDF presented a significantly ($p<0.05$) lower increase in the mitral valve area and thickness as compared to control animals treated with NDF (Figure 56).

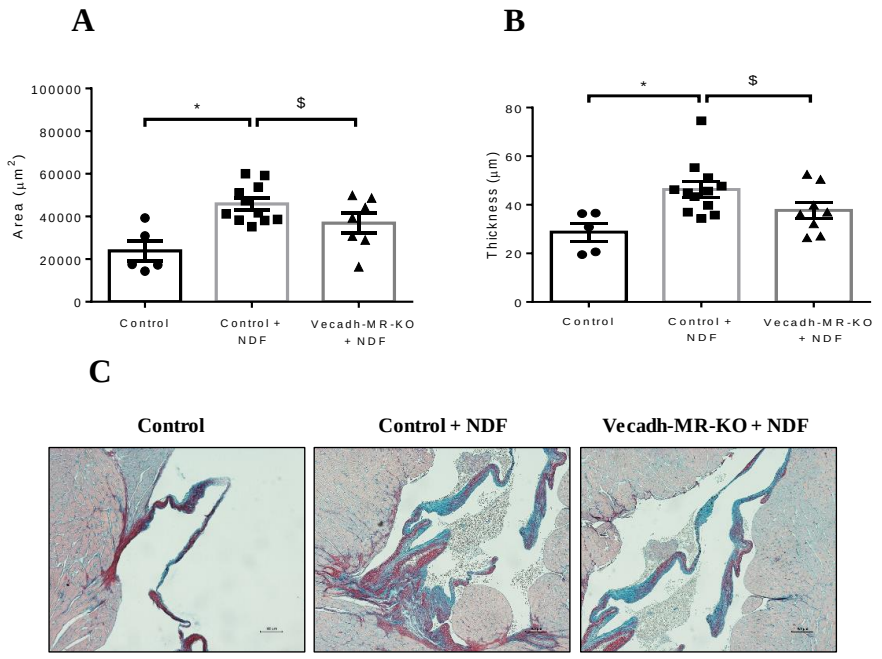

Figure 56. Effects of NDF administration on mitral valve area and thickness in Vecadh-MR-KO. Quantification of mitral valve area **(A)** and thickness **(B)**. Representative microphotographs of murine mitral valve sections stained for Sirius red and Alcian blue **(C)**. Histogram bars represent the mean ± SEM in arbitrary units versus control group. Magnification 20x. *p<0.05 vs. control. $p<0.05 vs. control + NDF.

Quantification of immunostaining showed a significant increment in proteoglycans content in control mice treated with NDF. However, NDF-treated Vecadh-MR-KO mice did not exhibit any changes in proteoglycans levels as compared to controls (Figure 57).

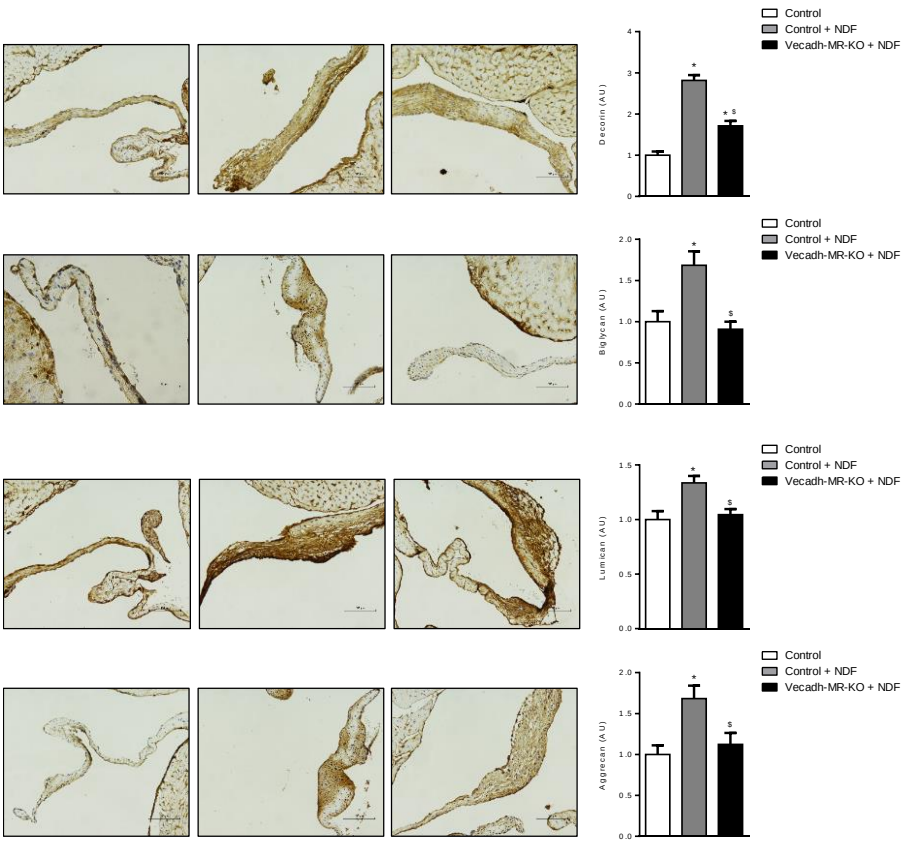

Figure 57. Effects of NDF administration on proteoglycan content in mitral valve from Vecadh-MR-KO mice. Representative microphotographs of murine mitral valve sections stained for decorin, biglycan, lumican and aggrecan and quantification of immunochemistry staining. Histogram bars represent the mean ± SEM in arbitrary units versus control group. Magnification 20x and 40x. *p<0.05 vs. control. $p<0.05 vs. control + NDF.

III. CLINICAL STUDY

12. Mitral valve remodeling in MVP patients

The last step of our study was to investigate if the treatment with a MRA in MVP patients could affect mitral valve composition. MVP patients treated with a MRA were selected from our cohort of patients and matched with patients that were not treated with a MRA by age, sex and cardiac function parameters. The decision of treatment with MRA was based upon clinician's criterion.

The baseline characteristics of the whole cohort of MVP patients are presented in Table 9. In keeping with the typical characteristics of patients presenting MVP, mean age was 68±10 years and 68% were male. A significant proportion suffered from concomitant coronary artery disease, hypertension, diabetes mellitus, and hyperlipidemia. Echocardiographic variables were those expected in patients with severe MVP.

Baseline characteristics of patients and controls	
n	103
Age (years ± SD)	68 ± 10
Male (%)	68 (65)
Hypertension (%)	59 (56)
Hypercolesterolemia (%)	48 (46)
Diabetes mellitus (%)	9 (9)
Coronary artery disease (%)	22 (21)
Heart failure	
NYHA functional class	
I	9 (9)
II	51 (49)
III	42 (40)
IV	2 (2)
Admission for heart failure (%)	20 (19)
BNP (pg/ml ± SD)	266 ± 342
Medications	
ACE inhibitors (%)	38 (36)
ARB (%)	21 (20)
Spironolactone (%)	6 (6)
Eplerenone (%)	3 (3)
Diuretics (%)	80 (76)
Betablockers (%)	52 (50)
Digoxin (%)	18 (17)
Echocardiographic parameters	
LVEF (mean % ± SD)	60.6±10.4
Systolic dysfunction (LVEF <60%) (%)	36 (34)
Severe systolic dysfunction (LVEF <35%) (%)	2 (2)
End diastolic diameter (mm ± SD)	59± 7
Indexed end diastolic diameter (mm/m^2 ± SD)	33±4
End systolic diameter (mm ± SD)	40±8
Indexed end systolic diameter (mm/m^2 ± SD)	23±7
Systolic pulmonary artery pressure (mmHg ± SD)	47±12
MVP etiologic subgroups	
Barlow disease (%)	70 (67)
Fibroelastic deficiency (%)	30 (30)
Syndromic MVP	1 (1)
Associated to hypertrophic cardiomyopathy	2 (2)

Table 9. Baseline characteristics of patients and controls. NYHA: New York Heart Association classification of heart failure. BNP: brain natriuretic peptide. ACE: angiotensin converting enzyme. ARB: angiotensin receptor blocker. LVEF: left ventricle ejection fraction.

The baseline characteristics of the groups of patients treated or not with a MRA are presented in Table 10. There were no significant differences between both groups regarding clinical variables, the rest of medications and echocardiographic parameters, with the exception of the systolic pulmonary arterial pressure.

Baseline characteristics of patients MRA and no MRA treatment			
	MRA	**No MRA**	**p**
n	9	14	
Age (years ± SD)	72±9	72±7	1.000
Male (%)	6 (67)	9 (64)	1.000
Hypertension (%)	9 (100)	9 (64)	0.116
Hypercolesterolemia (%)	2 (22)	5 (36)	0.657
Diabetes mellitus (%)	0 (0)	2 (14)	0.502
Coronary artery disease (%)	3 (33)	1 (7)	0.260
Heart failure			
NYHA functional class			
I	0 (0)	0 (0)	1.000
II	3 (33)	8 (57)	0.400
III	5 (55)	6 (43)	0.680
IV	1 (11)	0 (0)	0.391
Admission for heart failure (%)	5 (55)	2 (14)	0.179
BNP (pg/ml ± SD)	505±635	320±433	0.393
Medications			
ACE inhibitors (%)	4 (44)	4 (29)	0.657
ARB (%)	3 (33)	4 (29)	1.000
Spironolactone (%)	7 (78)	0 (0)	n/a
Eplerenone (%)	2 (22)	0 (0)	n/a
Diuretics (%)	9 (100)	10 (71)	0.127
Betablockers (%)	5 (55)	6 (43)	0.680
Digoxin (%)	4 (44)	1 (7)	0.056
Echocardiographic parameters			
LVEF (mean % ± SD)	55±16	57±13	0.734
Systolic dysfunction (LVEF <60%) (%)	5 (55)	7 (50)	1.0
Severe systolic dysfunction (LVEF <35%) (%)	1 (11)	1 (7)	1.0
End diastolic diameter (mm ± SD)	61±7	57±7	0.374
Indexed end diastolic diameter (mm/m^2 ± SD)	33±4	32±3	0.697
End systolic diameter (mm ± SD)	43±10	39±10	0.453
Indexed end systolic diameter (mm/m^2 ± SD)	23±6	22±3	0.627
Systolic pulmonary artery pressure (mmHg ± SD)	53±11	44±8	**0.033**

Table 10. Baseline characteristics of patients MRA and no MRA treatment. NYHA: New York Heart Association classification of heart failure. BNP: brain

natriuretic peptide. ACE: angiotensin converting enzyme. ARB: angiotensin receptor blocker. LVEF: left ventricle ejection fraction.

Mitral valves from patients treated with MRA presented a slightly increment in VECs markers as compared to mitral valves from patients without MRA treatment, although these differences did not reach statistical significance (Figure 58).

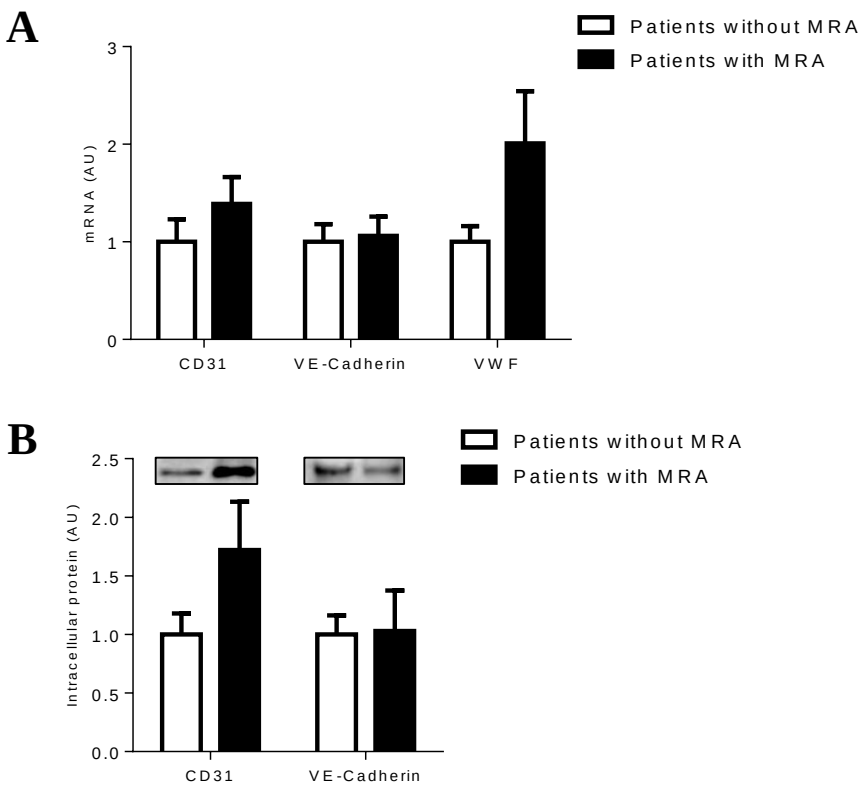

Figure 58. VECs markers in patients treated with MRA or without MRA. Quantification of VECs markers (CD31, VE-Cadherin and vWF) at mRNA **(A)** and protein levels **(B)**. Histograms with bars represents the mean ± SEM of each group

in arbitrary units (AU) normalized to HPRT, GADPH and β-actin or stain free gel for cDNA and protein respectively.

The expression of the quiescent VIC marker Chm-1did not change in mitral valves from patients treated with a MRA as compared with patients without MRA treatment. The expression of the VICs markers α-SMA, vimentin, MMP-2 and slug were slightly decreased in mitral valves from MRA-treated patients, being significantly ($p<0.05$) for α-SMA and MMP-2 at the mRNA levels as compared with MVP patients without MRA treatment (Figure 59).

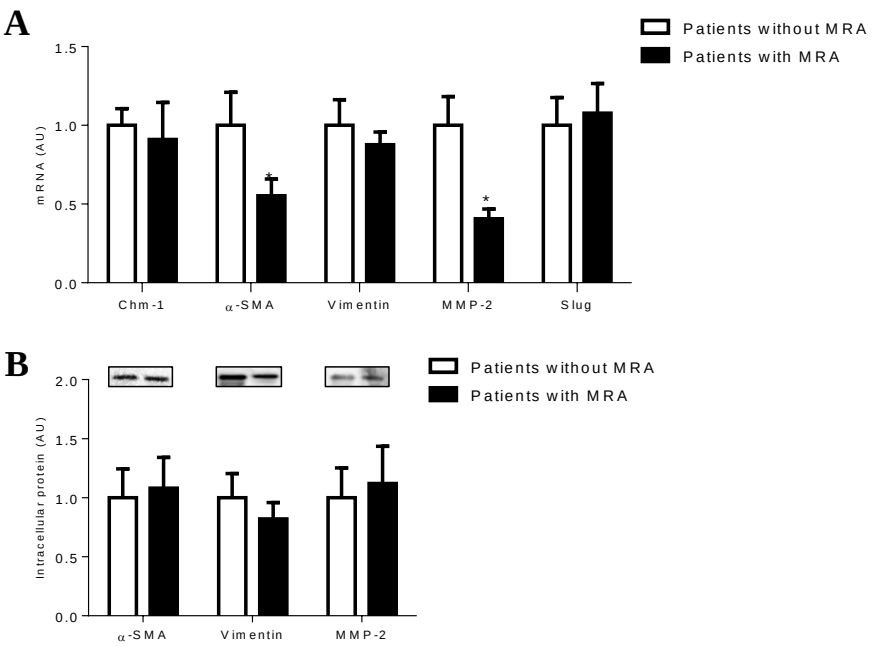

Figure 59. Quiescent and VICs activation markers in patients treated with or without MRA. Quantification of qVICs marker (Chm-1) and VICs activation markers (α-SMA, vimentin, MMP-2 and slug) at mRNA **(A)** and protein levels **(B)**. Histograms with bars represents the mean ± SEM of each group in arbitrary units (AU) normalized to HPRT, GADPH and β-actin or stain free gel for cDNA and protein respectively. * $p<0.05$ vs. Patients without MRA.

The expression of proteoglycans in the mitral valves was slightly decreased in MRA-treated patients, being significant ($p<0.05$) for lumican as compared with MVP patients without MRA treatment (Figure 60).

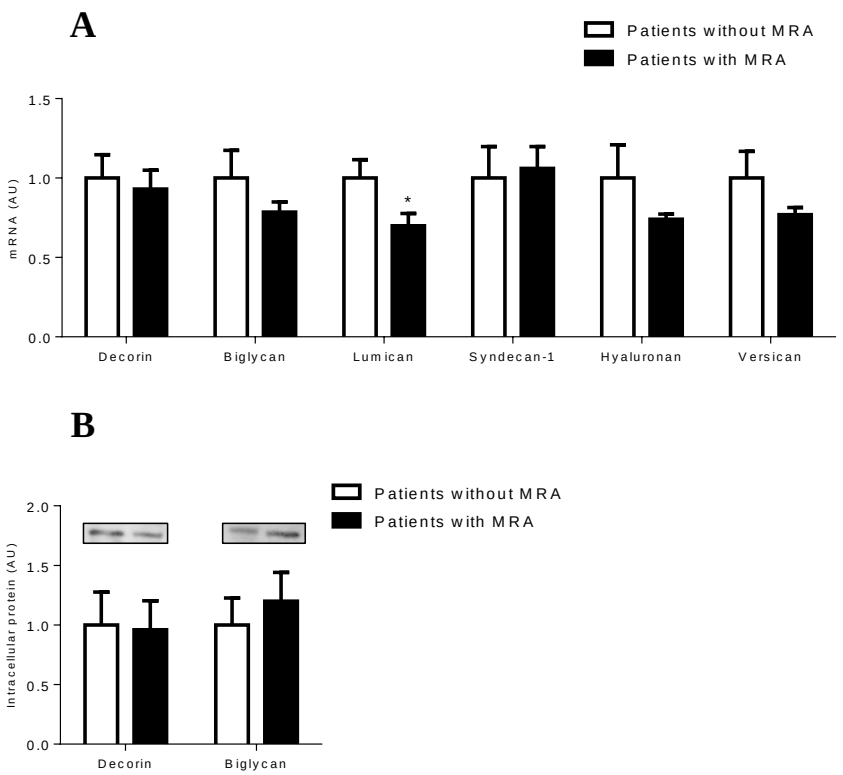

Figure 60. Proteoglycans expression in patients treated with or without MRA. Quantification of proteoglycans (decorin, biglycan, lumican, syndecan-1, hyaluronan and versican) at mRNA levels **(A)**. Quantification of proteoglycans (decorin and biglycan) at protein levels **(B)**. Histograms with bars represents the mean ± SEM of each group in arbitrary units (AU) normalized to HPRT, GADPH and β-actin or stain free gel for cDNA and protein respectively. * $p<0.05$ vs. Patients without MRA.

Interestingly, the expression of CT-1 and CD14 at the mRNA (Figure 61A) and the protein levels (Figure 61B) decreased significantly ($p<0.05$) in

MRA-treated mitral valves as compared with mitral valves from patients without MRA treatment.

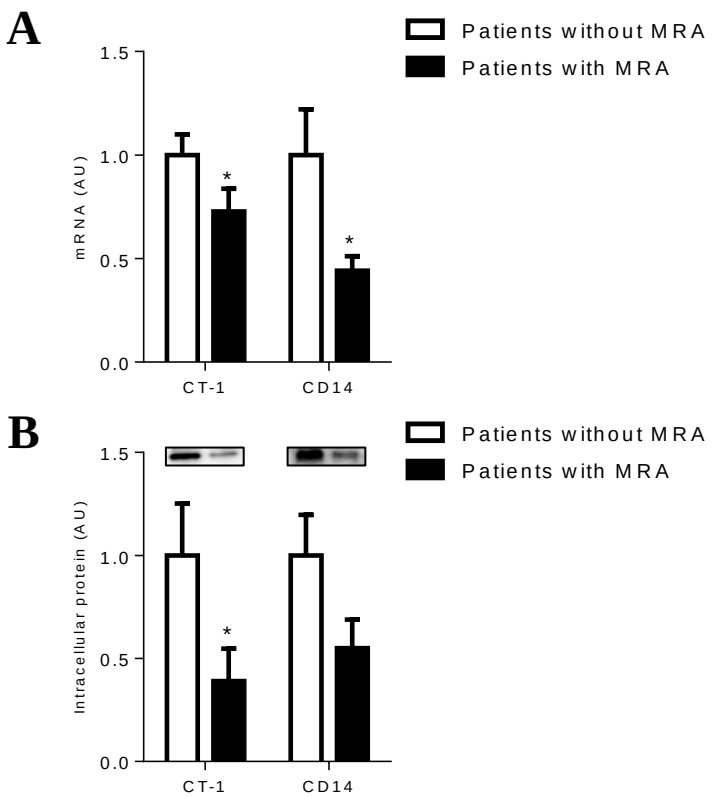

Figure 61. CT-1 and CD14 expression in patients treated with or without MRA. Quantification of CT-1 and CD14 at mRNA **(A)** and protein levels **(B)**. Histograms with bars represents the mean ± SEM of each group in arbitrary units (AU) normalized to HPRT, GADPH and β-actin or stain free gel for cDNA and protein respectively. * $p<0.05$ vs. Patients without MRA.

A decrease in the spongiosa layer thickness (marked with asterisk) and consequently in proteoglycans content (in blue) was observed in mitral valves from MVP patients treated with a MRA as compared with mitral valves from patients that did not receive a MRA.

Representative immunochemistry showed a reduction in the VECs markers VCAM-1 (classically considered marker of endothelial cell [145] and CD31 as well as in proteoglycans decorin, biglycan and versican in mitral valves from patients treated with a MRA as compared with mitral valves from patients that did not receive a MRA (Figure 62).

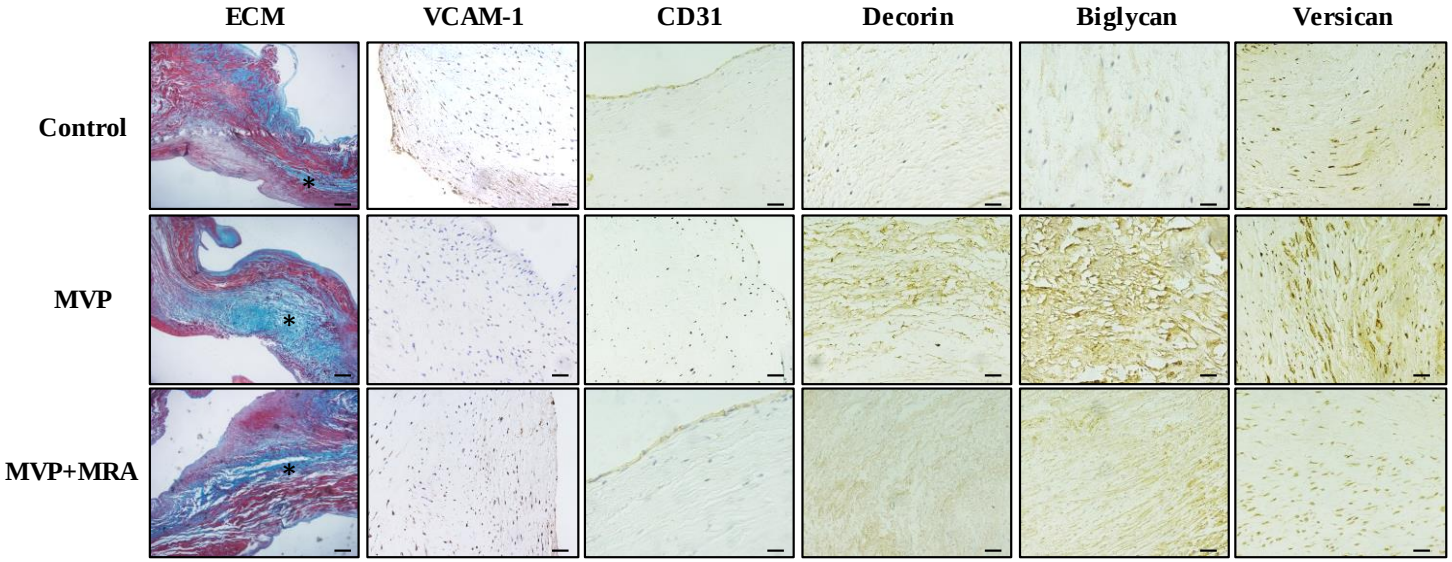

Figure 62. Extracellular proteoglycans expression in patients treated with or without MRA. Representative microphotographs of human mitral valve sections stained for Sirius red, Alcian blue, VCAM-1, CD31, decorin, biglycan and versican. Magnification 20x and 40x. * Marks Spongiosa layer.

DISCUSSION

MVP is one of the most common valvular abnormalities and currently there is not an effective treatment. Studies have focused on the discovery of new possible biomarkers in order to diagnose the valvular disease in the first stages and on exploring new possible treatments or combinations of treatments to revert or palliate the development of the disease.

The main goal of our project was to study the role of Aldo/MR pathway in the development of mitral valve alterations associated to MVP. Our results demonstrated for the first time the expression of MR in human mitral valve cells (VICs and VECs) and in human mitral valve tissue. Moreover, valvular tissue also expressed 11β-HSD2, identifying mitral valves as an Aldo-sensitive tissue. The *in vitro* experiments demonstrated that Aldo induced effects in both types of human mitral valve cells. In VICs, Aldo induced the activation of VICs through the mobilization of qVICs. Moreover, Aldo enhanced the secretion of proteoglycans. Aldo effects in VICs were mediated by CT-1 pathway. In VECs, Aldo promoted the differentiation into aVICs through the EndMT and increased proteoglycans expression. Aldo effects in VECs were mediated by CD14, a ligand of TLR-4 pathway. Furthermore, our *in vivo* studies showed that MR blockade by using a MRA exerted beneficial effects in a mouse model of MVP, preventing mitral valve remodeling and proteoglycans increase. The Vecadh-MR-KO-MVP mice revealed the implication of the endothelial MR in the development of MVP. Interestingly, the remodeling process in human mitral valves from MVP

patients treated with a MRA seemed to be attenuated as compared to mitral valves from MVP patients without MRA treatment.

1. Expression of enzymes controlling aldosterone synthesis and MR in the mitral valve.

Aldo is the main mineralocorticoid hormone that can binds to MR, a ligand-dependent transcription factor belonging to the nuclear receptor superfamily [146]. Aldo function is to stimulate renal sodium reabsorption and potassium excretion, therefore playing a major role in the control of blood pressure, electrolytic balance and extracellular volume homeostasis [88,94,147]. At cellular level, Aldo activity is dependent on the binding and activation of the cytoplasmic/nuclear MR. Aldo has a well-established pathophysiological role in hypertension and in cardiovascular disease due to the MR expression in cells such as cardiomyocytes, vascular smooth muscle cells, fibroblast, inflammatory cells and endothelial cells. In fact, some studies have demonstrated that alteration in Aldo levels and consequently MR hyperactivation can be either responsible or a factor in the onset and progression of several cardiovascular diseases, including metabolic syndrome, hypertension, coronary artery disease, and congestive HF [88,94,99]. Interestingly, in patients with these conditions, MR antagonism improves cardiac fibrosis and endothelial function [148,149]. Our study demonstrated for the first time the expression of MR in mitral valve cells, both VICs and

VECs. It has been proposed that endothelial cell MR could be a mediator of the switch from vascular health to disease in response to cardiovascular risk factors [150]. In line with these findings, our results leave open possibilities for the role of valvular MR as a new player in mitral valve diseases.

Importantly, MR is not a specific receptor on Aldo, because Aldo and cortisol bind to human MR with equal affinity and specificity, whereas the unique ligand of GR is cortisol [151,152]. For instance, the enzyme 11βHSD2, which prevents the binding of glucocorticoids to the MR by inactivating cortisol to the inactive metabolite 11-dehydrocorticosterone, confers to MR a high degree of selectivity for Aldo [153]. In contrast, in cells lacking this enzyme, the MR interacts with both Aldo and cortisol with a similar affinity [154,155]. We evidenced that 11βHSD2 was expressed in the mitral valve tissue. This is in line with other studies that analyze the expression of 11βHSD2 in other cardiac cells, such as cardiomyocytes, fibroblasts, smooth muscle cells and endothelial cells [91,140,156]. Thus, mitral valves emerge as a new Aldo-sensitive tissue.

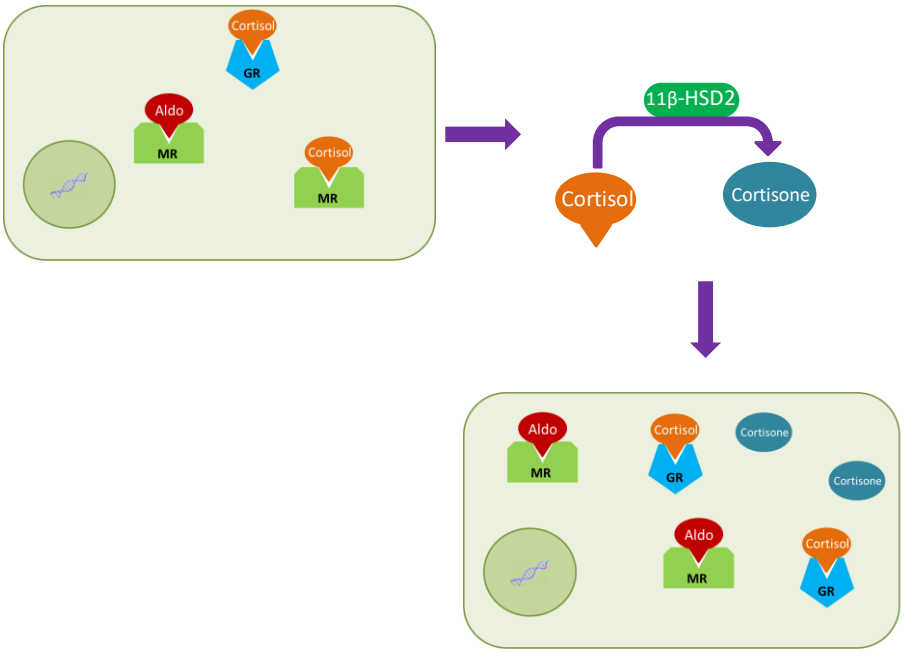

Figure 63. Schematic representation of MR and GR affinity to Aldo and Cortisol tissues where 11β-HSD2 is expressed.

2. Effects of Aldosterone in mitral valvular interstitial and endothelial cells

Several studies have demonstrated the involvement of Aldo in vascular remodeling, suppression of vascular endothelial function, induction of cardiac inflammation and fibrosis [88,157–159]. To our knowledge, this is the first study that analyze the effects of Aldo in valvular cells. Once demonstrated the presence of MR and the expression of 11βHSD2 in valvular cells, it is plausible to speculate that Aldo could exert actions in VICs and VECs. While VICs activation is characteristic of several different forms of valve

pathology, the stimulus and function of this process remain poorly understood.

Our study demonstrated for the first time that Aldo induced the activation of qVICs, resulting in an increment of proteoglycans expression. Moreover, these Aldo-dependent effects were prevented by prior administration of a MRA. Our data is in agreement with previous studies performed in cardiac fibroblasts and VSMCs where Aldo increases proliferation and ECM remodeling [160]. Aldo induces cardiac fibroblast activation resulting in an up-regulation of collagen expression, ECM remodeling and cardiac fibrosis [161–163]. In VSMCs, Aldo also enhances collagen production [164]. Complementarily, our results demonstrated for the first time that Aldo induced a differentiation of VECs into aVICs via EndMT, leading to an increment in proteoglycans expression. There are no studies that analyze the direct effects of Aldo on EndMT in endothelial cells; nevertheless, our result is in line with other observations showing that Aldo induces epithelial to mesenchymal transition via MR [165]. Moreover, in HUVECs, the use of MRAs blocks EndMT [113]. Furthermore, Aldo increases cardiac endothelial cell proliferation and pharmacological-specific blockade of MR inhibited endothelial cell proliferation in a preclinical model of HF [115]. Lastly, Aldo effects in VICs and VECs leaded to an increase in proteoglycans production, which is a hallmark in the development of MVP [14].

Interestingly, the conditioned medium experiments revealed that soluble factors produced by Aldo-treated VIC-VECs acted in paracrine manner,

promoting EndMT and VICs activation and proteoglycans secretion. Some authors tried to investigate the possible interactions and crosstalk between VECs and VICs in the development of valvulopathies [64] using co-cultures technology, conditioned medium, etc. to simulate the *in vivo* microenvironment. Two principal lines have been investigated; one where the signals and factors secreted between cells presented a protective role, and other where these signals and factors exacerbated the activation of VECs and/or VICs. Studies performed in sheep mitral valve cells demonstrated that mitral VECs and VICs secrete soluble factors that can reduce VIC activation and inhibit TGFβ-driven EndMT. These findings suggest that the endothelium of the mitral valve is critical for the maintenance of a quiescent VIC phenotype and that, in turn, VICs prevent EndMT [64]. However, our results demonstrated that one cell type was able to exacerbate Aldo effects on the other cell type. Accordingly, other studies have shown that in co-cultures there are paracrine factors and signals between both cells types able to aggravate VICs activation or VECs differentiation. Moreover, the ongoing reciprocal interactions between VECs and VICs may contribute to the thickened and fibrotic leaflets observed in ischemic mitral regurgitation and in other types of valve disease [166–168]. Nevertheless, more studies are needed to clarify this issue and to find the factors responsible of this effect.

Indeed, CT-1 emerges as a mediator of Aldo-induced VICs activation. CT-1 is a member of the IL-6 superfamily (group of inflammatory cytokines), which is expressed in different tissues including heart, vessels, skeletal

muscle, liver, lung, adipose tissue and kidney [169,170]. CT-1, a 201 amino acid protein, was originally isolated in 1995 for its ability to induce a hypertrophic response in neonatal cardiac myocytes. This cytokine mediates a pleiotropic set of growth and differentiation activities through the glycoprotein 130 (gp130)/leukemia inhibitory factor receptor (LIFR) heterodimer. Our results demonstrate that Aldo enhanced CT-1 expression in mitral valve cells. According with our findings, other studies described that CT-1 is upregulated by Aldo in cardiac cells [141,142,171]. Interestingly, CT-1 induced VICs activation and consequently an increment in proteoglycans expression. Furthermore, in VECs, CT-1 triggered EndMT and therefore VECs differentiation, as well as an increase in proteoglycans expression. Accordingly, experimental *in vitro* findings in rodent and canine fibroblasts [172–175] as well as in VSMCs [171] suggest that CT-1 behaves also as a pro-fibrotic factor in other cell types. In particular, CT-1 induces fibroblast growth and proliferation and collagen production [176]. Moreover, in human cardiac fibroblasts, CT-1 has been shown to stimulate myofibroblasts differentiation and ECM production [177]. In clinical populations, CT-1 positively correlates with left ventricular mass index and the serum concentration of carboxy-terminal propeptide of procollagen type I, a biomarker of collagen synthesis, reinforcing the idea that CT-1 may contribute to the development of cardiomyocyte hypertrophy, cardiac fibrosis, VSMC proliferation and endothelial dysfunction [142,176–179]. Furthermore, CT-1 has been described to mediate Aldo effects in cardiac

cells such as VSMCs, cardiomyocytes or cardiac fibroblasts [141,142,171]. In our experiments, CT-1 also mediated Aldo effects in VICs. Thus, CT-1-silenced VICs failed to express the VICs activation markers and secreted less amounts of proteoglycans than control cells. However, CT-1 did not emerged as an Aldo mediator in VECs. This is the first study that analyzes the role of CT-1 in the context of mitral valve disease, although it has been demonstrated a significant elevation in plasma CT-1 in patients with moderate/severe mitral regurgitation [180]. Further investigation is warranted to analyze if CT-1 could be a good biomarker or biotarget in MVP patients.

Looking at other possible mediators of Aldo effects in VECs, we explored CD14, a protein upregulated by Aldo. Our results showed that Aldo induced EndMT in VECs via CD14, a glycoprotein classically expressed by monocytes but also found in endothelial cells [181]. CD14 is the principal ligand of the TLR4 pathway [182]. Classically, the TLR4 signaling pathway has been related with the regulation of the inflammatory response and inflammation, but recent studies confirmed its role in endothelial cell proliferation and differentiation through EndMT [183–185]. Moreover, some studies demonstrated the implication of TLR4 pathway in myocardial infarction and HF, but the mechanism has been poorly studied [186]. Interestingly, Thalji NM. and coworkers observed an overexpression of CD14 (4.336-fold) in a microarray of human myxomatous mitral valves as compared with no myxomatous mitral valves [187], suggesting that TLR4/CD14 pathway could play a role in myxomatous valve diseases. Of

note, CD14 has been described as a mediator of Aldo/MR chronotropic effects in cardiomyocytes [143]. Finally, TLR4 signaling pathway has been involved in cardio-renal remodeling and dysfunction induced by Aldo in experimental models [188]. Besides, the inhibition of TLR-4 signaling attenuates Aldo-induced EndMT in a hypertension rat model [189]. In line with these papers, our results demonstrated the key role of CD14 as a mediator of Aldo effects in VECs.

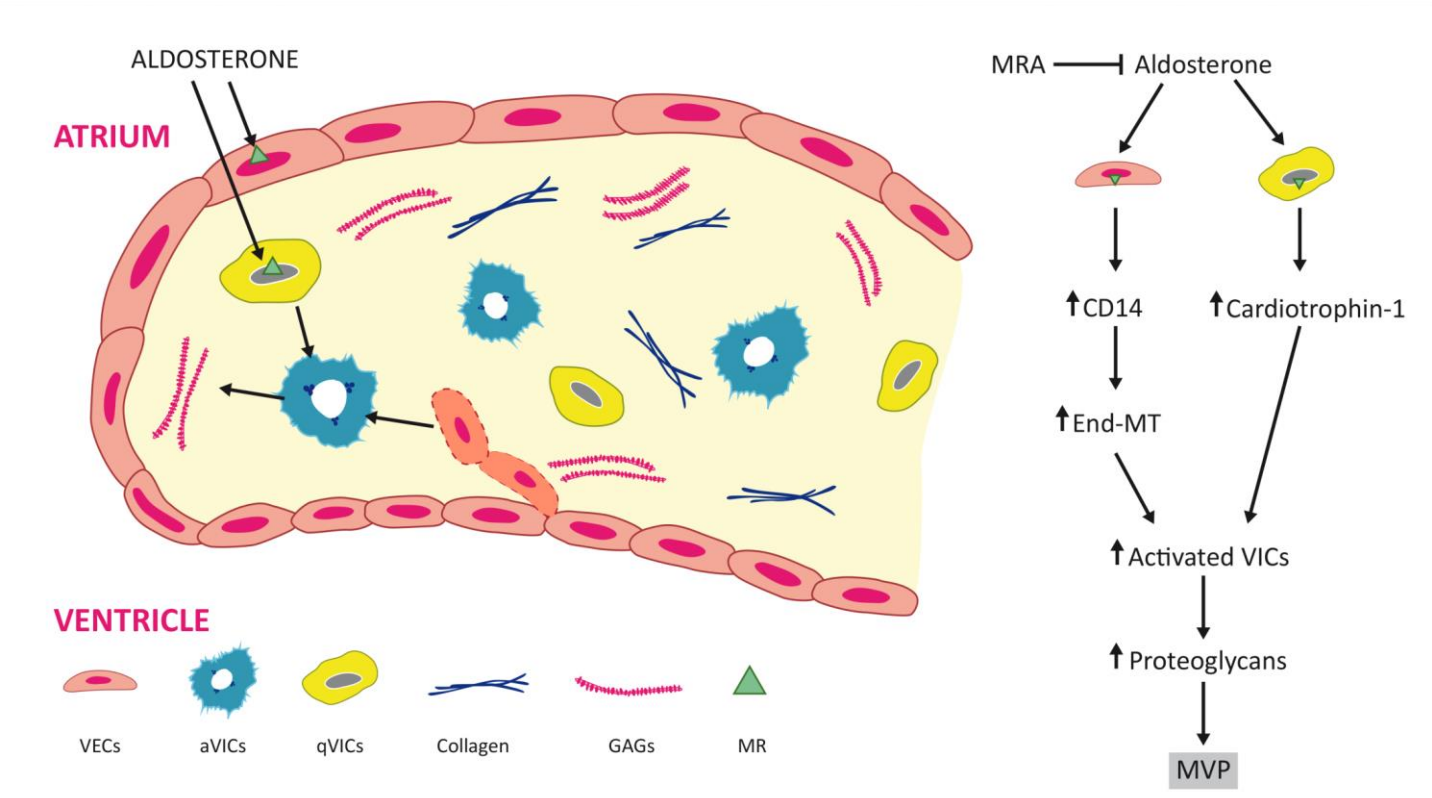

Figure 64. Schematic representations of our *in vitro* results.

3. Role of Mineralocorticoid Receptor antagonism in a Mitral Valve Prolapse mouse model.

Several drugs, such as anorectic compounds (fenfluramine, dexfenfluramine, nordexfenfluramine), have been associated with the remodeling of the mitral and aortic valves [190]. These drugs interact with the serotonergic system by targeting the Serotonin (5-HT)-2 receptor subtypes [191,192]. Principally, these drugs could be strong stimulators of the 5-HT2B receptor (5-HT2BR) in valvular cells. 5-HT2BR activation is known to cause VICs mitogenesis through the phosphorylation of non-receptor tyrosine kinases (SRC) and extracellular regulated kinases (ERK), and an inappropriate or exacerbation of 5-HT2BR activation has been associated with the development of clinically significant valve disease in humans [80,193]. Focusing in the mitral valve, the up-regulation of 5-HT2 receptors induces VICs activation and increases the expression of proteoglycans [73,193–196]. In fact, some studies have demonstrated that the inhibition of serotonin receptors could exert cardioprotective actions or effects [75,196–200]. In our study, we generated a MVP mouse model as described by Ayme-Dietrich et al [144]. They developed a murine model of drug-induced heart valve disease by continuous subcutaneous infusion of NDF. This treatment leads to the development of valve lesions characterized by cushions with a high density of endothelial progenitor cells (CD34+/CD31+) originated from bone marrow. Valve lesions are completely prevented by the inhibition of both 5-HT2A and 5-

HT2B receptors. This work also highlights the initiating mechanisms of valve lesions by indicating 5-HT as an important determinant in valvular cell recruitment that leads to valve remodeling [144]. In our hands, NDF-treated mice also presented increased area and thickness of the mitral valve as well as enhanced proteoglycans content as compared with controls. Similar studies in other MVD models show analogous characteristics, with proteoglycans synthesis and cellular proliferation [73,193–195]. *In vitro* data provide a mechanistic explanation of 5HT effects observed *in vivo.* In porcine VICs, 5-HT induces the phosphorylation of ERK1/2, an initiator of cellular proliferation and activity, and [3H] proline incorporation (index of ECM collagen synthesis), which is blocked by a potent 5-HT2A and 5-HT2B receptor antagonist [201]. Driesbaugh and colleagues showed that human MVP is associated with the up-regulation of 5HTR2B expression in the leaflets [196]. Moreover, the up-regulation of 5HTR2B is related with MVP development and valvular remodeling in a canine model [196].

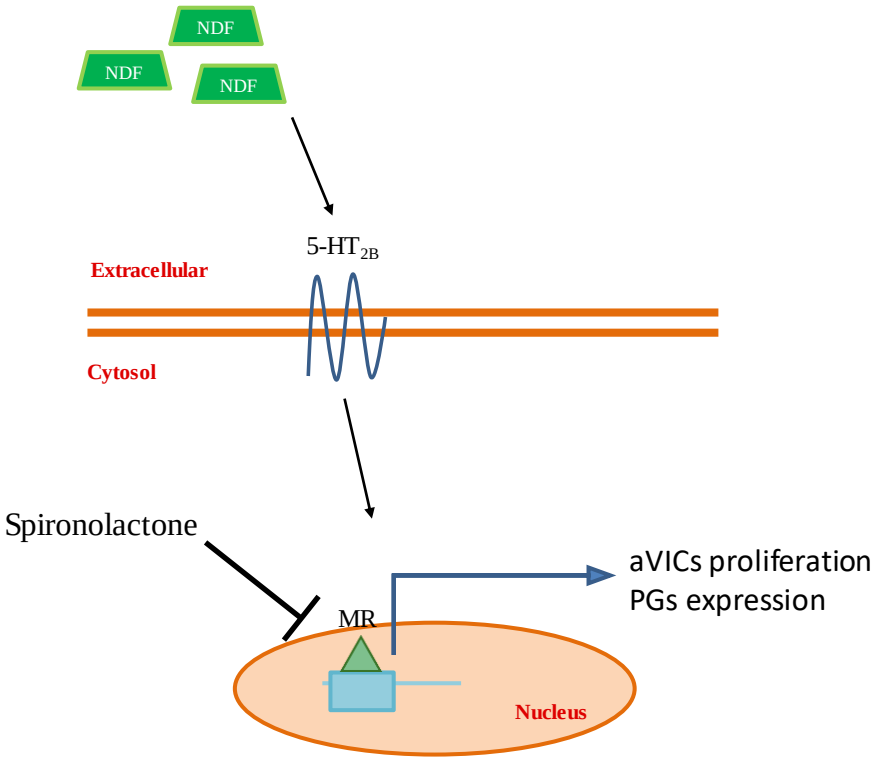

Figure 65. Mechanism of the drugs-induced 5-HT2BR the proliferation of VICs, increment of proteoglycans, where Spironolactone blocks the NDF effects.

Our results validate the implication of the serotonin pathway in the induction of mitral valve alterations associated with MVP. Importantly, our data showed that pharmacological intervention using a MRA could prevent the increment in area and thickness of mitral valve leaflets as well as proteoglycans expression. We observed for the first time the impact of MR in the development of MVP via serotonin pathway. Interestingly, in a sheep model of tachycardia-induced dilated cardiomyopathy presenting mitral

valve remodeling [32], Aldo levels have been found to be increased [202], suggesting the possible involvement of Aldo in mitral valve alterations. Moreover, it has been described that Spironolactone, in addition to conventional therapy, increases survival compared with conventional therapy in dogs with naturally occurring myxomatous mitral valve disease [203]. Moreover, in collaboration with Prof. Frédéric Jaisser in Paris (France) we used two different models of mice lacking MR specifically in smooth muscle cells (SMA-MR-KO mice) or endothelial cells (Vecadh-MR-KO mice). SMA-MR-KO mice treated with NDF exhibited an increase in mitral valve area and thickness and in the expression of proteoglycans as compared with NDF-control mice being these increases similar to those found in control mice treated with NDF. However, in Vecadh-MR-KO mice, NDF failed to increase mitral valve area, thickness and proteoglycans content.

Our findings support the idea that the endothelial MR in mitral valve is critical for the maintenance of normal Mitral valve structure.

Altogether these studies support our findings that demonstrated the involved of Aldo in mitral valve alterations associated to MVP.

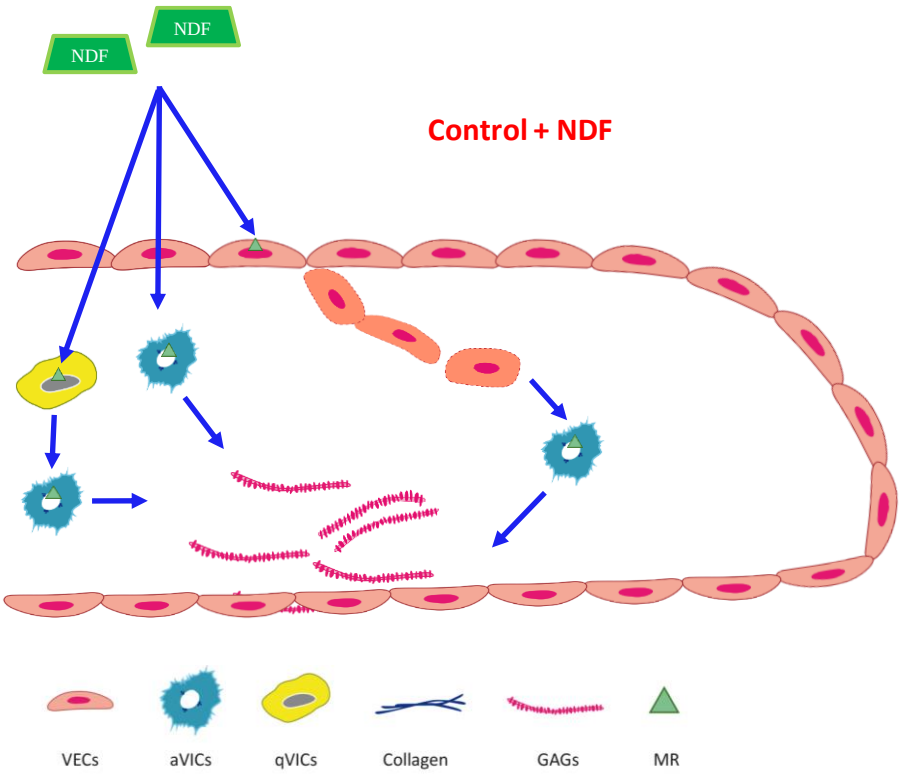

Figure 66. Schematic representation of the NDF effects in the control group treated with NDF.

Whether MR directly interferes with serotonin signaling or secondly affect the consequences of serotonin receptor activation in valve remains to be studied. However, in line with our findings, studies analyzing the interactions between MR and serotonin have been performed in brain diseases, mainly in depression. It has been established that in depression there is a down-regulation of the serotonin pathway. There is evidence that the expression and function of MR in the hippocampus is tightly regulated by serotonin in the median raphe nucleus [204,205]. Interestingly, serotonin is a key regulator of MR expression [205]. Thus, serotonin increases MR expression

in hippocampal neurons [205]. In accordance, some studies are investigating whether MRAs could disturb the serotonin pathway in depression [205–210]. Taking into account these studies, our mice model showed the impact of MR activity in the serotonin pathway, in the increment of mitral valve area and thickness as well as in the increase in proteoglycans content. However, our experiments were not focusedon the direct relation between the MR and the serotonin pathway and more studies are needed to clarify the crosstalk between MR and the serotonin pathway.

It has been well described that the serotonin pathway induces an increment of mitral valve area and thickness via the high proteoglycans expression by aVICs [80,144]. Our results in the MR-KO mouse models underlined the mandatory role of MR expressed in endothelial cells but no smooth muscle cells. It is important to point out that only aVICs are positive for α-SMA. Thus, it is interesting to speculate that NDF could exert its effects because the MR was presented in both qVICs and VECs that were able to maintain the aVICS population with the MR intact in the SMA-MR-KO model and therefore increase the proteoglycan content. We here proposed a mechanism where VECs are the first and the main cellular type responsible for the development MVP in the serotonin-induced pathway model. Thus, in pathological conditions, the absence of MR in VECs could protect VECs against EndMT, decreasing the number of aVICs in the mitral leaflets and leading to decreased proteoglycans expression. Nevertheless, more studies

are needed to analyze new possible interactions between MR and serotonin pathway.

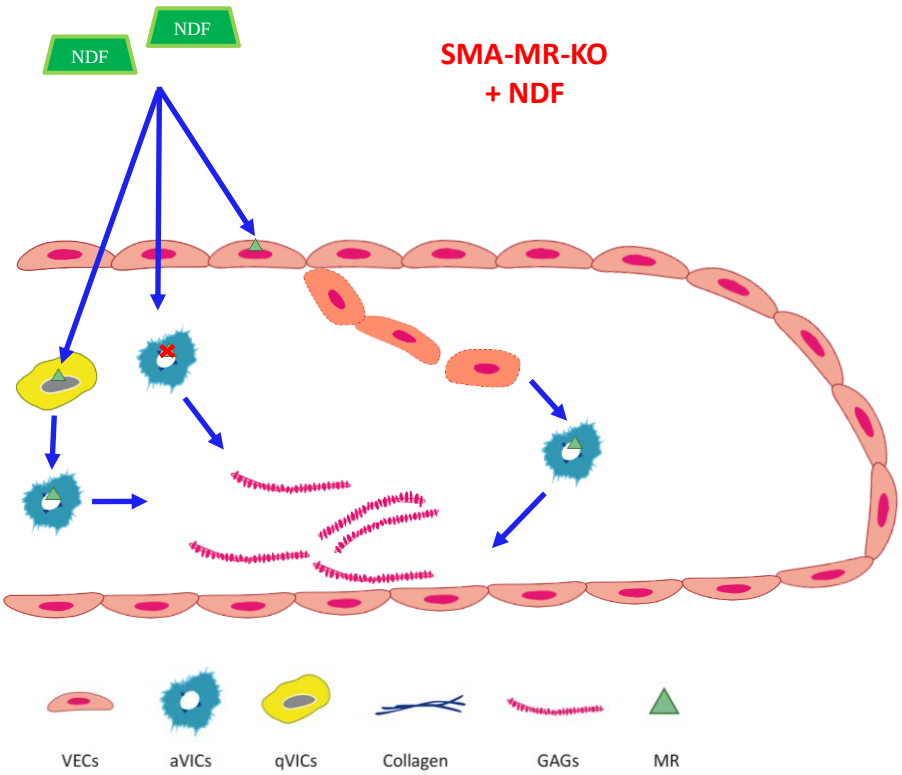

Figure 67. Schematic representation of the NDF effects in the SMA-MR-KO group treated with NDF.

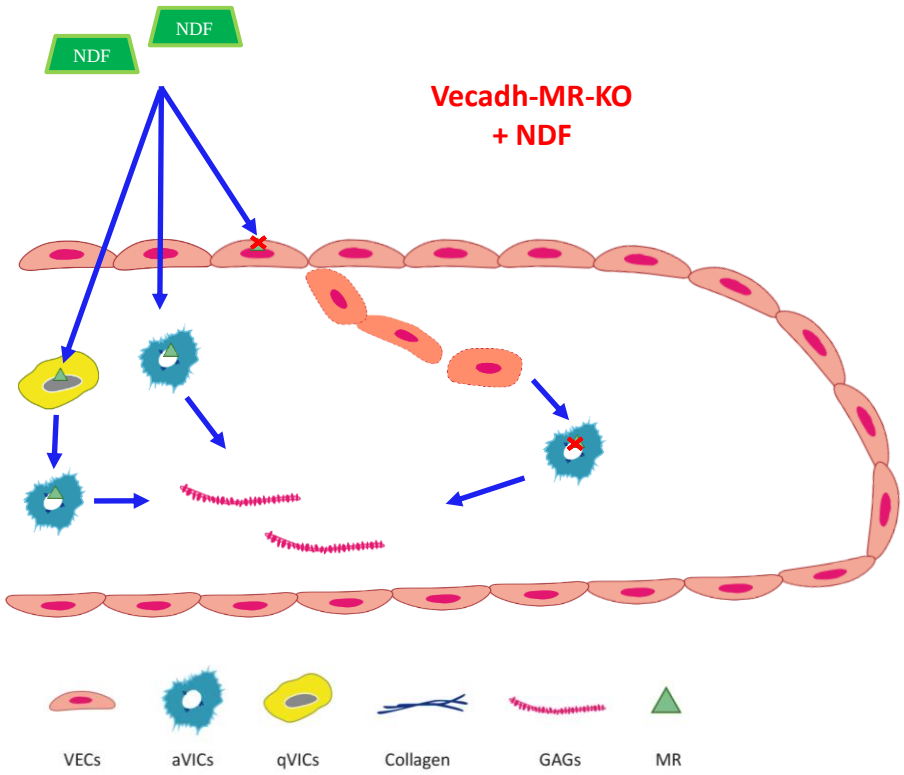

Figure 68. Schematic representation of the NDF effects in the Vecadh-MR-KO group treated with NDF.

4. Possible beneficial effects of MRA treatment in human MVP patients.

MVP is characterized by fibromyxomatous changes of the mitral leaflet that include thickening, enlargement, leaflet hooding, annular dilation, elongated and/or ruptured chordae. At the microscopic level, prolapsed mitral valves present fragmented, irregular elastin and collagen, abundant matrix metalloproteases, and an accumulation of glycosaminoglycans and proteoglycans particularly in the spongiosa layer of the leaflets [211].

Landmark clinical trials including RALES, EPHESUS and EMPHASIS-HF demonstrated the beneficial effects of MRAs in patients with HF, reducing mortality and hospitalizations. MRAs also have potential effects on vascular inflammation, macrophage activation, oxygen free radical formation, endothelial dysfunction, and myocardial fibrosis, and hence may provide more widespread benefits on cardiovascular disease states [212–215]. The EPHESUS trial, where eplerenone was administrated in acute myocardial infraction patients with HF, revealed a reduction in all-cause mortality, in cardiovascular mortality and in sudden cardiac death [216]. Moreover, MRAs have been shown to prevent hypertension-induced end organ damage [217]. Although experimental findings point out that the employment of MRAs could reduce myocardial fibrosis and hypertrophy among rodents with chronic aortic regurgitation [218] and in rats with aortic stenosis [219], the impact of the drug on the specific components of the mitral valve has not been

defined. A benefit for such therapy in human MVP remains to be demonstrated. Our results show that valves from MVP patients chronically treated with MRA prior to the surgical intervention presented an increment in VECs markers, a reduction in activated VICs markers and a reduction in proteoglycans content. In myxomatous mitral valves from human patients, Rabkin et al. observed an increase in the VICs activation marker α-SMA and vimentin as compared to controls [220]. Recently, a benefit of Angiotensin type 1a receptor antagonism using losartan has been demonstrated in mitral valve remodeling. Losartan blocks EndMT and prevents the growth and fibrosis in mitral leaflets after myocardial infarction [221,222]. Interestingly, angiotensin type 1a receptors are required for Aldo to induce vascular remodeling and inflammation, as well as endothelial dysfunction [223].

It is important to consider that the main indication for MRA administration in MVP patients according current clinical practice guidelines is the development of severe LV systolic dysfunction, which is related with a worse prognosis [224,225]. It should be pointed out that our study is not a clinical trial and thus the treatment with MRA was not randomized. Therefore, the group of MRA patients probably represent a group of patients in a more advanced stage of the disease, though we failed to demonstrate a significant difference between the clinical variables of both groups (with the exception of pulmonary hypertension), probably due to lack of statistical power. Even so, our results evidenced the partial beneficial effects of MRAs on proteoglycans content in mitral valve from patients with probably worse

prognosis and advance stages of valvulopathy. This opens the possibility of leaflet-specific therapy to improve mitral valve adaptation and reduce regurgitation, although specific studies and clinical trials are needed to confirm this hypothesis.

CLINICAL RELEVANCE AND PERSPECTIVES OF THE STUDY

As noted, the exact incidence and prevalence of mitral regurgitation is unknown, but it probably exceeds 176 million worldwide [226], and it is the second most common type of heart valve disease requiring surgery in Europe [227]. The condition is often associated with HF, one of the most common cardiovascular disorders worldwide, and one that poses a significant economic burden [228]. Moreover, the prevalence of mitral regurgitation in the population is strongly linked to ageing [229]. Consequently, in the next years it is expected that the prevalence of MVP patients will increase considerably. Despite being the most common cause of isolated mitral regurgitation requiring surgical repair, little is known about the cellular and molecular mechanisms underlying the pathogenesis and progression of MVP. Mitral valve repair is the surgical treatment of choice for MVP when feasible, if not, mitral valve replacement with a prosthetic valve is performed. In particular, in the *Complejo Hospitalario de Navarra*, the estimation of total economic cost per patient is around 40.000 euros. Per year, around 100 patients undergo mitral valve replacement in the *Complejo Hospitalario de Navarra.* Thus, the economic cost of these interventions per year is very high. The pathophysiology underlying MVP remains incompletely defined and the discovering of new druggable targets is an unmet clinical need. In this study, we have analyzed the involvement of Aldo/MR pathway in the development of MVP. Despite the fact that Aldo effects have been studied in other cardiovascular diseases, this is the first time that Aldo/MR is found to be involved in a valvular disease. The possibility to block Aldo effects by using a MRA opens a new therapeutic

approach that could delay the progression of MVP. Importantly, and due to the fact that MVP constitutes a public health problem, with rising clinical, social, and economic burden, our findings clearly propose that clinical trials aiming at analyzing the beneficial effects of MRA therapy in patients with MVP are needed. Our results have leaded to the better knowledge of the pathophysiology of MVP and paved the way for individualized options for MVP treatment.

LIMITATIONS

The current study presents a number of limitations to be considered when interpreting the data.

First, although VICs and VECs were isolated from human valves from MVP patients with similar age and risk factors, cells were not separated by individuals or sex.

MRA is not a conventional treatment for MVP patients. In consequence, our cohort of patients treated with MRA are very limited and accordingly, the statistical power is weak.

The treatment of patients with MRA depends on the clinician's criteria mainly based on the left ventricle dysfunction degree. Considering that this drug is indicated in more advanced stages of HF, it is possible that MRA treatment acts as a confounding factor by selecting patients with a higher degree of valvular disease. Overall the findings of the clinical study are largely observational and future studies are warranted to test whether MRA reduces mitral valve alterations as well as myocardial alterations in a larger cohort of patients with MVP.

CONCLUSIONS

1. Mitral valve is identified as an Aldo-sensitive tissue because it expresses MR and 11β-HSD2.

2. Aldo induces qVICs activation and enhances proteoglycans expression and secretion via CT-1.

3. Aldo induces EndMT in VECs leading to an increase in aVICs and consequently, an augmentation in proteoglycans expression and secretion. Aldo effects in VECs are mediated by CD14, the principal ligand of the TLR4 pathway.

4. In a mouse model of MVP, treatment with the MRA Spironolactone prevents mitral valve size and proteoglycans content.

5. In a MVP model that lacks specifically the MR in endothelial cells, mitral valve area and thickness as well as proteoglycans content are reduced.

6. Mitral valves from MVP patients treated with MRA present a reduction in proteoglycans content.

The conglomeration of the results presented in this study showed for the first time the involvement of the Aldo/MR pathway in the development of MVP. Finally, MRA treatment could be used as a novel therapeutic approach to reduce mitral valve remodeling associated to MVP.

CONCLUSIONES

1. La válvula mitral es un tejido sensible a los efectos de la Aldo debido a la expresión del receptor mineralocorticoide y de la enzima 11β-HSD2.

2. La Aldo induce la activación de las CIVs quiescentes y aumenta la expresión y secreción de proteoglicanos a través de la cardiotrofina- 1.

3. La Aldo estimula la TEM en las CEVs, induciendo la transfromación de las CEVs en CIVs activadas y consecuentemente aumentando la expresión y secreción de proteoglicanos. Los efectos de la Aldo en CEVs están mediados por el CD14, el principal ligando de la vía de señalización del TLR-4.

4. En el modelo murino de PVM, el tratamiento con Espironolactona reduce el área total de la válvula mitral y el contenido valvular de proteoglicanos.

5. En el modelo de ratón en el que el receptor mineralocorticoide está silenciado específicamente en las células endoteliales, el área total y el grosor de la válvula mitral, así como el contenido total de proteoglicanos está reducido.

6. Los pacientes con PVM tratados con un ARM presentan una reducción en los proteoglicanos de la válvula mitral.

El conglomerado de todos los resultados presentados en este estudio muestra por primera vez la implicación de la vía Aldo/RM en el desarrollo del PVM. Finalmente, el tratamiento con ARM podría ser usado como una nueva

estrategia terapéutica para reducir el remodelado de la válvula mitral asociado al PVM.

BIBLIOGRAPHY

1. Buckberg, G. D., Nanda, N. C., Nguyen, C. & Kocica, M. J. What Is the Heart? Anatomy, Function, Pathophysiology, and Misconceptions. *J. Cardiovasc. Dev. Dis.* **5**, 33 (2018).

2. Anderson, R. H., Razavi, R. & Taylor, A. M. Cardiac anatomy revisited. *J. Anat.* **205**, 159–77 (2004).

3. Yoganathan, A. P., He, Z. & Casey Jones, S. Fluid Mechanics of Heart Valves. *Annu. Rev. Biomed. Eng.* **6**, 331–362 (2004).

4. Yacoub, M. H. & Cohn, L. H. Novel approaches to cardiac valve repair: from structure to function: Part I. *Circulation* **109**, 942–50 (2004).

5. Anderson, R. H. The surgical anatomy of the aortic root. *Multimed. Man. Cardio-Thoracic Surg.* **2007**, 2527–0 (2007).

6. McCarthy, K. P., Ring, L. & Rana, B. S. Anatomy of the mitral valve: understanding the mitral valve complex in mitral regurgitation. *Eur. J. Echocardiogr.* **11**, i3–i9 (2010).

7. Liu, A. C., Joag, V. R. & Gotlieb, A. I. The emerging role of valve interstitial cell phenotypes in regulating heart valve pathobiology. *Am. J. Pathol.* **171**, 1407–18 (2007).

8. Carlhäll, C. *et al.* Contribution of mitral annular excursion and shape dynamics to total left ventricular volume change. *Am. J. Physiol.*

Heart Circ. Physiol. **287**, H1836-41 (2004).

9. Levine, R. A. *et al.* Three-dimensional echocardiographic reconstruction of the mitral valve, with implications for the diagnosis of mitral valve prolapse. *Circulation* **80**, 589–98 (1989).

10. Timek, T. A. & Miller, D. C. Experimental and clinical assessment of mitral annular area and dynamics: what are we actually measuring? *Ann. Thorac. Surg.* **72**, 966–74 (2001).

11. Salhiyyah, K., Yacoub, M. H. & Chester, A. H. Cellular mechanisms in mitral valve disease. *J. Cardiovasc. Transl. Res.* **4**, 702–9 (2011).

12. Levine, R. A. *et al.* Mitral valve disease--morphology and mechanisms. *Nat. Rev. Cardiol.* **12**, 689–710 (2015).

13. Chester, A. H. *et al.* The living aortic valve: From molecules to function. *Glob. Cardiol. Sci. Pract.* **2014**, 52–77 (2014).

14. Levine, R. A. *et al.* Mitral valve disease--morphology and mechanisms. *Nat. Rev. Cardiol.* **12**, 689–710 (2015).

15. Smith, S. *et al.* Force generation of different human cardiac valve interstitial cells: relevance to individual valve function and tissue engineering. *J. Heart Valve Dis.* **16**, 440–6 (2007).

16. Taylor, P. M., Batten, P., Brand, N. J., Thomas, P. S. & Yacoub, M. H. The cardiac valve interstitial cell. *Int. J. Biochem. Cell Biol.* **35**,

113–8 (2003).

17. Butcher, J. T., Penrod, A. M., García, A. J. & Nerem, R. M. Unique morphology and focal adhesion development of valvular endothelial cells in static and fluid flow environments. *Arterioscler. Thromb. Vasc. Biol.* **24**, 1429–34 (2004).

18. Grande-Allen, K. J. & Liao, J. The heterogeneous biomechanics and mechanobiology of the mitral valve: implications for tissue engineering. *Curr. Cardiol. Rep.* **13**, 113–20 (2011).

19. Bischoff, J. Endothelial-to-Mesenchymal Transition. *Circ. Res.* **124**, 1163–1165 (2019).

20. Rutkovskiy, A. *et al.* Valve Interstitial Cells: The Key to Understanding the Pathophysiology of Heart Valve Calcification. *J. Am. Heart Assoc.* **6**, (2017).

21. Latif, N., Sarathchandra, P., Taylor, P. M., Antoniw, J. & Yacoub, M. H. Localization and pattern of expression of extracellular matrix components in human heart valves. *J. Heart Valve Dis.* **14**, 218–27 (2005).

22. Hinton, R. B. & Yutzey, K. E. Heart Valve Structure and Function in Development and Disease. *Annu. Rev. Physiol.* **73**, 29–46 (2011).

23. Latif, N., Sarathchandra, P., Taylor, P. M., Antoniw, J. & Yacoub, M.

H. Molecules mediating cell-ECM and cell-cell communication in human heart valves. *Cell Biochem. Biophys.* **43**, 275–87 (2005).

24. Cleutjens, J. P. M. & Creemers, E. E. J. M. Integration of concepts: cardiac extracellular matrix remodeling after myocardial infarction. *J. Card. Fail.* **8**, S344-8 (2002).

25. Greenhouse, D. G. *et al.* Mitral valve prolapse is associated with altered extracellular matrix gene expression patterns. *Gene* **586**, 56–61 (2016).

26. Lockhart, M., Wirrig, E., Phelps, A. & Wessels, A. Extracellular matrix and heart development. *Birth Defects Res. A. Clin. Mol. Teratol.* **91**, 535–50 (2011).

27. Hadian, M., Corcoran, B. M. & Bradshaw, J. P. Molecular changes in fibrillar collagen in myxomatous mitral valve disease. *Cardiovasc. Pathol.* **19**, e141-8 (2010).

28. Akhtar, S., Meek, K. M. & James, V. Immunolocalization of elastin, collagen type I and type III, fibronectin, and vitronectin in extracellular matrix components of normal and myxomatous mitral heart valve chordae tendineae. *Cardiovasc. Pathol.* **8**, 203–11

29. Weber, K. T. Cardiac interstitium in health and disease: the fibrillar collagen network. *J. Am. Coll. Cardiol.* **13**, 1637–52 (1989).

30. Purushothaman, K.-R. *et al.* Association of altered collagen content and lysyl oxidase expression in degenerative mitral valve disease. *Cardiovasc. Pathol.* **29**, 11–18

31. Gupta, V. *et al.* Abundance and location of proteoglycans and hyaluronan within normal and myxomatous mitral valves. *Cardiovasc. Pathol.* **18**, 191–7 (2009).

32. Stephens, E. H. *et al.* Significant changes in mitral valve leaflet matrix composition and turnover with tachycardia-induced cardiomyopathy. *Circulation* **120**, S112-9 (2009).

33. Yanagishita, M. Function of proteoglycans in the extracellular matrix. *Acta Pathol. Jpn.* **43**, 283–93 (1993).

34. Iozzo, R. V. & Schaefer, L. Proteoglycan form and function: A comprehensive nomenclature of proteoglycans. *Matrix Biol.* **42**, 11–55 (2015).

35. George, E. L., Georges-Labouesse, E. N., Patel-King, R. S., Rayburn, H. & Hynes, R. O. Defects in mesoderm, neural tube and vascular development in mouse embryos lacking fibronectin. *Development* **119**, 1079–91 (1993).

36. Fayet, C., Bendeck, M. P. & Gotlieb, A. I. Cardiac valve interstitial cells secrete fibronectin and form fibrillar adhesions in response to injury. *Cardiovasc. Pathol.* **16**, 203–11 (2007).

37. Cleutjens, J. P. The role of matrix metalloproteinases in heart disease. *Cardiovasc. Res.* **32**, 816–21 (1996).

38. Grande-Allen, K. J., Griffin, B. P., Ratliff, N. B., Cosgrove, D. M. & Vesely, I. Glycosaminoglycan profiles of myxomatous mitral leaflets and chordae parallel the severity of mechanical alterations. *J. Am. Coll. Cardiol.* **42**, 271–7 (2003).

39. Zeng, Y. I. *et al.* Pathophysiology of valvular heart disease. *Exp. Ther. Med.* **11**, 1184–1188 (2016).

40. d'Arcy, J. L., Prendergast, B. D., Chambers, J. B., Ray, S. G. & Bridgewater, B. Valvular heart disease: the next cardiac epidemic. *Heart* **97**, 91–93 (2011).

41. Marciniak, A., Glover, K. & Sharma, R. Cohort profile: prevalence of valvular heart disease in community patients with suspected heart failure in UK. *BMJ Open* **7**, e012240 (2017).

42. Maganti, K., Rigolin, V. H., Sarano, M. E. & Bonow, R. O. Valvular Heart Disease: Diagnosis and Management. *Mayo Clin. Proc.* **85**, 483–500 (2010).

43. Ray, S. Changing epidemiology and natural history of valvular heart disease. *Clin. Med.* **10**, 168–71 (2010).

44. Suri, R. M. *et al.* Association between early surgical intervention vs

watchful waiting and outcomes for mitral regurgitation due to flail mitral valve leaflets. *JAMA* **310**, 609–16 (2013).

45. Baumgartner, H. *et al.* 2017 ESC/EACTS Guidelines for the management of valvular heart disease. *Eur. Heart J.* **38**, 2739–2791 (2017).

46. Mary Ann E. Zagaria. Mechanical Heart Valves: Contraindication for Dabigatran Therapy. *Geriatrics* **39(2)**, 32–34 (2014).

47. Zoghbi, W. A. *et al.* Recommendations for Noninvasive Evaluation of Native Valvular Regurgitation: A Report from the American Society of Echocardiography Developed in Collaboration with the Society for Cardiovascular Magnetic Resonance. *J. Am. Soc. Echocardiogr.* **30**, 303–371 (2017).

48. Chopra, P. & Gulwani, H. Pathology and pathogenesis of rheumatic heart disease. *Indian J. Pathol. Microbiol.* **50**, 685–97 (2007).

49. Chester, A. H. & Taylor, P. M. Molecular and functional characteristics of heart-valve interstitial cells. *Philos. Trans. R. Soc. Lond. B. Biol. Sci.* **362**, 1437–43 (2007).

50. Schmitto, J. D. *et al.* Functional mitral regurgitation. *Cardiol. Rev.* **18**, 285–91 (2010).

51. Otsuji, Y. *et al.* Restricted diastolic opening of the mitral leaflets in

patients with left ventricular dysfunction: evidence for increased valve tethering. *J. Am. Coll. Cardiol.* **32**, 398–404 (1998).

52. Connell, P. S. *et al.* Regurgitation Hemodynamics Alone Cause Mitral Valve Remodeling Characteristic of Clinical Disease States In Vitro. *Ann. Biomed. Eng.* **44**, 954–67 (2016).

53. Wallby, L. *et al.* Role of inflammation in nonrheumatic, regurgitant heart valve disease. A comparative, descriptive study regarding apolipoproteins and inflammatory cells in nonrheumatic heart valve disease. *Cardiovasc. Pathol.* **16**, 171–8 (2007).

54. Veinot, J. P. Pathology of inflammatory native valvular heart disease. *Cardiovasc. Pathol.* **15**, 243–251 (2006).

55. Breed, E. R. & Binstadt, B. A. Autoimmune valvular carditis. *Curr. Allergy Asthma Rep.* **15**, 491 (2015).

56. Freed, L. A. *et al.* Prevalence and clinical outcome of mitral-valve prolapse. *N. Engl. J. Med.* **341**, 1–7 (1999).

57. Freed, L. A. *et al.* Mitral valve prolapse in the general population: the benign nature of echocardiographic features in the Framingham Heart Study. *J. Am. Coll. Cardiol.* **40**, 1298–304 (2002).

58. Delling, F. N. & Vasan, R. S. Epidemiology and pathophysiology of mitral valve prolapse: new insights into disease progression, genetics,

and molecular basis. *Circulation* **129**, 2158–70 (2014).

59. Zoghbi, W. A. *et al.* Recommendations for Noninvasive Evaluation of Native Valvular Regurgitation. *J. Am. Soc. Echocardiogr.* **30**, 303–371 (2017).

60. Hulin, A. *et al.* Emerging pathogenic mechanisms in human myxomatous mitral valve: lessons from past and novel data. *Cardiovasc. Pathol.* **22**, 245–50 (2013).

61. Pellerin, D., Brecker, S. & Veyrat, C. Degenerative mitral valve disease with emphasis on mitral valve prolapse. *Heart* **88 Suppl 4**, iv20-8 (2002).

62. Hjortnaes, J. *et al.* Comparative Histopathological Analysis of Mitral Valves in Barlow Disease and Fibroelastic Deficiency. *Semin. Thorac. Cardiovasc. Surg.* **28**, 757–767

63. Dal-Bianco, J. P. *et al.* Active adaptation of the tethered mitral valve: insights into a compensatory mechanism for functional mitral regurgitation. *Circulation* **120**, 334–42 (2009).

64. Shapero, K. *et al.* Reciprocal interactions between mitral valve endothelial and interstitial cells reduce endothelial-to-mesenchymal transition and myofibroblastic activation. *J. Mol. Cell. Cardiol.* **80**, 175–85 (2015).

65. Wylie-Sears, J., Aikawa, E., Levine, R. A., Yang, J.-H. & Bischoff, J. Mitral valve endothelial cells with osteogenic differentiation potential. *Arterioscler. Thromb. Vasc. Biol.* **31**, 598–607 (2011).

66. Lin, F., Wang, N. & Zhang, T.-C. The role of endothelial-mesenchymal transition in development and pathological process. *IUBMB Life* **64**, 717–23 (2012).

67. van Meeteren, L. A. & ten Dijke, P. Regulation of endothelial cell plasticity by TGF-β. *Cell Tissue Res.* **347**, 177–86 (2012).

68. Horne, T. *et al.* Dynamic Heterogeneity of the Heart Valve Interstitial Cell Population in Mitral Valve Health and Disease. *J. Cardiovasc. Dev. Dis.* **2**, 214–232 (2015).

69. Mulholland, D. L. & Gotlieb, A. I. Cell biology of valvular interstitial cells. *Can. J. Cardiol.* **12**, 231–6 (1996).

70. Stephens, E. H., Post, A. D., Laucirica, D. R. & Grande-Allen, K. J. Perinatal changes in mitral and aortic valve structure and composition. *Pediatr. Dev. Pathol.* **13**, 447–58 (2010).

71. Stephens, E. H., Chu, C.-K. & Grande-Allen, K. J. Valve proteoglycan content and glycosaminoglycan fine structure are unique to microstructure, mechanical load and age: Relevance to an age-specific tissue-engineered heart valve. *Acta Biomater.* **4**, 1148–60 (2008).

72. Young, S. N. How to increase serotonin in the human brain without drugs. *J. Psychiatry Neurosci.* **32**, 394–9 (2007).

73. Elangbam, C. S. *et al.* 5-Hydroxytryptamine (5HT)-induced valvulopathy: Compositional valvular alterations are associated with 5HT2B receptor and 5HT transporter transcript changes in Sprague-Dawley rats. *Exp. Toxicol. Pathol.* **60**, 253–262 (2008).

74. Jian, B. *et al.* Serotonin mechanisms in heart valve disease I: serotonin-induced up-regulation of transforming growth factor-beta1 via G-protein signal transduction in aortic valve interstitial cells. *Am. J. Pathol.* **161**, 2111–21 (2002).

75. McDonald, P. C. *et al.* Quantitative analysis of human heart valves: does anorexigen exposure produce a distinctive morphological lesion? *Cardiovasc. Pathol.* **11**, 251–62

76. Driesbaugh, K. H. *et al.* Serotonin receptor 2B signaling with interstitial cell activation and leaflet remodeling in degenerative mitral regurgitation. *J. Mol. Cell. Cardiol.* **115**, 94–103 (2018).

77. Ayme-Dietrich, E. *et al.* The role of 5-HT $_{2B}$ receptors in mitral valvulopathy: bone marrow mobilization of endothelial progenitors. *Br. J. Pharmacol.* **174**, 4123–4139 (2017).

78. Goldberg, E. *et al.* Serotonin and catecholamines in the development and progression of heart valve diseases. *Cardiovasc. Res.* **113**, 849–

857 (2017).

79. Droogmans, S. *et al.* In vivo model of drug-induced valvular heart disease in rats: pergolide-induced valvular heart disease demonstrated with echocardiography and correlation with pathology. *Eur. Heart J.* **28**, 2156–2162 (2007).

80. Elangbam, C. S. Drug-induced Valvulopathy: An Update. *Toxicol. Pathol.* **38**, 837–848 (2010).

81. Ramamoorthy, S. & Cidlowski, J. A. Corticosteroids: Mechanisms of Action in Health and Disease. *Rheum. Dis. Clin. North Am.* **42**, 15–31, vii (2016).

82. Holst, J. P., Soldin, O. P., Guo, T. & Soldin, S. J. Steroid hormones: relevance and measurement in the clinical laboratory. *Clin. Lab. Med.* **24**, 105–18 (2004).

83. Wang, M. The role of glucocorticoid action in the pathophysiology of the Metabolic Syndrome. *Nutr. Metab. (Lond).* **2**, 3 (2005).

84. Hattangady, N. G., Olala, L. O., Bollag, W. B. & Rainey, W. E. Acute and chronic regulation of aldosterone production. *Mol. Cell. Endocrinol.* **350**, 151–62 (2012).

85. Bollag, W. B. Regulation of aldosterone synthesis and secretion. *Compr. Physiol.* **4**, 1017–55 (2014).

86. Connell, J. M. C. & Davies, E. The new biology of aldosterone. *J. Endocrinol.* **186**, 1–20 (2005).

87. Ye, P. *et al.* Effects of ACTH, dexamethasone, and adrenalectomy on 11beta-hydroxylase (CYP11B1) and aldosterone synthase (CYP11B2) gene expression in the rat central nervous system. *J. Endocrinol.* **196**, 305–11 (2008).

88. Jaisser, F. & Farman, N. Emerging Roles of the Mineralocorticoid Receptor in Pathology: Toward New Paradigms in Clinical Pharmacology. *Pharmacol. Rev.* **68**, 49–75 (2016).

89. Marzolla, V. *et al.* Mineralocorticoid receptor in adipocytes and macrophages: a promising target to fight metabolic syndrome. *Steroids* **91**, 46–53 (2014).

90. Chapman, K., Holmes, M. & Seckl, J. 11β-hydroxysteroid dehydrogenases: intracellular gate-keepers of tissue glucocorticoid action. *Physiol. Rev.* **93**, 1139–206 (2013).

91. De-An, P. *et al.* Increased Expression of Mineralocorticoid Receptor and 11β-Hydroxysteroid Dehydrogenase Type 2 in Human Atria During Atrial Fibrillation. *Clin. Cardiol.* **33**, 23–29 (2010).

92. Viengchareun, S. *et al.* The mineralocorticoid receptor: insights into its molecular and (patho)physiological biology. *Nucl. Recept. Signal.* **5**, e012 (2007).

93. Messaoudi, S., Azibani, F., Delcayre, C. & Jaisser, F. Aldosterone, mineralocorticoid receptor, and heart failure. *Mol. Cell. Endocrinol.* **350**, 266–272 (2012).

94. Cannavo, A. *et al.* Aldosterone and Mineralocorticoid Receptor System in Cardiovascular Physiology and Pathophysiology. *Oxid. Med. Cell. Longev.* **2018**, 1–10 (2018).

95. Bauersachs, J., Jaisser, F. & Toto, R. Mineralocorticoid receptor activation and mineralocorticoid receptor antagonist treatment in cardiac and renal diseases. *Hypertens. (Dallas, Tex. 1979)* **65**, 257–63 (2015).

96. Martínez-Martínez, E. *et al.* Differential proteomics reveals S100-A11 as a key factor in aldosterone-induced collagen expression in human cardiac fibroblasts. *J. Proteomics* **166**, 93–100 (2017).

97. Martínez-Martínez, E. *et al.* Differential Proteomics Identifies Reticulocalbin-3 as a Novel Negative Mediator of Collagen Production in Human Cardiac Fibroblasts. *Sci. Rep.* **7**, 12192 (2017).

98. Ibarrola, J. *et al.* Aldosterone Impairs Mitochondrial Function in Human Cardiac Fibroblasts via A-Kinase Anchor Protein 12. *Sci. Rep.* **8**, 6801 (2018).

99. White, P. C. Aldosterone: Direct Effects on and Production by the Heart. *J. Clin. Endocrinol. Metab.* **88**, 2376–2383 (2003).

100. Martínez-Martínez, E. *et al.* Differential Proteomics Identifies Reticulocalbin-3 as a Novel Negative Mediator of Collagen Production in Human Cardiac Fibroblasts. *Sci. Rep.* **7**, 12192 (2017).

101. Ferreira, J. P. *et al.* Mineralocorticoid receptor antagonist pattern of use in heart failure with reduced ejection fraction: findings from BIOSTAT-CHF. *Eur. J. Heart Fail.* **19**, 1284–1293 (2017).

102. Ferreira, J. P., Mentz, R. J., Pizard, A., Pitt, B. & Zannad, F. Tailoring mineralocorticoid receptor antagonist therapy in heart failure patients: are we moving towards a personalized approach? *Eur. J. Heart Fail.* **19**, 974–986 (2017).

103. Stienen, S. *et al.* Estimated Long-Term Survival With Eplerenone. *J. Am. Coll. Cardiol.* **73**, 2357–2359 (2019).

104. Rossignol, P. *et al.* Spironolactone and Resistant Hypertension in Heart Failure With Preserved Ejection Fraction. *Am. J. Hypertens.* **31**, 407–414 (2018).

105. Pitt, B. *et al.* Eplerenone, a Selective Aldosterone Blocker, in Patients with Left Ventricular Dysfunction after Myocardial Infarction. *N. Engl. J. Med.* **348**, 1309–1321 (2003).

106. Pitt, B. *et al.* The effect of spironolactone on morbidity and mortality in patients with severe heart failure. Randomized Aldactone Evaluation Study Investigators. *N. Engl. J. Med.* **341**, 709–17 (1999).

107. Zannad, F. *et al.* Eplerenone in Patients with Systolic Heart Failure and Mild Symptoms. *N. Engl. J. Med.* **364**, 11–21 (2011).

108. Hatakeyama, H. *et al.* Vascular aldosterone. Biosynthesis and a link to angiotensin II-induced hypertrophy of vascular smooth muscle cells. *J. Biol. Chem.* **269**, 24316–20 (1994).

109. Montezano, A. C. & Touyz, R. M. Networking between systemic angiotensin II and cardiac mineralocorticoid receptors. *Hypertens. (Dallas, Tex. 1979)* **52**, 1016–8 (2008).

110. Montezano, A. C. *et al.* Aldosterone and angiotensin II synergistically stimulate migration in vascular smooth muscle cells through c-Src-regulated redox-sensitive RhoA pathways. *Arterioscler. Thromb. Vasc. Biol.* **28**, 1511–8 (2008).

111. Bunda, S. *et al.* Aldosterone Stimulates Elastogenesis in Cardiac Fibroblasts via Mineralocorticoid Receptor-independent Action Involving the Consecutive Activation of $G\alpha_{13}$, c-Src, the Insulin-like Growth Factor-I Receptor, and Phosphatidylinositol 3-Kinase/Akt. *J. Biol. Chem.* **284**, 16633–16647 (2009).

112. Stockand, J. D. & Meszaros, J. G. Aldosterone stimulates proliferation of cardiac fibroblasts by activating Ki-RasA and MAPK1/2 signaling. *Am. J. Physiol. Heart Circ. Physiol.* **284**, H176-84 (2003).

113. Chen, X. *et al.* Protective Effect of Spironolactone on Endothelial-to-Mesenchymal Transition in HUVECs via Notch Pathway. *Cell. Physiol. Biochem.* **36**, 191–200 (2015).

114. Sun, Y. *et al.* Aldosterone-Induced Inflammation in the Rat Heart. *Am. J. Pathol.* **161**, 1773–1781 (2002).

115. Gravez, B. *et al.* Aldosterone promotes cardiac endothelial cell proliferation in vivo. *J. Am. Heart Assoc.* **4**, e001266 (2015).

116. NEHME, J. *et al.* Spironolactone improves carotid artery fibrosis and distensibility in rat post-ischaemic heart failure. *J. Mol. Cell. Cardiol.* **39**, 511–519 (2005).

117. Virdis, A. *et al.* Spironolactone improves angiotensin-induced vascular changes and oxidative stress. *Hypertens. (Dallas, Tex. 1979)* **40**, 504–10 (2002).

118. Farquharson, C. A. & Struthers, A. D. Spironolactone increases nitric oxide bioactivity, improves endothelial vasodilator dysfunction, and suppresses vascular angiotensin I/angiotensin II conversion in patients with chronic heart failure. *Circulation* **101**, 594–7 (2000).

119. Farquharson, C. A. J. & Struthers, A. D. Aldosterone induces acute endothelial dysfunction in vivo in humans: evidence for an aldosterone-induced vasculopathy. *Clin. Sci. (Lond).* **103**, 425–31 (2002).

120. McCurley, A., McGraw, A., Pruthi, D. & Jaffe, I. Z. Smooth muscle cell mineralocorticoid receptors: role in vascular function and contribution to cardiovascular disease. *Pflügers Arch. - Eur. J. Physiol.* **465**, 1661–1670 (2013).

121. Kanno, N. *et al.* Effects of pimobendan for mitral valve regurgitation in dogs. *J. Vet. Med. Sci.* **69**, 373–7 (2007).

122. Häggström, J. *et al.* Short-term hemodynamic and neuroendocrine effects of pimobendan and benazapril in dogs with myxomatous mitral valve disease and congestive heart failure. *J. Vet. Intern. Med.* **27**, 1452–62 (2013).

123. Suzuki, S. *et al.* Comparative Effect of Carperitide and Furosemide on Left Atrial Pressure in Dogs with Experimentally Induced Mitral Valve Regurgitation. *J. Vet. Intern. Med.* **27**, 1097–1104 (2013).

124. Falk, T. *et al.* Cardiac troponin-I concentration, myocardial arteriosclerosis, and fibrosis in dogs with congestive heart failure because of myxomatous mitral valve disease. *J. Vet. Intern. Med.* **27**, 500–6 (2013).

125. Bernay, F. *et al.* Efficacy of Spironolactone on Survival in Dogs with Naturally Occurring Mitral Regurgitation Caused by Myxomatous Mitral Valve Disease. *J. Vet. Intern. Med.* **24**, 331–341 (2010).

126. Lefebvre, H. P. *et al.* Safety of spironolactone in dogs with chronic

heart failure because of degenerative valvular disease: a population-based, longitudinal study. *J. Vet. Intern. Med.* **27**, 1083–91 (2013).

127. Bartko, P. E. *et al.* Effect of Losartan on Mitral Valve Changes After Myocardial Infarction. *J. Am. Coll. Cardiol.* **70**, 1232–1244 (2017).

128. Leszek, P. *et al.* Usefulness of 6-minute walk test, plasma neurohumoral and cytokine activation in the assessment of symptomatic patients with left ventricle dysfunction caused by chronic severe mitral valve regurgitation. *Acta Cardiol.* **65**, 43–51 (2010).

129. Hayashi, Y. *et al.* Left atrial diameter is a simple indicator of a deficiency in atrial natriuretic peptide secretion in patients with mitral stenosis: efficacy of postoperative supplementation with synthetic human alpha-atrial natriuretic peptide. *J. Cardiovasc. Pharmacol.* **44**, 709–17 (2004).

130. Qian, Y. *et al.* Circulating and local renin-angiotensin-aldosterone system express differently in atrial fibrillation patients with different types of mitral valvular disease. *J. Renin. Angiotensin. Aldosterone. Syst.* **14**, 204–11 (2013).

131. Bischoff, J. *et al.* CD45 Expression in Mitral Valve Endothelial Cells After Myocardial Infarction. *Circ. Res.* **119**, 1215–1225 (2016).

132. Barrera-Chimal, J. *et al.* Benefit of Mineralocorticoid Receptor

Antagonism in AKI: Role of Vascular Smooth Muscle Rac1. *J. Am. Soc. Nephrol.* **28**, 1216–1226 (2017).

133. Clausen, B. E., Burkhardt, C., Reith, W., Renkawitz, R. & Förster, I. Conditional gene targeting in macrophages and granulocytes using LysMcre mice. *Transgenic Res.* **8**, 265–77 (1999).

134. Mueller, K. B. *et al.* Endothelial Mineralocorticoid Receptors Differentially Contribute to Coronary and Mesenteric Vascular Function Without Modulating Blood Pressure. *Hypertens. (Dallas, Tex. 1979)* **66**, 988–97 (2015).

135. Fraccarollo, D. *et al.* Deletion of cardiomyocyte mineralocorticoid receptor ameliorates adverse remodeling after myocardial infarction. *Circulation* **123**, 400–8 (2011).

136. Wang, Y. *et al.* Ephrin-B2 controls VEGF-induced angiogenesis and lymphangiogenesis. *Nature* **465**, 483–6 (2010).

137. Wendling, O., Bornert, J.-M., Chambon, P. & Metzger, D. Efficient temporally-controlled targeted mutagenesis in smooth muscle cells of the adult mouse. *Genesis* **47**, 14–8 (2009).

138. Livak, K. J. & Schmittgen, T. D. Analysis of relative gene expression data using real-time quantitative PCR and the 2(-Delta Delta C(T)) Method. *Methods* **25**, 402–8 (2001).

139. Margioris, A. N. & Tsatsanis, C. *ACTH Action on the Adrenals*. *Endotext* (2000).

140. Chapman, K., Holmes, M. & Seckl, J. 11β-Hydroxysteroid Dehydrogenases: Intracellular Gate-Keepers of Tissue Glucocorticoid Action. *Physiol. Rev.* **93**, 1139–1206 (2013).

141. López-Andrés, N., Iñigo, C., Gallego, I., Díez, J. & Fortuño, M. A. Aldosterone induces cardiotrophin-1 expression in HL-1 adult cardiomyocytes. *Endocrinology* **149**, 4970–8 (2008).

142. López-Andrés, N. *et al.* A role for cardiotrophin-1 in myocardial remodeling induced by aldosterone. *Am. J. Physiol. Circ. Physiol.* **301**, H2372–H2382 (2011).

143. Mannic, T. *et al.* CD14 as a Mediator of the Mineralocorticoid Receptor-Dependent Anti-apolipoprotein A-1 IgG Chronotropic Effect on Cardiomyocytes. *Endocrinology* **156**, 4707–19 (2015).

144. Ayme-Dietrich, E. *et al.* The role of 5-HT2B receptors in mitral valvulopathy: bone marrow mobilization of endothelial progenitors. *Br. J. Pharmacol.* **174**, 4123–4139 (2017).

145. Golias, C. *et al.* Review. Leukocyte and endothelial cell adhesion molecules in inflammation focusing on inflammatory heart disease. *In Vivo* **21**, 757–69

146. Jaisser, F. & Farman, N. Emerging Roles of the Mineralocorticoid Receptor in Pathology: Toward New Paradigms in Clinical Pharmacology. *Pharmacol. Rev.* **68**, 49–75 (2015).

147. Verrey, F. Transcriptional control of sodium transport in tight epithelial by adrenal steroids. *J. Membr. Biol.* **144**, 93–110 (1995).

148. Thum, T. *et al.* Impairment of endothelial progenitor cell function and vascularization capacity by aldosterone in mice and humans. *Eur. Heart J.* **32**, 1275–1286 (2011).

149. Garg, R. *et al.* Mineralocorticoid Receptor Blockade Improves Coronary Microvascular Function in Individuals With Type 2 Diabetes. *Diabetes* **64**, 236–242 (2015).

150. Davel, A. P., Anwar, I. J. & Jaffe, I. Z. The endothelial mineralocorticoid receptor: mediator of the switch from vascular health to disease. *Curr. Opin. Nephrol. Hypertens.* **26**, 97–104 (2017).

151. Gorini, S., Marzolla, V., Mammi, C., Armani, A. & Caprio, M. Mineralocorticoid Receptor and Aldosterone-Related Biomarkers of End-Organ Damage in Cardiometabolic Disease. *Biomolecules* **8**, 96 (2018).

152. Arriza, J. L. *et al.* Cloning of human mineralocorticoid receptor complementary DNA: structural and functional kinship with the

glucocorticoid receptor. *Science* **237**, 268–75 (1987).

153. Odermatt, A. & Kratschmar, D. V. Tissue-specific modulation of mineralocorticoid receptor function by 11β-hydroxysteroid dehydrogenases: an overview. *Mol. Cell. Endocrinol.* **350**, 168–86 (2012).

154. Young, M. & Funder, J. Mineralocorticoid Action and Sodium-Hydrogen Exchange: Studies in Experimental Cardiac Fibrosis. *Endocrinology* **144**, 3848–3851 (2003).

155. Wilson, P., Morgan, J., Funder, J. W., Fuller, P. J. & Young, M. J. Mediators of mineralocorticoid receptor-induced profibrotic inflammatory responses in the heart. *Clin. Sci. (Lond).* **116**, 731–9 (2009).

156. Caprio, M. *et al.* Functional mineralocorticoid receptors in human vascular endothelial cells regulate intercellular adhesion molecule-1 expression and promote leukocyte adhesion. *Circ. Res.* **102**, 1359–67 (2008).

157. Gaddam, K. K., Pimenta, E., Husain, S. & Calhoun, D. A. Aldosterone and cardiovascular disease. *Curr. Probl. Cardiol.* **34**, 51–84 (2009).

158. He, B. J. & Anderson, M. E. Aldosterone and cardiovascular disease: the heart of the matter. *Trends Endocrinol. Metab.* **24**, 21–30 (2013).

159. Fu, G.-X., Xu, C.-C., Zhong, Y., Zhu, D.-L. & Gao, P.-J. Aldosterone-induced osteopontin expression in vascular smooth muscle cells involves MR, ERK, and p38 MAPK. *Endocrine* **42**, 676–83 (2012).

160. Pruthi, D. *et al.* Aldosterone Promotes Vascular Remodeling by Direct Effects on Smooth Muscle Cell Mineralocorticoid Receptors. *Arterioscler. Thromb. Vasc. Biol.* **34**, 355–364 (2014).

161. Martínez-Martínez, E. *et al.* Aldosterone Target NGAL (Neutrophil Gelatinase-Associated Lipocalin) Is Involved in Cardiac Remodeling After Myocardial Infarction Through NFκB Pathway. *Hypertens. (Dallas, Tex. 1979)* **70**, 1148–1156 (2017).

162. Martinez-Martinez, E. *et al.* Differential Proteomics Identifies Reticulocalbin-3 as a Novel Negative Mediator of Collagen Production in Human Cardiac Fibroblasts. *Sci. Rep.* **7**, 12192 (2017).

163. Martínez-Martínez, E. *et al.* Differential proteomics reveals S100-A11 as a key factor in aldosterone-induced collagen expression in human cardiac fibroblasts. *J. Proteomics* **166**, 93–100 (2017).

164. Calvier, L. *et al.* Galectin-3 Mediates Aldosterone-Induced Vascular Fibrosis. *Arterioscler. Thromb. Vasc. Biol.* **33**, 67–75 (2013).

165. Zhang, A., Jia, Z., Guo, X. & Yang, T. Aldosterone induces epithelial-mesenchymal transition via ROS of mitochondrial origin.

Am. J. Physiol. Renal Physiol. **293**, F723-31 (2007).

166. Brown, D. J. *et al.* Endothelial cell activation of the smooth muscle cell phosphoinositide 3-kinase/Akt pathway promotes differentiation. *J. Vasc. Surg.* **41**, 509–16 (2005).

167. Rzucidlo, E. M., Martin, K. A. & Powell, R. J. Regulation of vascular smooth muscle cell differentiation. *J. Vasc. Surg.* **45 Suppl A**, A25-32 (2007).

168. Lin, C.-H. & Lilly, B. Endothelial cells direct mesenchymal stem cells toward a smooth muscle cell fate. *Stem Cells Dev.* **23**, 2581–90 (2014).

169. López-Yoldi, M. *et al.* Role of cardiotrophin-1 in the regulation of metabolic circadian rhythms and adipose core clock genes in mice and characterization of 24-h circulating CT-1 profiles in normal-weight and overweight/obese subjects. *FASEB J.* **31**, 1639–1649 (2017).

170. Lopez-Andres, N. *et al.* Cardiotrophin 1 Is Involved in Cardiac, Vascular, and Renal Fibrosis and Dysfunction. *Hypertension* **60**, 563–573 (2012).

171. Lopez-Andres, N. *et al.* Vascular effects of cardiotrophin-1: a role in hypertension? *J. Hypertens.* **28**, 1261–72 (2010).

172. Tsuruda, T. *et al.* Cardiotrophin-1 stimulation of cardiac fibroblast growth: roles for glycoprotein 130/leukemia inhibitory factor receptor and the endothelin type A receptor. *Circ. Res.* **90**, 128–34 (2002).

173. Freed, D. H. *et al.* Cardiotrophin-1: expression in experimental myocardial infarction and potential role in post-MI wound healing. *Mol. Cell. Biochem.* **254**, 247–56 (2003).

174. Freed, D. H., Borowiec, A. M., Angelovska, T. & Dixon, I. M. C. Induction of protein synthesis in cardiac fibroblasts by cardiotrophin-1: integration of multiple signaling pathways. *Cardiovasc. Res.* **60**, 365–75 (2003).

175. Drobic, V. *et al.* Differential and combined effects of cardiotrophin-1 and TGF-beta1 on cardiac myofibroblast proliferation and contraction. *Am. J. Physiol. Heart Circ. Physiol.* **293**, H1053-64 (2007).

176. Calabrò, P. *et al.* Novel insights into the role of cardiotrophin-1 in cardiovascular diseases. *J. Mol. Cell. Cardiol.* **46**, 142–8 (2009).

177. Martínez-Martínez, E. *et al.* CT-1 (Cardiotrophin-1)-Gal-3 (Galectin-3) Axis in Cardiac Fibrosis and Inflammation. *Hypertension* **73**, (2019).

178. Wollert, K. C. *et al.* Cardiotrophin-1 activates a distinct form of

cardiac muscle cell hypertrophy. Assembly of sarcomeric units in series VIA gp130/leukemia inhibitory factor receptor-dependent pathways. *J. Biol. Chem.* **271**, 9535–45 (1996).

179. Pennica, D. *et al.* Expression cloning of cardiotrophin 1, a cytokine that induces cardiac myocyte hypertrophy. *Proc. Natl. Acad. Sci. U. S. A.* **92**, 1142–6 (1995).

180. Talwar, S., Squire, I. B., Davies, J. E. & Ng, L. L. The effect of valvular regurgitation on plasma Cardiotrophin-1 in patients with normal left ventricular systolic function. *Eur. J. Heart Fail.* **2**, 387–391 (2000).

181. Jersmann, H. P. A., Hii, C. S. T., Hodge, G. L. & Ferrante, A. Synthesis and Surface Expression of CD14 by Human Endothelial Cells. *Infect. Immun.* **69**, 479–485 (2001).

182. Vaure, C. & Liu, Y. A Comparative Review of Toll-Like Receptor 4 Expression and Functionality in Different Animal Species. *Front. Immunol.* **5**, (2014).

183. Adamczak, D. M. The Role of Toll-Like Receptors and Vitamin D in Cardiovascular Diseases-A Review. *Int. J. Mol. Sci.* **18**, 2252 (2017).

184. Lu, C.-C. *et al.* Developmental pathways and endothelial to mesenchymal transition in canine myxomatous mitral valve disease. *Vet. J.* **206**, 377–84 (2015).

185. Jagavelu, K. *et al.* Endothelial cell toll-like receptor 4 regulates fibrosis-associated angiogenesis in the liver. *Hepatology* **52**, 590–601 (2010).

186. Liu, L. *et al.* Up-regulated TLR4 in cardiomyocytes exacerbates heart failure after long-term myocardial infarction. *J. Cell. Mol. Med.* **19**, 2728–40 (2015).

187. Thalji, N. M. *et al.* Nonbiased Molecular Screening Identifies Novel Molecular Regulators of Fibrogenic and Proliferative Signaling in Myxomatous Mitral Valve Disease. *Circ. Cardiovasc. Genet.* **8**, 516–28 (2015).

188. Zhang, Y. *et al.* TAK-242, a Toll-Like Receptor 4 Antagonist, Protects against Aldosterone-Induced Cardiac and Renal Injury. *PLoS One* **10**, e0142456 (2015).

189. Yu, L. & Feng, Z. The Role of Toll-Like Receptor Signaling in the Progression of Heart Failure. *Mediators Inflamm.* **2018**, 1–11 (2018).

190. Connolly, H. M. *et al.* Valvular heart disease associated with fenfluramine-phentermine. *N. Engl. J. Med.* **337**, 581–8 (1997).

191. Fitzgerald, L. W. *et al.* Possible role of valvular serotonin 5-HT(2B) receptors in the cardiopathy associated with fenfluramine. *Mol. Pharmacol.* **57**, 75–81 (2000).

192. Rothman, R. B. *et al.* Evidence for possible involvement of 5-HT(2B) receptors in the cardiac valvulopathy associated with fenfluramine and other serotonergic medications. *Circulation* **102**, 2836–41 (2000).

193. Goldberg, E. *et al.* Serotonin and catecholamines in the development and progression of heart valve diseases. *Cardiovasc. Res.* **113**, 849–857 (2017).

194. McDonald, P. C. *et al.* Quantitative analysis of human heart valves: does anorexigen exposure produce a distinctive morphological lesion? *Cardiovasc. Pathol.* **11**, 251–62

195. Droogmans, S. *et al.* In vivo model of drug-induced valvular heart disease in rats: pergolide-induced valvular heart disease demonstrated with echocardiography and correlation with pathology. *Eur. Heart J.* **28**, 2156–62 (2007).

196. Driesbaugh, K. H. *et al.* Serotonin receptor 2B signaling with interstitial cell activation and leaflet remodeling in degenerative mitral regurgitation. *J. Mol. Cell. Cardiol.* **115**, 94–103 (2018).

197. Droogmans, S. *et al.* In vivo model of drug-induced valvular heart disease in rats: pergolide-induced valvular heart disease demonstrated with echocardiography and correlation with pathology. *Eur. Heart J.* **28**, 2156–62 (2007).

198. Bharti, S., Rani, N., Bhatia, J. & Arya, D. S. 5-HT2B receptor blockade attenuates β-adrenergic receptor-stimulated myocardial remodeling in rats via inhibiting apoptosis: role of MAPKs and HSPs. *Apoptosis* **20**, 455–65 (2015).

199. Elangbam, C. S. *et al.* 5-Hydroxytryptamine (5HT)-induced valvulopathy: Compositional valvular alterations are associated with 5HT2B receptor and 5HT transporter transcript changes in Sprague-Dawley rats. *Exp. Toxicol. Pathol.* **60**, 253–262 (2008).

200. Goldberg, E. *et al.* Serotonin and catecholamines in the development and progression of heart valve diseases. *Cardiovasc. Res.* **113**, 849–857 (2017).

201. Kekewska, A., Görnemann, T., Jantschak, F., Glusa, E. & Pertz, H. H. Antiserotonergic properties of terguride in blood vessels, platelets, and valvular interstitial cells. *J. Pharmacol. Exp. Ther.* **340**, 369–76 (2012).

202. Leopold, J. A. Aldosterone, mineralocorticoid receptor activation, and cardiovascular remodeling. *Circulation* **124**, e466-8 (2011).

203. Bernay, F. *et al.* Efficacy of spironolactone on survival in dogs with naturally occurring mitral regurgitation caused by myxomatous mitral valve disease. *J. Vet. Intern. Med.* **24**, 331–41 (2010).

204. Increase of tryptophan hydroxylase enzyme protein by

dexamethasone in adrenalectomized rat midbrain. - PubMed - NCBI. Available at: https://www.ncbi.nlm.nih.gov/pubmed/?term=8254360. (Accessed: 31st May 2019)

205. Lai, M. *et al.* Differential regulation of corticosteroid receptors by monoamine neurotransmitters and antidepressant drugs in primary hippocampal culture. *Neuroscience* **118**, 975–84 (2003).

206. Wu, T.-C. *et al.* Mineralocorticoid receptor antagonist spironolactone prevents chronic corticosterone induced depression-like behavior. *Psychoneuroendocrinology* **38**, 871–83 (2013).

207. Hesen, W. & Joëls, M. Modulation of 5HT1A responsiveness in CA1 pyramidal neurons by in vivo activation of corticosteroid receptors. *J. Neuroendocrinol.* **8**, 433–8 (1996).

208. Wissink, S., Meijer, O., Pearce, D., van Der Burg, B. & van Der Saag, P. T. Regulation of the rat serotonin-1A receptor gene by corticosteroids. *J. Biol. Chem.* **275**, 1321–6 (2000).

209. Térouanne, B. *et al.* A stable prostatic bioluminescent cell line to investigate androgen and antiandrogen effects. *Mol. Cell. Endocrinol.* **160**, 39–49 (2000).

210. Azmitia, E. C., Liao, B. & Chen, Y. S. Increase of tryptophan hydroxylase enzyme protein by dexamethasone in adrenalectomized rat midbrain. *J. Neurosci.* **13**, 5041–55 (1993).

211. Whittaker, P., Boughner, D. R., Perkins, D. G. & Canham, P. B. Quantitative structural analysis of collagen in chordae tendineae and its relation to floppy mitral valves and proteoglycan infiltration. *Br. Heart J.* **57**, 264–9 (1987).

212. Parviz, Y. *et al.* Emerging cardiovascular indications of mineralocorticoid receptor antagonists. *Trends Endocrinol. Metab.* **26**, 201–11 (2015).

213. Pitt, B. *et al.* The effect of spironolactone on morbidity and mortality in patients with severe heart failure. Randomized Aldactone Evaluation Study Investigators. *N. Engl. J. Med.* **341**, 709–17 (1999).

214. Zannad, F. *et al.* Eplerenone in patients with systolic heart failure and mild symptoms. *N. Engl. J. Med.* **364**, 11–21 (2011).

215. Nayar, P. *et al.* Risk Factors for In-Hospital Mortality in Heart Failure Patients: Does Rurality, Payer or Admission Source Matter? *J. Rural Health* **34**, 103–108 (2018).

216. Pitt, B. *et al.* Eplerenone, a selective aldosterone blocker, in patients with left ventricular dysfunction after myocardial infarction. *N. Engl. J. Med.* **348**, 1309–21 (2003).

217. Pitt, B. *et al.* Effects of eplerenone, enalapril, and eplerenone/enalapril in patients with essential hypertension and left ventricular hypertrophy: the 4E-left ventricular hypertrophy study.

Circulation **108**, 1831–8 (2003).

218. Zendaoui, A., Lachance, D., Roussel, E., Couet, J. & Arsenault, M. Effects of spironolactone treatment on an experimental model of chronic aortic valve regurgitation. *J. Heart Valve Dis.* **21**, 478–86 (2012).

219. Okoshi, M. P. *et al.* Effects of early aldosterone antagonism on cardiac remodeling in rats with aortic stenosis-induced pressure overload. *Int. J. Cardiol.* **222**, 569–575 (2016).

220. Rabkin, E. *et al.* Activated interstitial myofibroblasts express catabolic enzymes and mediate matrix remodeling in myxomatous heart valves. *Circulation* **104**, 2525–32 (2001).

221. Wylie-Sears, J., Levine, R. A. & Bischoff, J. Losartan inhibits endothelial-to-mesenchymal transformation in mitral valve endothelial cells by blocking transforming growth factor-β-induced phosphorylation of ERK. *Biochem. Biophys. Res. Commun.* **446**, 870–5 (2014).

222. Bartko, P. E. *et al.* Effect of Losartan on Mitral Valve Changes After Myocardial Infarction. *J. Am. Coll. Cardiol.* **70**, 1232–1244 (2017).

223. Briet, M. *et al.* Aldosterone-Induced Vascular Remodeling and Endothelial Dysfunction Require Functional Angiotensin Type 1a Receptors. *Hypertens. (Dallas, Tex. 1979)* **67**, 897–905 (2016).

224. Borer, J. S. & Sharma, A. Drug Therapy for Heart Valve Diseases. *Circulation* **132**, 1038–45 (2015).

225. Ponikowski, P. *et al.* 2016 ESC Guidelines for the diagnosis and treatment of acute and chronic heart failure: The Task Force for the diagnosis and treatment of acute and chronic heart failure of the European Society of Cardiology (ESC). Developed with the special contribution of the Heart Failure Association (HFA) of the ESC. *Eur. J. Heart Fail.* **18**, 891–975 (2016).

226. Bonow, R. O. *et al.* 2008 Focused Update Incorporated Into the ACC/AHA 2006 Guidelines for the Management of Patients With Valvular Heart Disease. *Circulation* **118**, e523-661 (2008).

227. Iung, B. *et al.* Valvular heart disease in the community: a European experience. *Curr. Probl. Cardiol.* **32**, 609–61 (2007).

228. Braunschweig, F. *et al.* Transient repolarization instability following the initiation of cardiac resynchronization therapy. *Europace* **13**, 1327–1334 (2011).

229. Nkomo, V. T. *et al.* Burden of valvular heart diseases: a population-based study. *Lancet (London, England)* **368**, 1005–11 (2006).

ANNEX

Cytokine	VIC
	Aldo (24 h)
MMP-13	1,54
MMP-9	1,53
BMP-7	1,46
IL-21R	1,42
Endoglin	1,41
TGF β 2	1,40
IL-18 R β	1,38
IL-5Rα	1,35
IL-2 R β	1,33
CXCL-16	1,32
Cardiotrophin-1	1,32
BMP-5	1,31
IL-9	1,31
ErbB3	1,31
Tie-1	1,31
E-Selectin	1,30
IL-2 R g	1,30
MMP-1	1,28
MMP-3	1,28
MPIF-1	1,28
TGF-α	1,27
IP-10	1,26
Fas Ligand	1,25
IL-18 BPα	1,25
PDGF AA	1,24
LAP	1,24
CD14	1,24
NGF R	1,23
PDGF Bβ	1,22
VE-Cadherin	1,22
PDGF-AB	1,22
ICAM-2	1,20
DR6	1,19
Tie-2	1,18
IL-10 Rβ	1,18
VEGF R2	1,18
IGF-II	1,18
ALCAM	1,17
PDGF R β	1,17
IL-13 R α 2	1,16
Activin A	1,16
IL-1 R II	1,16
B7-1 (CD80)	1,15
Siglec-5	1,14
Leptin R	1,14
PECAM-1	1,14
M-CSF R	1,13
LIF	1,13
VEGF R3	1,11
SDF-1β	1,10
L-Selectin	1,09
SCF R	1,08
Prolactin	1,08
TIMP-4	0,87

Cytokine	VEC	
	Aldo (24 h)	**Aldo (96 h)**
DR6	14,732	0,514
TIMP-4	13,113	0,771
IL-2 R g	8,665	0,446
NGF R	6,274	0,364
CXCL-16	5,685	0,701
Tie-2	3,414	0,974
MPIF-1	2,577	0,456
IL-2 R β	2,444	0,538
CD14	2,293	1,006
Tie-1	2,276	1,205
Fas Ligand	2,068	1,011
LAP	1,993	1,204
LIF	1,979	1,146
Leptin R	1,921	1,086
Cardiotrophin-1	1,919	1,386
L-Selectin	1,790	1,283
IL-1 R II	1,784	1,248
IP-10	1,780	1,045
BMP-7	1,761	0,917
IL-18 BPα	1,753	1,172
IL-18 R β	1,732	1,386
MMP-9	1,723	0,578
MMP-3	1,723	0,619
IL-10 Rβ	1,722	1,208
TGF β 2	1,703	1,061
IGF-II	1,661	1,140
M-CSF R	1,654	1,352
E-Selectin	1,631	1,077
IL-13 R α 2	1,619	1,309
BMP-5	1,615	1,142
TGF-α	1,592	1,017
ICAM-2	1,492	1,095
B7-1 (CD80)	1,491	1,056
MMP-13	1,490	0,768
Siglec-5	1,482	1,044
ALCAM	1,445	1,107
PECAM-1	1,383	0,878
IL-9	1,263	1,105
Activin A	1,235	1,146
PDGF R β	1,166	1,140
MMP-1	1,163	1,549
ErbB3	1,140	1,114
SDF-1β	1,117	0,960
Prolactin	1,028	1,122
SCF R	0,966	1,113
IL-5Rα	0,658	1,136
PDGF AA	0,560	1,187
PDGF Bβ	0,512	1,175
Endoglin	0,477	1,092
PDGF-AB	0,419	1,244
IL-21R	0,276	1,165
VEGF R3	0,144	1,138
VEGF R2	0,140	1,227
VE-Cadherin	0,123	0,850